APPLICATIONS OF SENSITIVITY ANALYSIS IN PLANNING AND OPERATION OF MODERN POWER SYSTEMS

By

Mohammed Ben-Idris

A DISSERTATION

Submitted to
Michigan State University
in partial fulfillment of the requirements
for the degree of

Electrical Engineering - Doctor of Philosophy

2014

ABSTRACT

APPLICATIONS OF SENSITIVITY ANALYSIS IN PLANNING AND OPERATION OF MODERN POWER SYSTEMS

By

Mohammed Ben-Idris

More large blackouts in power systems have been encountered in the last few years than in any other period in history. Although the evolution of a large blackout is a complex process, it usually starts with a small triggering event that by successive events can cascade and evolve into a complete blackout. Therefore, hardening power systems against such events and improving power system reliability are of necessity.

Several reliability indices for composite systems have been introduced such as loss of load probability, loss of load frequency, loss of load expectation, expected energy not supplied, expected demand not supplied, etc. Although these indices are of a great importance in both planning and operational power system reliability evaluation, they lack the ability to identify the influence of each area or equipment on system reliability. Moreover, these indices cannot determine the most effective way to improve the system in order to keep it reliable. Due to these reasons, significant efforts have been devoted to this area in recent years to evaluate what the system's reliability justifications are and to determine the best location in which to invest.

One of the promising methods that can identify the most vulnerable component(s), bus(es), or area(s) is performing sensitivity analysis of the possible load shedding with respect to component parameters and operating limits. The sensitivity analysis provides a measure of the amount of load to be curtailed in response to the violation of the operating limits or component characteristics.

The task of performing sensitivity analysis is amply used in power system reliability planning and operational studies. However, the application of sensitivity analysis in the changing operating environment such as the newly imposed emission constraints, penetration of the renewable energy sources and cascading failures in power systems has not been given much attention. Sensitivity analyses of the reliability indices can be conducted either analytically such as using state space enumeration or by means of simulations. Therefore, performing sensitivity analyses over a large set of variables for large systems is computationally expensive and often intractable.

The work presented in thesis develops and proposes new expressions for sensitivity analysis that can be used to identify the most vulnerable components in power systems. Also, this work proposes a heuristic technique in conjunction with the population-based intelligent search methods (PIS) to reduce the computation burden. The work in this thesis is divided into three parts. Part I presents the concept of the sensitivity analyses and provides the mathematical derivations of the proposed expressions. Also, this part introduces new techniques to reduce the computational time and burden based on PIS methods and their applications in power system reliability evaluation. Furthermore, it introduces a new technique to classify the search space into success, failure and unclassified subspaces. Part II presents the application of the derived expressions on power system reliability planning studies such as the effect of each parameter on system reliability and the effect of emission constraints on power system reliability. Also, this part examines the proposed algorithms to speed up the computational time against the existing techniques. Part III conducts the application of the sensitivity analysis in power system reliability operation such as mitigation of cascading failures and prevention of the unfolding events.

My parents, wife and my two little daughters

ACKNOWLEDGMENTS

TABLE OF CONTENTS

LIST OF TABLES

LIST OF FIGURES

Chapter 1

Introduction

Due to the ongoing changes in generation portfolios and environmental concerns, reliability evaluation of composite generation and transmission systems has received a great attention. The task of composite power system reliability evaluation has become more complicated due to the rapid increase in electrical demand and the liberalization of the electricity markets. Several reliability indices for composite systems have been introduced such as loss of load probability, loss of load frequency, loss of load expectation, expected energy not supplied, expected demand not supplied, etc. Although these indices are of a great importance in both planning and operational power system reliability evaluation, they lack the ability of identifying the influence of each area or equipment on system reliability. Moreover, these indices cannot determine the most-effective way to improve the system in order to keep it reliable.

One of the promising methods that can identify the most vulnerable component, bus, or area is performing sensitivity analysis of the possible load shedding with respect to component parameters and operating limits. The sensitivity analysis provides a measure for the amount of load to be curtailed in response to the violation of the operating limits or component characteristics. Sensitivity analysis of the power system reliability indices is intended to determine the effect of the capacity and reliability parameters such as failure and repair rates of each component on system reliability. Also, it examines the effect of power quality such as voltage and reactive power reserve on system behavior. Furthermore, sensitivity analysis

1

can be used and is being used in mitigating the unfolding events in case of cascading failures.

The task of performing sensitivity analysis is amply used in power system reliability planning and operational studies. However, the application of sensitivity analysis in the changing operating environment such as the newly imposed emission constraints, penetration of the renewable energy sources and cascading failures in power systems has not been given much attention. Sensitivity analyses of the reliability indices can be conducted either analytically such as using state space enumeration or by means of simulations. Therefore, performing sensitivity over a large set of variables for large systems is computationally expensive.

In response to the growing need to harden power systems against unfolding events with efficient computation tools, this thesis provides a framework for performing sensitivity analysis for the risk indices with respect system variables. To make the analyses feasible in terms of computation time and burden, a state space reduction technique in conjunction with the population-based intelligent search methods is proposed.

In addition to component parameters such as component availability/unavailability, failure rate and repair rate, the operating limits are also included in this work. The operating limits studied in this work are emission caps and voltage and reactive power limits. The work provided in this thesis is the first work in the literature that addresses the effects of the emission limits on power system planning from reliability prospective. Although the effects of voltage and reactive power limits on power system reliability have been considered, the sensitivity of the load shedding with respect to these limits is the first time introduced in this thesis.

1.1 Motivation

In response to the rapid growth of the global economics, large power grids are interconnected in order to provide the required energy. As a result of these interconnections, the number of failures also increases and may spread through these interconnections and cause cascading failures. Also, due to the integration of renewable energy sources, voltage and reactive power limits should be included in the planning and operating reliability assessments. Further, after the introduction of the regulations and amendments to reduce the emissions from the power generation sector, emission constraints should also be included in the reliability assessments.

The time and computation effort to evaluate the robustness of power systems against the triggering events are of concern in both planning and operation prospective. Developing tools that can reduce the computation burden will help in applying strategies to harden power systems against catastrophic failures.

1.2 Challenges

The challenges that were addressed in this thesis are summarized as follows:

A. Determining the most vulnerable components in power systems that can lead to power interruptions is a challenging task. Several indices have been introduced in the literature of power system reliability evaluation but they lack the ability of identifying which component that has the highest effect on system deficiency.

B. The task of power system reliability evaluation is becoming more computationally demanding due to the increase in the complexity of the power industry infrastructure. The time and computation effort to evaluate power system reliability indices and their

3

sensitivities with respect to component parameters and system operating limits are of concern in both planning and operation prospective. As the number of system components increases, the number of states that need to be tested to assess power system reliability exponentially increases (2^n in case of state space enumeration where n is the number of system components).

C. Most of the existing power system reliability evaluation methods do not account for the effects of the operating constraints such as voltage and reactive power limits. Also, new regulations such as emission reduction regulations should be included in performing power system reliability evaluation.

D. Mitigation of cascading failures in power systems has become of necessity especially after the recent blackouts. Cascading failures usually develop in a sequence of events within a time horizon of seconds to hours. If the potential causes of the cascading failures are incorporated with the load shedding procedure, cascading failure could be mitigated.

1.3 Approaches

In addressing the aforementioned challenges, the following approaches were used:

A. Sensitivity analysis of the reliability indices are used to identify the most vulnerable components in a power system. The sensitivity analysis can identify which component that contributes in most and most sever load interruptions.

B. A state space reduction technique is proposed and used in reducing the computational effort. This technique classifies the state space into success, failure and unclassified subspace by using heuristic devices. Controlled population-based intelligent search methods,

4

in particular, dynamically directed particle swarm optimization search method, are used to search for the desired states in the unclassified subspace.

C. The effects of the voltage and reactive power constraints on power system availability are considered by utilizing the AC power flow model and a linearized power flow model. Also, the constraints of the emission limits are accommodated by piecewise linearizing the quadratic heat rate equations.

D. The sensitivity of the risk of load curtailments with respect to voltage and reactive power limits are used in mitigating cascading failures in power systems. After identifying the buses that hit the limits, reactive power compensation and/or generation rescheduling are suggested to prevent voltage collapse.

1.4 Contributions

The contributions of the presented work can be summarized as follows:

A. Developing and proposing new sensitivity analysis expressions that can relate the expected load curtailment to the component parameters as well as operating limits.

B. Proposing a new state space reduction technique that can classify the state space of a given system into success, failure and unclassified subspaces. The validity and effectiveness of the proposed technique are tested through comparing the results with those obtained using Monte Carlo simulation.

C. Proposing a dynamically directed particle swarm optimization search method to search for failure states in the unclassified subspace or in any desired subspace.

D. Introducing a complementary concept that can be used with the population-based intelligent search methods to estimate the reliability of power systems without the need of testing the entire state space.

E. Inclusion of emission constraints in power system reliability evaluation.

F. Proposing new indices to include the effects of voltage and reactive power limits on power system reliability.

G. Developing a method to mitigate cascading failures in power systems through the use of the sensitivity analysis concept.

1.5 Organization of the Thesis

The remainder of this thesis is organized as follows: Chapter 2 presents the power flow models that are used in this thesis and the incorporation of minimum load curtailments in an optimization framework. Chapter 3 discusses the developments of the sensitivity analysis expressions that are used to estimate the sensitivity of power reliability indices with respect to component parameters and the operating limits. Chapter 4 introduces the proposed state space reduction technique and the dynamically directed particle swarm optimization search method. Chapter 5 describes the use of the shadow price concept (Lagrange multipliers) in evaluating the sensitivity of power system reliability indices with respect to component parameters. Also, chapter 5 provides benchmark results that can be used to test the effectiveness of the proposed approaches. Chapter 6 shows the applications of the proposed approaches on performing sensitivity analysis of the reliability indices. Chapter 7 shows the applications of the proposed methods with considering emission constraints. Chapter 8 con-

siders the effects of voltage and reactive power limits on power system reliability. Chapter 9 shows the applications of sensitivity analysis in hardening power systems against cascading failures. Chapter 10 provides concluding remarks and possible future work.

Chapter 2

Power Flow Modeling and Optimization Framework

2.1 Introduction

Power flow in power system networks plays a significant part of power system planning and operating studies. Incorporation of a power flow model and redispatch optimization problem with minimizing operation costs and load curtailment is commonly used in planning and operation decisions. Two types of power flow models have been commonly used in the literature in modeling power system networks which are AC power flow and DC power flow. The DC power flow ignores the effect of line resistances and the reactive power and assumes voltages magnitudes are 1 p.u. These assumptions make the DC power flow less accurate because in some scenarios the voltage collapse due to voltage limits and insufficient reactive power support can lead to under-voltage load shedding. The full AC power flow model is the most accurate power flow model but it is computationally expensive especially for the applications that require repetitive runs of power flow. In this thesis, in addition to the AC and DC power flow models, we have used another power flow model which is a linearized version of the AC power flow that closely represents power system networks. This model was developed by the authors in [1]. This model can be considered as a modified version of the DC power flow model or a linearized form of the full AC load flow model.

2.2 Power Flow Models

In evaluating the reliability indices of composite systems, an optimal power flow with an objective of minimum load curtailment is performed. This section provides a brief overview of the AC, DC and the linearized power flow models.

2.2.1 AC Power Flow Model

AC power flow model has been amply explained in the literature. This section provides a brief introduction about the formulation of the AC power flow. The AC power flow equations at bus k can be presented as follows (in the polar form),

$$P_k = V_k \sum_{m \in k} V_m \left(G_{km} \cos \delta_{km} + B_{km} \sin \delta_{km} \right) \tag{2.1}$$

$$Q_k = V_k \sum_{m \in k} V_m \left(G_{km} \sin \delta_{km} - B_{km} \cos \delta_{km} \right) \tag{2.2}$$

where $m \in k$ means the set of the buses connected to bus k, P_k and Q_k are the real and reactive power injected at bus k, V_k and V_m are the voltage magnitudes at buses k and m, G_{km} is the conductance between buses k and m, B_{km} is the susceptance between buses k and m and δ_{km} is the angle difference between voltages of buses k and m $(\delta_{km} = \delta_k - \delta_m)$.

In solving the AC power flow equations, each bus has four variables which are P_k, Q_k, V_k and δ_{km}. There are three types of buses, load buses, generation buses and a slack or reference bus. For load buses, which are sometimes called PQ buses, the P_k and Q_k are pre-specified for constant power load model. For generation buses, which are commonly known as PV buses, P_k and V_k are pre-specified. For the slack bus (one slack bus), P_k and δ_{km} are pre-specified.

2.2.2 DC Power Flow model

DC power flow model has been amply explained in the literature. This section provides a brief introduction about the formulation of the DC power flow. The DC power flow model is an approximated version of the AC power flow model with the following assumptions:

1. Bus voltage magnitudes are assumed 1.0 p.u.,

2. Voltage angles, δ_{km}, between buses are small such that $\cos(\delta_{km}) \approx 1$ and $\sin(\delta_{km}) \approx \delta_{km} = \delta_k - \delta_m$,

3. Line resistances are much smaller than the line reactances so that line impedances can be approximated as $Z_{km} = jx_{km}$ (line susceptance $B_{km} = -j/x_{km}$),

4. Susceptances between buses and the ground are neglected.

The real power flow between buses can be expressed as,

$$P_{km} = \frac{|V_k||V_m|}{x_{km}} \sin \delta_{km} \tag{2.3}$$

From the above assumptions, the real power flow between buses can be approximated as,

$$P_{km} = \frac{\delta_k - \delta_m}{x_{km}} \tag{2.4}$$

Then, the real power at buses can expressed as follows,

$$P_k = \sum_{m \in k} P_{km}. \tag{2.5}$$

2.2.3 Linearized Power Flow model

The development of the linearized power flow model starts with the well-known AC real and reactive power injection equations at bus k (equations (2.1) and (2.2)). If the voltage at bus k is assumed 1 p.u. for calculating the power injection equations, then equations (2.1) and (2.2) can be approximated as follows,

$$P_k \approx \sum_{m \in k} V_m \left(G_{km} \cos \delta_{km} + B_{km} \sin \delta_{km} \right) \tag{2.6}$$

$$Q_k \approx \sum_{m \in k} V_m \left(G_{km} \sin \delta_{km} - B_{km} \cos \delta_{km} \right). \tag{2.7}$$

It should be noted that, this assumption will not prevent the voltage at bus k from being calculated, rather it approximates the power injection at bus k. In other words, this is only an approximation that enables the linearization; it is not an assumption that the voltage magnitude equals 1.0 p.u.

Differences in bus voltage angles usually are very small and equations (2.6) and (2.7) can be further approximated by applying the cosine and sine rules. When δ is very small, $\cos(\delta) \approx 1$ and $\sin(\delta) \approx \delta$. Therefore,

$$P_k \approx \sum_{m \in k} \left(V_m G_{km} + V_m B_{km} \delta_{km} \right) \tag{2.8}$$

$$Q_k \approx \sum_{m \in k} \left(V_m G_{km} \delta_{km} - V_m B_{km} \right). \tag{2.9}$$

With further manipulation, the above equations can be rewritten as shown in equation

(2.10).

$$\begin{bmatrix} P_K \\ Q_K \end{bmatrix} = \begin{bmatrix} -B' & G \\ -G' & -B \end{bmatrix} \begin{bmatrix} \delta_K \\ V_K \end{bmatrix} \tag{2.10}$$

where B and G are the susceptance and conductance sub matrices of the Y_{bus} and B' and G' are the susceptance and conductance sub matrices of the Y_{bus} without including the susceptances and conductances of the lines. The diagonal elements of B' and G' can be expressed as,

$$B'_{kk} = B_{kk} - b_{kk}$$

$$G'_{kk} = G_{kk} - g_{kk}$$

where b_{kk} is the sum of susceptances of the shunt elements that are connected at bus k and g_{kk} is the sum of conductances of the shunt elements that are connected at bus k.

This model has been applied on several known systems and the results show its validity and it closely approximates the full AC power flow model. For further details about this model, the readers are suggested to refer to [1].

The developed linearized power flow model does not include the losses in the transmission lines. In large power systems with thousands of buses, real power losses can be substantial which is not advisable to be neglected.

If we keep the term of $-\frac{\delta_{km}^2}{2}$ of the Tylor expansion of the cosine function, while neglecting other higher order terms, then we obtain,

$$P_k \approx \sum_{m \in \Omega_k} (V_m G_{km} + B_{km}\delta_{km}) - \frac{1}{2} \sum_{m \in \Omega_k} G_{km}\delta_{km}^2 \tag{2.11}$$

Note that the first part of (2.11) describes the real power flow that other buses receive

from bus k, while the second part indicates the real power loss in the power transition. Let us define,

$$P_{loss}^k = -\frac{1}{2} \sum_{m \in \Omega_k} G_{km} \delta_{km}^2 \tag{2.12}$$

Similarly, the reactive power losses can be expressed as,

$$Q_{loss}^k = \frac{1}{2} \sum_{m \in \Omega_k} B_{km} \delta_{km}^2 \tag{2.13}$$

Equations (2.12) and (2.13) explicitly indicate active and reactive power losses are quadratic forms of δ_{km}. G_{km}, the real part of Y_{km}, is always non-positive, hence P_{loss}^k is a non-negative number. Ref. [2–4] described a piecewise method to linearize transmission line losses.

Note that (2.12) and (2.13) only include the losses produced by the series impedances of transmission lines. Losses produced from the shunt part of the transmission lines have already been considered in the original formulation expressed by (2.10).

2.3 Optimization Problem for Minimum Load Curtailment

In composite system reliability studies, power flow analyses are usually carried out in solving optimization problems of minimum load curtailment. Optimization with minimum load curtailment has been extensively used in calculating the reliability indices of composite power systems. If, under any scenario, the curtailment is unavoidable, the optimization problem tries to minimize the amount of load to be shed.

2.3.1 Network Modeling using Nonlinear Programming and the AC Power Flow Model

This section describes the formulation and incorporation of the objective function of minimum load curtailment in the nonlinear programming problem with the AC power flow model. This objective function is subjected to equality and inequality constraints of the power system operating limits. The equality constraints include the power balance at each bus and the inequality constraints are the capacity limits of generating units, power carrying capabilities of transmission lines, voltage limits at the nodes and reactive power capability limits. The minimization problem is formulated as follows [5],

$$\text{Loss of Load} = \min \left(\sum_{i=1}^{N_b} C_i \right) \tag{2.14}$$

Subject to

$$P(V, \delta) - P_D + C = 0$$

$$Q(V, \delta) - Q_D = 0$$

$$P_G^{min} \leq P(V, \delta) \leq P_G^{max}$$

$$Q_G^{min} \leq Q(V, \delta) \leq Q_G^{max} \tag{2.15}$$

$$V^{min} \leq V \leq V^{max}$$

$$S(V, \delta) \leq S^{max}$$

$$0 \leq C \leq P_D$$

$$\delta \ \text{unrestricted.}$$

In (2.14) and (2.15), C_i is the load curtailment at bus i, C is the vector of load curtailments ($N_d \times 1$), V is the vector of bus voltage magnitudes ($N_b \times 1$), δ is the vector of

bus voltage angles $(N_b \times 1)$, P_D and Q_D are the vectors of real and reactive power loads $(N_d \times 1)$, P_G^{min}, P_G^{max}, Q_G^{min} and Q_G^{max} are the vectors of real and reactive power limits of the generators $(N_g \times 1)$, V^{max} and V^{min} are the vectors of maximum and minimum allowed voltage magnitudes $(N_b \times 1)$, $S(V, \delta)$ is the vector of power flows in the lines $(N_t \times 1)$, S^{max} is the vector of power rating limits of the transmission lines $(N_t \times 1)$ and $P(V, \delta)$ and $Q(V, \delta)$ are the vectors of real and reactive power injections $(N_b \times 1)$. Also, N_b is the number of buses, N_d is the number of load buses, N_t is the number of transmission lines and N_g is the number of generators.

In the standard minimization problem given by (2.14) and (2.15), all generation and network constraints have been taken into consideration. Also, it has been assumed that one of the bus angles is zero in the constraints (2.15) to work as a reference bus.

2.3.2 Network Modeling using Linear Programming and the DC Power Flow Model

The DC power flow model has been widely utilized in reliability assessment of power systems due to its simplicity of formulation and implementation [6–8,10–17]. Moreover, the DC power flow model has the advantage of being suitable for studies that require extensive computational burden such as composite system reliability and security assessment. Using DC power flow, there are three main constraints which are power balance equation, generation capacity limits and transmission lines power carrying capabilities. The linear programming model of the network with DC power flow is given in equation (2.16) which is adapted from [7],

$$\text{Loss of Load} = \min \left(\sum_{i=1}^{N_b} C_i \right) \tag{2.16}$$

subject to

$$
\begin{aligned}
\widehat{B}\delta + G + C &= D \\
G &\leq G^{max} \\
C &\leq D \\
b\widehat{A}\delta &\leq F_f^{max} \\
-b\widehat{A}\delta &\leq F_r^{max} \\
G, C &\geq 0 \\
\delta &\quad \text{unrestricted}
\end{aligned}
\tag{2.17}
$$

where N_b is number of buses, N_t is number of transmission lines, $\widehat{B}$ is the augmented node susceptance matrix $(N_b \times N_b)$, b is the transmission line susceptance matrix $(N_t \times N_t)$, $\widehat{A}$ is the element-node incidence matrix $(N_t \times N_b)$, δ is the vector of node voltage angles $(N_b \times 1)$, C is the vector of bus load curtailments $(N_b \times 1)$, D is the vector of bus demand $(N_b \times 1)$, G^{max} is the vector of maximum available generation $(N_b \times 1)$, F_f^{max} is the vector of forward flow capacities of lines $(N_t \times 1)$, F_r^{max} is the vector of reverse flow capacities of lines $(N_t \times 1)$, and G is the solution vector of the generation at buses $(N_b \times 1)$.

In the standard minimization problem given by (2.16) and (2.17), all generation and network constraints have been taken into consideration. Moreover, it has been assumed that one of the bus angles is zero in the constraints (2.17) to work as a reference bus.

2.3.3 Network Modeling using Linear Programming and the Linearized Power Flow Model

In this section, the linear programming optimization problem is incorporated with the linearized power flow to minimize load curtailments. Using the linearized power flow model, in addition to the power balance equation, generation capacity limits and transmission lines power carrying capabilities, more constraints can be added. These constraints are voltage allowable limits and generation reactive power limits. This section provides explanations for the incorporation of theses constraints to the optimization problem.

2.3.3.1 Power Balance Constraints

Power balance equation is an equality equation represents the sum of the complex power at a bus. The balance equation can be derived from equation (2.10) as follows:

$$B'\delta - GV + P_G = P_D$$
$$G'\delta + BV + Q_G = Q_D$$
(2.18)

where δ is the vector of bus voltage angles, V is the vector of bus voltage magnitudes, P_G and Q_G are the vectors of the real and reactive power of the generators respectively and P_D and Q_D are the vectors of the real and reactive power of the bus loads respectively.

Since the problem is to minimize the curtailment, equation (2.18) is augmented by fictitious generators that are equivalent to the required curtailment. Therefore, equation (2.18)

becomes,

$$B' \delta - GV + P_G + P_C = P_D$$

$$G' \delta + BV + Q_G + Q_C = Q_D$$

(2.19)

where P_C and Q_C are the vectors of the real and reactive power of the load curtailments respectively.

2.3.3.2 Real and Reactive Power Constraints of the Generators

Real power limits of the generators are bounded by maximum available capacity and minimum power where the latter is considered zero. Reactive power limits are the maximum reactive power provided by a generator and the minimum reactive power assigned for each generator. Therefore, the constraints of real and reactive power of the generators can be expressed as,

$$0 \leq P_G \leq P_G^{max}$$

$$Q_G^{min} \leq Q_G \leq Q_G^{max}$$

(2.20)

where P_G^{max} is the maximum available capacity for each generator, Q_G^{min} is minimum reactive power can be absorbed by a generator and Q_G^{max} is the maximum reactive power can be produced by a generator.

2.3.3.3 Voltage Limits Constraints

Voltage constraints are limited according to the allowed voltage fluctuations. The maximum voltage limit, V^{max}, and the minimum voltage limit, V^{min}, which are assumed throughout this work as 1.05 p.u. and 0.95 p.u. respectively, are expressed as follows,

$$V^{min} \leq V \leq V^{max}.$$

(2.21)

2.3.3.4 Line Current Limit

The current flowing through a line connecting buses k and m can be calculated from the voltage difference and branch impedance as follows,

$$\widehat{I}_{km} = \frac{\widehat{V}_k - \widehat{V}_m}{\widehat{Z}_{km}} \tag{2.22}$$

Equation (2.22) can be manipulated to produce a linearized expression for the line current. This approximation is based on the assumption that the differences between bus voltage angles are very small such that $\cos \delta_{km} \approx 1$ and $\sin \delta_{km} \approx \delta_{km}$ and line resistances is much smaller than line reactances, i.e., $R_{ik} \ll X_{ik}$. Therefore,

$$|I_{km}| \approx \sqrt{(\delta_k - \delta_m)^2 + (V_k - V_m)^2} / |Z_{km}|$$

$$\tag{2.23}$$

$$= \sqrt{\left(I_{km}^p\right)^2 + \left(I_{km}^q\right)^2}$$

where

$$I_{km}^p = \frac{(\delta_k - \delta_m)}{|Z_{km}|}$$

$$I_{km}^q = \frac{(V_k - V_m)}{|Z_{km}|}$$

where I_{km}^p and I_{km}^q are the real and imaginary components of the line current respectively. Therefore, the line current can be expressed by two linear components but the magnitude of these two components is non-linear.

With a constant maximum line current, the locus of the real and imaginary components forms a circle as shown in Figure 2.1. To linearize the current, the ratio of the reactive power to the real power flowing through a line needs to be known in advance which is not possible in
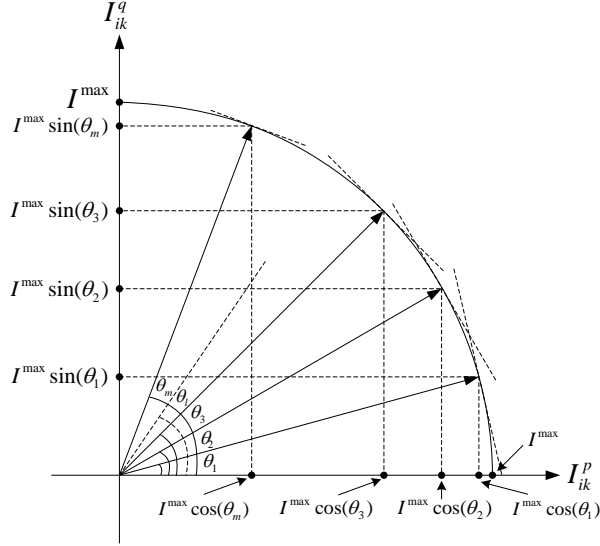
Figure 2.1: Line Current Linearization

solving linear programming problem. However, this ratio also can be linearly approximated around the operating point. This can be done by running unconstrained linear programming problem for several load scenarios to evaluate the average and standard deviation of these ratios. From the average and standard deviation of these ratios, the two components of the line current can be approximated by n linear segments according to the required accuracy. Therefore, the curve around the average ratio can be linearized as mentioned above. The angle θ_l in Figure 2.1 is the tangent inverse of the ratio that corresponds to segment l.

From the analysis of Figure 2.1 the linear equations of the linear segments can be expressed as,

$$I_{kml}^p \ cos \ \theta_l + I_{kml}^q \ sin \ \theta_l - I_{km}^{max} = 0 \tag{2.24}$$

where $l = 1, 2, ..., n$

Therefore, by choosing the number of linear segments, n, the current limit constraints will be increased with order of n times. The current limit constraints in the linear programming

20

problem can be expressed as:

$$bA'\delta + bA'V \leq I_f^{max}$$

$$-bA'\delta - bA'V \leq I_r^{max}$$

(2.25)

where b is a diagonal matrix of the transmission line admittances ($N_t \times N_t$), A is the element-node incidence matrix ($N_t \times N_a$) and

$$bA' = bA \cos \theta_l$$

$$bA' = bA \sin \theta_l$$

As mentioned above, as the number of linear segments increases, the number of line constraints increases accordingly which it may slow down the computation speed. However, in most practical power systems it is not economical to transmit reactive power through transmission lines; therefore, the ratio of reactive power flowing in a line to the real power is usually small. Hence, linear segments can be limited to one or two segments around the maximum real power limits.

2.3.3.5 Linear Programming Formulation

The Linear Programming is used here to minimize load curtailments similar to the formulation of the DC power flow model [7] with incorporating voltage and reactive power constraints. From the above constraints, the minimization problem can be formulated as,

$$\text{Loss of Load} = \min \left(\sum_{i=1}^{Na} C_i \right)$$

(2.26)

Subject to:

$$B^{'}\delta - GV + P_G + P_C = P_D$$

$$G^{'}\delta + BV + Q_G + Q_C = Q_D$$

$$0 \le P_G \le P_G^{max}$$

$$Q_G^{min} \le Q_G \le Q_G^{max}$$

$$0 \le P_C \le P_D \qquad (2.27)$$

$$0 \le Q_C \le Q_D$$

$$V^{min} \le V \le V^{max}$$

$$bA'\delta + bA'V \le I_f^{max}$$

$$-bA'\delta - bA'V \le I_r^{max}$$

$$\delta \quad \text{unrestricted}$$

where N_a is number of buses, N_t is number of transmission lines, $B^{'}$, B, $G^{'}$ and G are as given in section II with dimensions of $(N_a \times N_a)$, δ is the vector of node voltage angles $(N_a \times 1)$, V is the vector of bus voltage magnitudes $(N_a \times 1)$, P_G is the vector of real power generation $(N_a \times 1)$, Q_G is the vector of reactive power generation $(N_a \times 1)$, P_C is the vector of real load curtailments $(N_a \times 1)$, Q_C is the vector of reactive load curtailments $(N_a \times 1)$, P_D is the vector of bus real loads $(N_a \times 1)$, Q_D is the vector of bus reactive loads $(N_a \times 1)$, P_G^{max} is the vector of maximum available real power generation $(N_a \times 1)$, Q_G^{max} is the vector of maximum available reactive power generation $(N_a \times 1)$, Q_G^{min} is the vector of minimum available reactive power generation $(N_a \times 1)$, V^{max} is the vector of maximum allowable voltages $(N_a \times 1)$, V^{min} is the vector of minimum allowable voltages $(N_a \times 1)$,

22

F_{f-real}^{max} is the vector of real forward flow capacities of lines ($N_t \times 1$), $F_{f-imaginary}^{max}$ is the vector of imaginary forward flow capacities of lines ($N_t \times 1$), F_{r-real}^{max} is the vector of real reverse flow capacities of lines ($N_t \times 1$) and $F_{r-imaginary}^{max}$ is the vector of imaginary reverse flow capacities of lines ($N_t \times 1$).

In (2.26) and (2.27) all generation availability and network constrains have been taken into considerations. Also, in order to get a feasible solution for the standard problem, it has been assumed that one of the bus angles is zero in the constraints of equation (2.26).

Formulation of the optimization problem in this manner may produce a solution with different curtailments for the active and reactive powers. In other words, if a load is assumed to be curtailed in case of insufficient real power generation, this formulation may shed the real part of the load and leaves the reactive part. To insure that the curtailment solves for real and reactive powers, an additional constraint has to be added. This constraint can be expressed as,

$$P_C - (P_D/Q_D)\, Q_C = 0 \tag{2.28}$$

The factor (P_D/Q_D) is the ratio between the real load to the reactive load at each bus. Therefore, this constraint will insure that both the active and reactive power will be curtailed if there is no enough real power as well as if there is no enough reactive power.

2.3.4 Other Constraints

Other constraints can be incorporated into the optimization problem such as emission constraints, transient stability constraints, etc. In this thesis, the emission caps and limits have been included in performing sensitivity analysis for the reliability indices.

The emission constraints are used in this work to determine the point at which the

action of buying or selling the emission allowances can be decided. Also, the shadow prices of emission constraints at each power plant are used in estimating the sensitivity of the objective function with respect to the emission limits. The emission constraints are derived as follows,

$$ECO_{2j} \leq ECO_{2j}^{max} \quad \forall j. \tag{2.29}$$

In (2.29), ECO_{2j} is the total emission of CO_2 in tonne/t at the power plant j and ECO_{2j}^{max} is the cap on the CO_2 emission at the power plant j. More details about the incorporation of the emission constraints are given in chapter 7.

Chapter 3

Power System Reliability Indices and Sensitivity Analysis

3.1   Introduction

Due to the ongoing changes in generation portfolios and environmental concerns several reliability indices for composite systems have been introduced. Even though these indices are of a great importance in both planning and operational power system reliability evaluation, they lack the ability of identifying the influence of each area or equipment on the system reliability. Moreover, these indices do not give a full picture of the most-effective way to revamp the system in order to keep it reliable. Due to these reasons, significant efforts have been devoted to this area in recent years to evaluate what the system's reliability justifications are and where the best location to invest is. This chapter provides explanations for the reliability indices and the developments of the sensitivity of these indices with respect to the component parameters.

3.2   Calculation of the Reliability Indices

In this work, we have evaluated the well know composite power system reliability indices, namely loss of load probability (LOLP), expected demand not supplied (EDNS), loss of

energy expectation (LOEE), loss of load expectation (LOLE), loss of load frequency (LOLF) and expected duration of load curtailment (EDLC).

3.2.1   Calculation of System Probability Indices

Failure probability indices evaluate the probability of failure of the system to meet the demand. Another index was introduced which is the probability of load availability. This index represents the probability of the system to succeed to meet the demand. Through the search process, if the state under consideration is a failure state, the probability of this state is added to the failure probability index, q; otherwise, the probability of this state is added to the success probability index, p. The failure probability index and the success probability index are bounded between 0 and 1.0. If the algorithm were to visit the entire state space, the sum of q and p would equal to 1.0. In other words, q and $1 - p$ would reach each other and would evaluate the same index, loss of load probability.

The probability of system failure to meet the demand is given by

$$q = \sum_{i=1}^{n_f} P\left\{x_i : x_i \in X_f\right\} \tag{3.1}$$

where X is the set of all states, X_f is the set of failure states $(X_f \subset X)$ and n_f is the number of failure states.

The probability of system success to meet the demand is given by

$$p = \sum_{i=1}^{n_s} P\left\{x_i : x_i \in X_s\right\} \tag{3.2}$$

where X_s is the set of success states $(X_s \subset X)$ and n_s is the number of success states.

26

The estimated q, $(\hat{q})$, index can be calculated based on the complementary concept (the complementary concept is introduced in chapter 4) as follows,

$$\hat{q} = \frac{q}{q+p} \tag{3.3}$$

The estimated loss of load expectation can be calculated in the same manner. Let L_q denote loss of load expectation index. The estimated L_q, $(\hat{L}_q)$, index can be calculated directly from the $\hat{q}$ index as follows,

$$\hat{L}_q = \frac{q}{q+p} \times T \tag{3.4}$$

where T is the period of study in hours.

3.2.2 Calculation of System Energy Indices

The well-known reliability energy indices are expected demand not supplied and expected energy not supplied. Let d_n denote the expected demand not supplied index and e_n denote the expected energy not supplied index. In this work, another index was introduced which is expected demand supplied and denoted as d_s. This index estimates the amount of power supplied to system loads. For every tested state, if the state is a success state, the product of the probability of this state and the peak load is added to the d_s index. On the other hand, if the state is a failure state, the product of the probability of this state and the amount of load curtailment is added to the d_n index and the product of the probability of this state and the amount of supplied load (the supplied load is the peak load minus the curtailed load) is added to the d_s index. The expected demand not supplied and the expected demand

27

supplied indices are bounded between 0 and the peak load. If the algorithm were to visit the entire state space, the sum of d_n and d_s would equal to the peak load. In other words, d_n and (Peak Load $- d_s$) would reach each other and would evaluate the same index, expected demand not supplied.

The expected demand not supplied is given by,

$$d_n = \sum_{i=1}^{n_f} P\left\{x_i : x_i \in X_f\right\} \times Lc\left\{x_i : x_i \in X_f\right\} \tag{3.5}$$

where Lc is amount of load curtailment of state x_i.

The expected demand supplied is given by,

$$d_s = \sum_{i=1}^{n_f} P\left\{x_i : x_i \in X_f\right\} \times Ls\left\{x_i : x_i \in X\right\} \tag{3.6}$$

where Ls is amount of load supplied of state x_i and can be expressed as,

$$Ls\left\{x_i : x_i \in X\right\} = \begin{cases} \text{Peak Load}, & x_i \in X_s \\ \text{Peak Load} - \text{Lc}, & x_i \in X_f \end{cases} \tag{3.7}$$

The estimated value of d_n, $(\hat{d}_n)$, index can be evaluated as follows,

$$\hat{d}_n = \frac{d_n}{d_n + d_s} \times \text{Peak Load} \tag{3.8}$$

The e_n index can be calculated from the estimated d_n index. The estimated value of e_n,

$(\hat{e}_n)$, can be calculated as follows,

$$\hat{e}_n = \frac{d_n}{d_n + d_s} \times \text{Peak Load} \times T. \tag{3.9}$$

3.2.3 Calculation of System Frequency and Duration Indices

Calculation of frequency and duration indices is generally more difficult than calculation of probability and energy indices. As it has been mentioned, the probability indices are bounded between 0 and 1 and energy indices are bounded between 0 and the peak load. On the other hand, frequency and duration indices do not have this property. However, as a result of the frequency balance property, $\left(F_f = F_s \right)$, failure frequency can be calculated either from the success states that have downward transitions crossing the boundary between the success and failure states, F_s, or from the failure states that have upward transitions crossing the boundary between the success and failure states, F_f. If the algorithm were to visit the entire state space, these two frequencies would converge to the same value. Since the search method is not intended to visit the entire state space (as shown in chapter 4) and the frequency is related to the probabilities of the states, frequency of failure index can be estimated by taking the average of these frequencies, $\left(F_s \text{ and } F_f \right)$, over the visited subspace. If we denote the frequency of the failure index as F, then the estimated value of F, $(\hat{F})$, can be expressed as follows,

$$\hat{F} = \frac{F_f + F_s}{2\left(q + p \right)} \tag{3.10}$$

After estimating the probability of failure index, $\hat{q}$, and the frequency of failure index,

$\hat{F}$, it is trivial to estimate the expected duration of load curtailment, $\hat{T}_c$, index as follows,

$$\hat{T}_c = \frac{\hat{q}}{\hat{F}} = \frac{2\,q}{F_f + F_s} \tag{3.11}$$

The approach used in this work to calculate frequency and duration indices was adapted from [8, 18, 19]. The work presented in [8, 18] was based on concepts described in details in [20, 21]. We will not reproduce the rigorous derivation here; rather, the expressions will be presented for convenience.

Every failure state comprises of functional components and failed components. Failure states can transit to higher states by upward transitions, and the resulted states can be success or failure states. These transitions are said to be crossed the boundary between the success and failure states if the failure states transit to success states. Also, the same procedure can be applied on the success states that transit downwards to failure states. The frequency of encountering success states (or failure states) is the sum of the individual frequencies associated with those transitions of the failure states (or success states) which cross the boundary.

The sum of the frequencies of the upward transitions from the failed states can be expressed as,

$$F^{(+)} = \sum_{i=1}^{n_f} \left(P\left\{x_i : x_i \in X_f\right\} \sum_{j \in F_i} \mu_j \right) \tag{3.12}$$

where F_i is the set of failed components in state i, and μ_j is the repair rate of component j.

The sum of the frequencies of the downward transitions from the failed states can be expressed as,

$$F^{(-)} = \sum_{i=1}^{n_f} \left(P\left\{x_i : x_i \in X_f\right\} \sum_{k \in S_i} \lambda_k \right) \tag{3.13}$$

30

where S_i is the set of functional components in state i, and λ_k is the failure rate of component k.

Some of $F^{(+)}$ transitions will cross the boundary and the others will not. Also, by the assumption that the system is coherent, none of $F^{(-)}$ will cross the boundary. As a result of frequency balance property, all those transitions included in $F^{(+)}$ which do not cross the boundary are balanced by corresponding transitions included in $F^{(-)}$. Consequently, the frequency of system success can be calculated as,

$$F_s = F^{(+)} - F^{(-)} \tag{3.14}$$

In the steady state, the frequency of system success and frequency of system failure will balance, that is $F_f = F_s$. Therefore, the frequency of system failure can be calculated from failure states as follows,

$$F_f = \sum_{i=1}^{n_f} \left[P\left\{x_i : x_i \in X_f\right\} \left(\sum_{j \in F_i} \mu_j - \sum_{k \in S_i} \lambda_k \right) \right] \tag{3.15}$$

Following the similar approach, frequency of system failure can be calculated from the success states as follows,

$$F_s = \sum_{i=1}^{n_s} \left[P\left\{x_i : x_i \in X_s\right\} \left(\sum_{k \in S_i} \lambda_k - \sum_{j \in F_i} \mu_j \right) \right] \tag{3.16}$$

where X_s is the set of success states and n_s is the number of success states.

3.2.4 Calculation of Bus Indices

Calculation of bus indices utilizing optimization problems produces multiple solutions and hence bus indices will not be unique [22]. Depending on the manner in which the program scans the vertices of the feasible polytopes, it can favor curtailing power at certain buses depending on how the buses are numbered. In the literature, load priority philosophy technique is usually used to overcome this problem. Such philosophies can be the priority of each load or part of each load. Also, load can be curtailed according to closeness to the fault location. In this method, the loads are divided into several parts with different weighting factors. Each part is assumed to represent a percentage of the total load. However, if the amount of load curtailment at each bus is less than the load priority level, the multi-optimum problem will occur. This bias can be removed by dynamic numbering of the buses, i.e., altering the bus numbers after the occurrence of each event in the simulation.

In this work we have combined both approaches by adapting the load priority philosophy technique and dynamic numbering of the buses. Loads were divided into three parts with different weighting factors for each part, e.g., w_1, w_2 and w_3 respectively. The first two parts were assumed to represent 25% of the total load and the third part was assumed to represent 50% of the total load. The weighting factor of the first part is assumed to be less than that of the second part and the weighting factor of the second part is assumed to be less than that of the third part or in other words, $w_1 < w_2 < w_3$.

3.2.5 Modeling of System Components

There several methods to model system components in power system reliability studies. This section presents the modeling of generators, loads and transmission lines.

3.2.5.1 Modeling of Available Generation

Most buses have several generators which may be similar or different. The unit addition algorithm [23] is used to construct a discrete probability distribution function for each bus which is known as capacity outage probability and frequency table, COPAFT. This table is constructed based on the capacity states and forced outage rates of units at each bus.

3.2.5.2 Modeling of System Load

Loads at the buses is modeled based on the cluster load model technique [23–26]. From the chronological loads, clusters are constructed according to the load level and its probability. These clusters are used for each load bus as a percentage of the peak load of the given bus.

3.2.5.3 Modeling of Transmission Lines

A discrete probability density function is constructed for every transmission line. If a line is tripped for some system state, the line is removed from the bus admittance matrix and its capacity is set to zero.

3.2.6 A Stopping Criterion

A convergence criterion should be applied to stop the algorithm if there is not much change in the reliability indices. In power system reliability analysis using Monte Carlo simulation, it was found to be that energy indices are the slowest indices from convergence view point [22]. In this work, we have applied the stopping criterion on the EDNS index.

The stopping criterion considering the EDNS index can be expressed as,

$$\sigma = \frac{\sqrt{Var(\text{EDNS})}}{E\left[\text{EDNS}\right]} \tag{3.17}$$

where $E\left[.\right]$ is the expectation operator and $Var\left(.\right)$ is the variance function.

After few iterations, the amount of the change in σ is calculated, if this amount is less than or equal to the specified tolerance, the algorithm is to be terminated; otherwise, the simulation will continue. This stopping criterion can be used for both the Monte Carlo simulation method and the population-based intelligent search methods.

3.3   Concept of the Sensitivity Analysis

Lagrange multipliers based method is proposed for performing sensitivity analysis in composite system reliability. Lagrange multipliers are defined as the sensitivity of the value of the objective function to the change in the right hand side of the linear/non-linear programming problem constraints [27–30]. Lagrange multipliers are used in evaluating the sensitivity analysis of the reliability indices with respect to component parameters. The sensitivity of the reliability indices with respect to the component parameters are used as a decision making tool in identifying the system's component or area that has the highest impact on system reliability; and which area or component need to be reinforced to enhance the overall system reliability. Lagrange multipliers can be determined by solving for the dual solution of the optimization problem with an objective function of minimizing buses load curtailments. The proposed method relies on component availability data, generation capacity, transmission line capability and load scenarios. In most of the practical applications reported in the literature, the sensitivity evaluation techniques include approximations in generating capacity model, load model and the evaluation techniques. The proposed method uses Monte Carlo simulation and population-based intelligent search methods that do not necessitate such approximations.

3.4 Sensitivity Analysis of the Reliability Indices

Sensitivity analyses of reliability indices reported in the literature have been based on calculating the amount of change of these indices with respect to component parameters such as availability/unavailability, capacity, failure rate and repair rate. These analyses have been conducted either by examining every single state of the system or by Monte Carlo simulation. The analyses have been performed by casting the dispatch operation as an optimization problem, through minimizing load curtailment or maximizing load supplying capability. The optimization has been constrained by generator and transmission line capacities. The LOLP and LOLF indices from their definitions are based on reliability parameters and cannot be directly related to the operating limits. On the other hand, the EDNS index is based on failure rates, repair rates and unit capacities. In this section, we provide a brief description of the sensitivity analysis of the reliability indices and the detailed derivations are given in the appendix.

3.4.1 Sensitivity Analysis of the LOLP and LOLF Indices with Respect to Component Parameters

Sensitivity studies of LOLP and LOLF to component reliability have been amply described in the literature. Sensitivity analysis can be conducted analytically by enumerating all system states or by simulation. Refs. [16, 31–33] provide relationships that are suitable for use in state space enumeration.

The sensitivity of LOLP with respect to unavailability u_i of component i can be calculated as follows,

$$\partial LOLP/\partial u_i = \sum_{x \in X} I_f(x)P(x)[(1/u_i) - S_i/(a_i u_i)] \tag{3.18}$$

where X is the set of all states, x is the state of the system, $P(x)$ is the probability of occurrence of state x, u_i is the probability of failure of component i and a_i is the probability of success of component i. S_i is the state indicator of component i, i.e., $S_i = 0$ if component i is in the down state (failure state) and $S_i = 1$ if component i is in the up state (success state) and $I_f(x)$ is the system state indicator function which can be expressed as follows,

$$I_f(x) = \begin{cases} 1 & \text{if } x \text{ is failure state} \\ 0 & \text{if } x \text{ is success state} \end{cases} \qquad (3.19)$$

The sensitivity of LOLP with respect to component failure rate λ_i is given by

$$\partial LOLP/\partial \lambda_i = \sum_{x \in X} I_f(x) P(x) [a_i/\lambda_i - S_i/\lambda_i] \qquad (3.20)$$

The sensitivity of LOLP with respect to component repair rate μ_i is given by

$$\partial LOLP/\partial \mu_i = \sum_{x \in X} I_f(x) P(x) [-a_i/\mu_i + S_i/\mu_i] \qquad (3.21)$$

The sensitivity of LOLF with respect to unavailability u_i of component i can be calculated as follows.

$$\partial LOLF/\partial u_i = \sum_{x \in X} \Big[-I_f(x) P(x) S_i \mu_i / a_i^2$$
$$+ F(x) P(x) \left((1/u_i) - S_i/(a_i u_i) \right) \Big] \qquad (3.22)$$

where $F(x)$ is the sum of the repair rates of a failure state x that crosses the boundary and

can be expressed as:

$$F(x) = I_f(x) \sum_{i=1}^{m} \lambda_i^{in}(x)$$

where m is the number of components, and

$$\lambda_i^{in}(x) = (1 - S_i)\,\mu_i - S_i\mu_i u_i/a_i$$

The sensitivity of LOLF with respect to component failure rate λ_i is given by

$$\partial LOLF/\partial \lambda_i = \sum_{x \in X} \big[-I_f(x)P(x)S_i$$

$$+ F(x)P(x)\,(a_i/\lambda_i - S_i/\lambda_i)\big] \tag{3.23}$$

The sensitivity of LOLF with respect to component repair rate μ_i is given by

$$\partial LOLF/\partial \mu_i = \sum_{x \in X} \big[I_f(x)\,(1 - S_k)\,P(x)$$

$$+ F(x)P(x)\,(-a_i/\mu_i + S_i/\mu_i)\big] \tag{3.24}$$

3.4.2 Sensitivity Analysis of the EDNS index with Respect to Component Capacities

The expected demand not supplied (EDNS) is an important index because it inherently reflects the severity of the events. The sensitivities of this index with respect to u_i, λ_i and μ_i are the same as for the LOLP index except that they are multiplied by the amount of load curtailments. The sensitivity analysis of the EDNS with respect component capacities

was derived as follows [16, 32, 33],

$$\partial EDNS/\partial C_i = \sum_{x \in X} I_f(x) P(x) \partial L_c(x) / \partial C_i \tag{3.25}$$

where C_i is the capacity of component i and $L_c(x)$ is the total load curtailment when the system is at state x.

The derivative of the total load curtailment with respect to component capacity can be expressed as

$$\partial L_c(x) / \partial C_i = \begin{cases} \pi_{g,i} & \text{if component } i \text{ is a generator} \\ \pi_{t,i} & \text{if component } i \text{ is a circuit element} \end{cases}$$

where $\pi_{g,i}$ and $\pi_{t,ij}$ are the Lagrange multipliers or shadow prices of generation capacity constraints and transmission lines carrying capability constraints respectively. $\pi_{g,i}$ can be calculated directly from the optimization problem. However, $\pi_{t,ij}$ depends on circuit parameters which are circuit capacity and susceptance. These two parameters are dependent variables and cannot be treated separately. Pereira and Pinto [34], combined the effect of circuit capacity and susceptance on circuit sensitivity and developed the following expression.

$$\pi_{t,ij} = \left(\pi_{d,i} - \pi_{d,j}\right)\left(\theta_j - \theta_i\right) \tag{3.26}$$

where $\pi_{d,i}$ and $\pi_{d,j}$ are Lagrange multipliers or shadow prices of load constraints of buses i and j respectively and θ_j and θ_i are voltage angles of buses j and i respectively.

Chapter 4

State Space Reduction and Population-based Intelligent Search Methods

4.1 Introduction

Composite system reliability evaluation aims at determining the reliability of the given power system taking into consideration both transmission and generation systems. Numerous techniques have been proposed in the literature to assess composite system reliability. In this context, analytical methods [7, 35, 36] and Monte Carlo simulation [37] have been used for composite system reliability evaluation. In evaluating the reliability indices of composite power systems, a power flow or optimal power flow with an objective of minimum load curtailment is usually required to test whether the state under consideration is a failure or success state. Performing optimal power flow for huge number of scenarios can be computationally demanding. Consequently, numerous techniques have been proposed in the literature to reduce the computational burden and the time spent in evaluating the reliability indices of composite systems.

This chapter introduces a heuristic technique, which classifies the search space into fail-

ure, success, and unclassified subspaces, and introduces an algorithm, which is developed based on a directed binary particle swarm optimization search method, to search for failure states in the unclassified subspace. The proposed heuristic technique is developed based on calculating the maximum capacity flow of the transmission lines and the available generation. A key element in using particle swarm optimization to search for failure states in the unclassified subspace lies in selecting the weighting factors associated with the objective function. Appropriate values of these weighting factors should be carefully selected in order to prevent the swarm from being trapped to one corner of the state space. The work presented in this chapter proposes an intelligent particle swarm optimization based search method to adjust these weighting factors in a dynamic fashion. The effectiveness of the proposed method is demonstrated on several test systems which are given in the next chapters. The results show not only that the reliability indices obtained using the proposed method correspond closely with those obtained using Monte Carlo simulation, but also the computational burden can be significantly reduced using the proposed method.

The use of binary particle swarm optimization in power system reliability is found to be an efficient tool in evaluating the reliability indices. However, the task of choosing the weighting factors associated with the objective function tends to be tedious and time consuming as trial and error approaches are often times being used to prevent the particles from being flying in one direction. Consequently, the development of an automated approach to adjust these weighting factors could save some effort in solving the task of reliability evaluation efficiently.

This work proposes a technique to search for failure states in the unclassified subspace, which is developed based on an intelligent bounded and directed binary particle swarm optimization. This technique dynamically adjusts the weighting factors associated with the

40

objective function of the binary particle swarm optimization so that the swarm has always forced to fly on the unclassified subspace. A dynamically directed binary particle swarm optimization search method was developed by the authors in [11] to search for failure states in the *entire* state space. In this work, instead of using the dynamically directed binary particle swarm optimization search method to search for failure states in the *entire* state space, we use this technique to search for failure states in the *unclassified* subspace. Another intelligence factor is added to the binary particle swarm optimization that reverses the direction of the particles to search in the unclassified subspace if the algorithm discovers that some particles have entered the success and/or failure subspaces. The proposed algorithm tracks the behavior of the particles and then adjusts the objective function coefficients correspondingly. The behavior of the swarm can be evaluated by examining the probabilities of the visited states.

4.2 State Space Reduction Technique

Searching for failure states in the entire state space is time consuming; and hence, a reduction technique is required to reduce the computational time. Several methods have been introduced in the power system literature to reduce the search space and the computational effort. Singh and Mitra [6] have introduced the concept of the state space pruning. In [6], an arbitrary set of coherent acceptable subspaces were pruned out from the state space using the concept of partitioning vectors. Then, Monte Carlo simulation was performed for the remaining subspaces. The number of pruned subspaces is system dependent and it is a tradeoff between the required time to prune the acceptable subspaces and the required time to perform Monte Carlo simulation for the rest of the subspace. The application of

the state space pruning to calculate the frequency and duration indices of composite power systems was carried out by Mitra and Singh in [8]. State space partitioning has been introduced in [9]. Some other researchers have developed the concept of state space pruning using population-based intelligent search methods [38–44]. The genetic algorithm and the modified genetic algorithm have been used in [38–40] to prune the state space and Monte Carlo simulation has been then used for the remaining part of the state space. Binary particle swarm optimization technique has been utilized in [42, 44] to prune the state space. Green et al. [43] have applied the artificial immune systems optimization technique in pruning the state space. A comparative study of using population-based intelligent search methods, in particular, genetic algorithms, repulsive binary particle swarm optimization, and binary ant colony optimization has been held in [41]. It is worth to point out here that in the work presented in [38–44], population-based intelligent search methods have been utilized as heuristic techniques and the selection of the acceleration factors was a key element in guaranteeing the best performance of these methods.

In this section, a heuristic technique is introduced to prune the state space; and thereby reduces the computational effort. This heuristic technique is developed based on calculating the line flow capacity limits of the transmission lines. This technique models power system networks based on network configuration, available generation, loading conditions and transmission line availabilities, and power carrying capabilities.

By examining the optimization problems presented in chapter 2, it can be noted that for any sampled state if at least one of the following two conditions is satisfied, we can conclude that this state is a failure state: (1) total generation is less than the total load and (2) sum of the capacity of the lines connected to a bus is less than the loading of that bus as shown in Figure 4.1. Given these conditions, we can construct a heuristic technique that reduces

42

the search space significantly. The procedures can be described as follows,

Bus K

Line i-k   Line k-j

Generator   Load
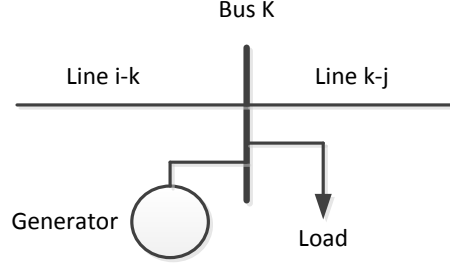
Figure 4.1: A bus connecting two transmission lines. If the total generation at this bus and the sum of line capacities are less than the load, then this state is a failure state

1. Subtract the loads connected to the generation buses from the sampled amount of generation at these buses.

2. Construct a line capacity capability flow matrix (LCM) for the given sampled config-uration. This matrix can be constructed in the same manner as constructing a "Y_{bus}" from the branch-node incidence matrix $(\widehat{A})$ except that instead of using "-1" for the branch that is assumed to enter a node, we use "1". In this case, the incidence matrix is denoted A. Further, instead of using the diagonal susceptance matrix, we use a diagonal capacity matrix (K) so that the diagonal entries of this matrix are the line capacities. The LCM can be expressed as follows,

$$\text{LCM} = A^T \ K \ A \tag{4.1}$$

3. At any bus, if the total generation is larger than the corresponding diagonal element of the LCM, adjust the generation at that bus downward to the corresponding diagonal element.

4. For a state x, if the value of any of the diagonal elements of the LCM is less than the

43

absolute value of the power injection at the corresponding bus or the total generation

is less than the total demand, this state is guaranteed to be a failure state.

After reading system data, system states are sampled. For every sampled state, the above

search space reduction technique is applied. Then, failure states are passed to the optimiza-

tion problem and the reliability indices are updated. These processes are repeated for every

sampled system state.

As an example, consider the hypothetical system shown in Figure 4.2. This system

consists of five buses and 6 transmission lines. Line capacities are shown on the figure and

denoted as C_1, C_2, ... and C_6.

The LCM is shown in (4.2) and (4.3). The diagonal entries of (4.3) represents the sum

of available line capacities at each bus.

$$
\text{LCM} =
\begin{bmatrix}
1 & 1 & 1 & 0 & 0 & 1 \\
1 & 0 & 0 & 0 & 0 & 0 \\
0 & 1 & 0 & 1 & 0 & 0 \\
0 & 0 & 1 & 0 & 1 & 0 \\
0 & 0 & 0 & 1 & 1 & 1
\end{bmatrix}
\begin{bmatrix}
C_1 & 0 & 0 & 0 & 0 & 0 \\
0 & C_2 & 0 & 0 & 0 & 0 \\
0 & 0 & C_3 & 0 & 0 & 0 \\
0 & 0 & 0 & C_4 & 0 & 0 \\
0 & 0 & 0 & 0 & C_5 & 0 \\
0 & 0 & 0 & 0 & 0 & C_6
\end{bmatrix}
\begin{bmatrix}
1 & 1 & 0 & 0 & 0 \\
1 & 0 & 1 & 0 & 0 \\
1 & 0 & 0 & 1 & 0 \\
0 & 0 & 1 & 0 & 1 \\
0 & 0 & 0 & 1 & 1 \\
1 & 0 & 0 & 0 & 1
\end{bmatrix}
\tag{4.2}
$$

$$
\text{LCM} =
\begin{bmatrix}
C_1 + C_2 + C_3 & 0 & 0 & 0 & 0 \\
0 & C_1 + C_6 & 0 & 0 & 0 \\
0 & 0 & C_2 + C_4 & 0 & 0 \\
0 & 0 & 0 & C_3 + C_5 & 0 \\
0 & 0 & 0 & 0 & C_4 + C_5 + C_6
\end{bmatrix}
\tag{4.3}
$$
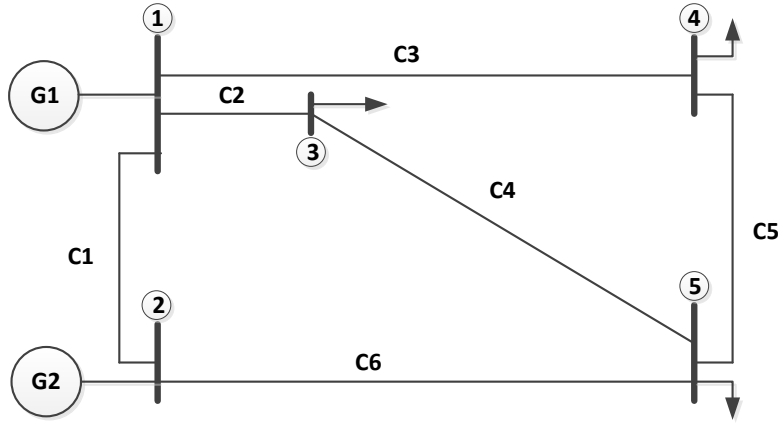
Figure 4.2: A hypothetical system to demonstrate the application of the state space reduction technique

This heuristic technique was first developed by the authors in [10]. The heuristic technique is different from the pruning techniques, which are already presented in the literature, in the sense that it classifies the state space into success, failure, and unclassified subspaces. The method developed in [10] has given satisfactory results in evaluating energy indices due to the fact that it sums up the probabilities of the visited states, and not the estimated values of the indices. In section 4.5, we introduce a new method, which is developed based on the complementary concept, to estimate the energy indices with less computational effort.

4.3 Power System Reliability Evaluation using Binary Particle Swarm Optimization Search Method

Population-based intelligent search methods have been amply used in power system studies [45–47]. Genetic algorithm and bacterial foraging have been applied in power system reliability evaluation in [48, 49]. Applications of binary particle swarm optimization in

power system studies have reviewed in [50]. Binary particle swarm optimization has been used as a searching tool for success or failure states in power system reliability evaluation in [14, 38–43, 51–55]. Binary particle swarm optimization has been used in the reliability evaluation of distribution systems and microgrids in [56–59]. The objective function of the binary particle swarm optimization can be single objective or multi-objective. The two objective functions were intended to prevent the particles from being trapped to one corner of the state space. The weighting factors associated with the objective functions have been carefully selected in order to keep the particles to search in the entire state space [12, 13]. Even with two objective functions, if the weighting factors are not carefully chosen, the particles might be trapped to one corner of the search space. To circumvent this difficulty, an effective approach that adjusts these weighting factors and using an appropriate fitness function are presented in this work.

4.4   Non-Sequential Monte Carlo Simulation vs. Binary Particle Swarm Optimization Search Method

One of the differences between using binary particle swarm optimization in power system reliability evaluation and non-sequential Monte Carlo simulation is that binary particle swarm optimization sums up the values of the reliability indices of the visited states, whereas in non-sequential Monte Carlo simulation, the reliability indices are evaluated by dividing the number of encountered failure states to the number of samples. It is well known that non-sequential Monte Carlo simulation takes long time to calculate reliability indices for the designated accuracy; however, it is obvious that by using non-sequential Monte Carlo simulation, no need to visit all system states since it calculates the estimated values not the

exact values. Therefore, through the sampling process, Monte Carlo simulation reaches the designated index from both sides, under estimation and over estimation. On the other hand, intelligent search methods such as binary particle swarm optimization accumulate the values of the designated indices as the search progresses. Therefore, all failure states or success states need to be visited to calculate reliability indices which are computationally expensive if it is not impossible for large systems. Hence, the values of these indices will be always less than the exact values unless the search method visits all the failure states or all the success states or the entire state space. Therefore, another way to overcome this necessity is required.

New indices have been introduced in [12, 13] which are normalized LOLP, (LOLP_{norm}) and projected LOLP, (LOLP_{proj}) to eliminate the necessity of visiting all the failure and success states. The LOLP_{norm} is the ratio between the sum of the probabilities of the failure states (LOLP) to the sum of probabilities of the states encountered so far (1+LOLP-DLOLP); where DLOLP is the dual value of the LOLP which is one minus the sum of probabilities of the success states encountered so far (1-sum of the probabilities of the visited success states). The LOLP_{proj} is the crossings between the tangents of the LOLP and DLOLP. The normalized LOLP can be expressed as follows,

$$\text{LOLP}_{norm} = \frac{\text{LOLP}}{1 + \text{LOLP} - \text{DLOLP}} \tag{4.4}$$

Again, LOLP_{norm} and LOLP_{proj} are the same as the weighted LOLP index used in Monte Carlo simulation. However, LOLP_{proj} converges to the approximate value of the LOLP faster than LOLP_{norm} [13]. It can be noted that even though binary particle swarm optimization and Monte Carlo simulation both evaluate the weighted index, the number of

states to be visited using binary particle swarm optimization is significantly less than the number of states to be visited using Monte Carlo simulation [13].

The binary particle swarm optimization is used in this work to search intelligently for the most relevant states rather than randomly searching for failure states. Also, we present comparisons between using binary particle swarm optimization and the conventional Monte Carlo simulation.

The assumptions made in [12,13] are only valid for calculating loss of load probability not for the energy, frequency and duration indices. In this work, we have used the complementary concept (section 4.5) to evaluate all the well-known composite systems reliability indices.

4.5   The complementary Concept

The concept of complementary has been applied in several disciplines to calculate/estimate a parameter from its complementary value. The complementary concept in composite power system reliability evaluation can be defined as "every reliability index that can be evaluated from the failure states, has a complementary value that can be evaluated from the success states as long as the boundaries of an index and its complementary value are known such as probability and energy indices or the index can be equally likely determined from the success or failure states such failure frequency indices". For example, the boundaries (minimum and maximum values) of the probability of system failure and the probability of system success are between 0 and 1. Also, the boundaries of expected load curtailment and the expected load supplied are between 0 and the peak load. Frequency indices can be evaluated either from the failure states that transit upwards to success states or from success states that transit downwards to failure states. The complementary concept estimates reliability indices

from visited states; rather than the entire state space.

4.5.1 Theoretical Background

The complementary concept starts with the fact that the sum of the probabilities of the state space is one. Therefore, the sum of the probabilities of the success states and the failure states is also one. The number of states in a state space is 2^n where n is the number of the components. Most power system components (generation and transmission) are highly reliable. Therefore, the state that all system components are in the up state has the highest probability. Not only that, the probability of a state with only one component being in the down state usually less than the probability of the state with all the components are in the up states of order of $1/q_i$ where q_i is the unavailability of component i. This probability order can be generalized for the rest of the states, that is the probability of a state that has two components in the down state (i and j) is less than the probability of a state with all the components are in the up state of order of $1/(q_i q_j)$. Therefore, as the number of the components in the down state increases, the probability of a state decreases with reciprocal of the multiplication of the un-availabilities. Therefore, if an intelligent search method discards the states with very small probabilities and captures the states that have most effect on system reliability, the number of states that need to be evaluated can be decreased significantly.

For example, consider a system with ten identical components with availability of 0.95. The probability of all the components are in the up state is 0.59874 and the probability of one component being in the down state is 0.03151. Therefore, the probability order between the two states is 19. The probability of a state with two components are in the down state is 0.00166. The probability order between this state and the state with all components are

up state is 361. The probability of the state with all components are in the down state is 9.76563×10^{-14}. Therefore, even with ignoring the states that have small probabilities, we can accurately evaluate the behavior of the system.

For this system, if we consider at most one component being in the down state, we need to evaluate 11 states out of 1024 states and the sum of the probabilities of these states is 0.91386. If we consider at most two components are in the down state, we need to evaluate 56 states out of 1024 states and the sum of the probabilities of these states is 0.98850. This behavior is trivial for small systems with identical components; however, for large systems with non-identical components, it is difficult to trace the behavior of the system analytically. Therefore, if we allow some error tolerance, an intelligent search method can capture the states that have most effect on system reliability. Having said that, the reliability of the system can be approximately evaluated based on these states. The indices evaluated from these states, however, will not be equal to the exact indices. Therefore, a method to estimate these indices from the specified states is of necessity. In this work we introduced the concept of complementary to estimate reliability indices.

As the algorithm searches through the state space, the reliability indices and their complementary values become close to each other. For example, the difference between the probability of system failure calculated from the failure states, q, and the probability of system failure calculated from the success states, $(1-p)$, goes gradually to zeros as the search progresses. Since, the search method is not intended to visit the entire state space and the reliability indices can approximately evaluated from the relevant states, the reliability indices can be referred to the relevant subspace. Since the sum of probabilities of the entire state space is 1 and the sum of probabilities of the visited states is $q + p$, then a reliability index

can estimated over the evaluated subspace as follows,

$$\hat{f}_i(x) = f_i(x) \times \frac{1}{q+p} \tag{4.5}$$

where, $f_i(x)$ is the reliability index under consideration and $\hat{f}_i(x)$ is its estimated value.

4.5.2 Mathematical Justification

If we evaluate the entire state space and if we denote the loss of load probability as q and the probability of load availability as p, then the following relationship holds,

$$p + q = 1$$

On the other hand, if we evaluate part of the state space, then $q + p < 1$. In this case the estimated value of q, $(\hat{q})$, and estimated value of p, $(\hat{p})$, will be less than or equal to the exact values, that is $\hat{q} \leq q$ and $\hat{p} \leq p$.

If the search tool were able to visit all the failure states without the need to visit the entire state space, then $\hat{q} = q$ and $\hat{p} < p$. On the other hand, if the search tool were able to visit all the success states without the need to visit the entire state space, then $\hat{q} < q$ and $\hat{p} = p$.

Searching for all the failure states or all the success states is computationally expensive and equivalent to state space enumeration. If the search tool intelligently searches uniformly for both success and failure states and if the algorithm does not evaluate the entire state space, then $\hat{q} < q$ and $\hat{p} < p$.

If the algorithm searches for the states that have the most effect on system reliability, then a high cumulative probability of the state space can be evaluated through a small

51

fraction of the state space. Therefore, q and p can be approximated as,

$$q + p \approx 1$$

Through the search process, the q index represents the sum of the probabilities of the failed states visited so far and p index represents the sum of the probabilities of the success states visited so far. The sum of the probabilities of the states visited so far is $q + p$. Therefore, the estimated value of the probabilities of failure over the visited subspace can be expressed as follows,

$$\hat{q} = \frac{q}{q + p}$$

and the estimated value of the probabilities of the success over the visited subspace can be expressed as follows,

$$\hat{p} = \frac{p}{q + p}$$

Same relations can be applied for the other indices that can be calculated from the failure states as well as from the success states as shown in chapter 3.

4.6 Particle Swarm Optimization

Particle swarm optimization (PSO) is a population-based intelligent search method, which has been proposed by Kennedy and Eberhart in [60]. Later, Kennedy and Eberhart proposed a discrete binary particle swarm optimization to solve combinatorial optimization problems [61]. PSO has been proven to be an effective optimization technique and has, therefore, been used in the presented work. We use the binary PSO to search for success and failure states rather than looking for optimal solution. Further, generation and transmission lines states

are represented as up states or down states so that up states are represented by 1's and down states are represented by 0's. Moreover, we apply bi-objective function that searches through the entire state space for success and failure states. Such objective function is also capable to prevent particles from being trapped to one area of the search space. It is worth noting here that the size of the state space is 2^n, where n is the number of system components. Therefore, even for medium systems, the number of states is very large and it is impractical to test the entire state space. Hence, the concept of the complementary is used in this work so that the condition of searching for all failure states over the entire state space is eliminated.

The binary PSO technique searches through the state space and tests the visited states for a possibility of load curtailment. In performing the search process, for every iteration, particle velocity v_i or the direction of movement of particle i from position x_i can be governed by an objective function (sections 4.6.1 and 4.6.2).

The change in particles positions can be defined by a sigmoid limiting transformation function and a uniformly distributed random number in [0,1] as following,

$$x_{id} = \begin{cases} 1, & \text{rand}() < S(v_{id}) \\ 0, & \text{otherwise} \end{cases} \qquad (4.6)$$

where, x_{id} is the dth component of particle i and $S(v_{id})$ is the sigmoid function of dth's component of particle i which can be expressed as,

$$S(v_{id}) = \frac{1}{1 + e^{(-v_{id})}} \qquad (4.7)$$
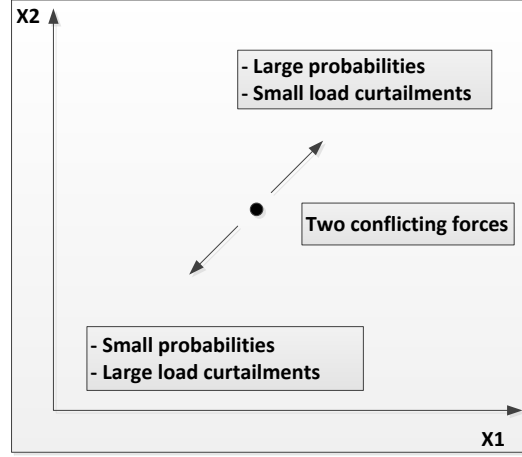
Figure 4.3: State space representation with two conflicting objective functions

The objective function of the BPSO can be single objective (section 4.6.2) or multi-objective (section 4.6.1). In [38–43], single objective function has been used which is minimum load curtailment to search for success states to be pruned from the state space. BPSO with two objective functions has been proposed in [12, 13] to calculate reliability indices. In [12, 13], one objective function has been used to maximize load curtailments and the other has been used to maximize states probabilities. These two conflicting objective functions have been intended to prevent the particles from being trapped to one corner of the state space. The representation of the state space with these two objective functions is depicted in Figure 4.3 where x_1 and x_2 represent the possible states for two system components. State space pruning using BPSO with two objective functions has been introduced in [44]. The BPSO has been used with two objective functions to prune the success states from the state space and then to apply Monte Carlo Simulation on the remaining part of the state space [44]. Even with two objective functions, if the weighting factors are not chosen carefully, the particles might be trapped to one corner of the search space. Therefore, using multi-objective function does not guarantee that the particles will fly on the entire state space unless the right weighting factors are chosen as shown in section 4.7.2.

4.6.1 Multiple Objective Functions

The two objective function can be described as follows [12, 13, 61]:

$$
\begin{aligned}
v_i = v_i \quad &+ \quad rand() \times c_1 \times (Ppbest_i - x_i) \\
&+ \quad rand() \times c_2 \times (Pgbest - x_i) \\
&+ \quad rand() \times c_3 \times (Cpbest_i - x_i) \\
&+ \quad rand() \times c_4 \times (Cgbest - x_i)
\end{aligned}
\tag{4.8}
$$

where $rand()$ is a uniformly distributed random number between [0,1], $Ppbest_i$ is the particle best position from the probability of a state prospective particle i has ever encountered, $Pgbest$ is the group of particles best position from the probability of a state prospective the group has ever encountered, $Cpbest_i$ is the particle best position from the load curtailment of a state prospective particle i has ever encountered, $Cgbest$ is the group of particles best position from load curtailment of a state prospective the group has ever encountered and c_1, c_2, c_3 and c_4 are acceleration factors.

4.6.2 Single Objective Function

To circumvent the difficulty of choosing appropriate weighting factors, a fitness function based on the severity of the states should be used. In this work, we propose a fitness function that is based on the risk index for each state which is the product of state probability and amount of load curtailment. This fitness function eliminates the need to use multi-objective function and guides the swarm to search around the states that have most effect on system reliability and prevents the swarm from being trapped to one corner of the search space.

The proposed fitness function can be expressed as follows,

$$\rho(x) = p(x) \times Lc(x) \tag{4.9}$$

where $p(x)$ is the probability of state x and $Lc(x)$ is the amount of load curtailment of state x. The objective function becomes,

$$
\begin{aligned}
v_i = v_i \ &+ \ rand() \times c_1 \times \left(\rho_{pbest-i} - x_i\right) \\
&+ \ rand() \times c_2 \times \left(\rho_{gbest} - x_i\right)
\end{aligned} \tag{4.10}
$$

where $\rho_{pbest-i}$ is the particle best position from the risk of a state prospective particle i has ever encountered and ρ_{gbest} is the group of particles best position from the risk of a state prospective the group has ever encountered.

4.7 Dynamically-directed Binary Particle Swarm Optimization Search Method

In performing the heuristic technique, some failure events may not be captured. In this context, three failure scenarios can exist. In the first scenario, an area of the system is isolated from the generation areas (area with loads only) and the transmission lines connecting the loads of this area are sufficient to carry the loads. In the second scenario, an area of only load buses is connected to the rest of the system through a tie-line that cannot withstand the total load of this area, but the transmission lines can do. In the third scenario, line impedances force the power to flow through some capacity limited lines and the power flow will not converge without load curtailment. These scenarios cannot be detected by considering the

power carrying capabilities of the transmission lines. Therefore, a search tool should be used to capture these events. However, the search space can be bounded by definite failure subspace and definite success subspace, which makes the search method converges to these events with lower computational effort.

4.7.1 State Space Description

Figure 4.4 shows the state space of a three dimension system. The above reduction technique can detect the definite failure subspace, but cannot determine the boundary of the definite success subspace. However, since the reliability indices and their sensitivities are evaluated based on the failure states, analysis of the entire success subspace is not important. If the boundary of the success subspace is known, then an algorithm can be developed to search for failure states outside the success subspace. A large part of the success subspace can be truncated by considering all the transmission lines in the up state and determining the vector of minimum generation that satisfies the load. Any state in the state space that has a generation vector larger than or equal to the minimum generation vector is guaranteed to be a success state. Therefore, the boundary of the success subspace can be used to control the binary particle swarm optimization search method. Also, most of the unclassified failure states lay around the boundary of the definite failure subspace. Therefore, an intelligent search method that is bounded between the boundaries of the success and failure subspaces can efficiently converge to the failure states in the unclassified subspace. In this work, we use a method based on a dynamically directed binary particle swarm optimization to search for these states.
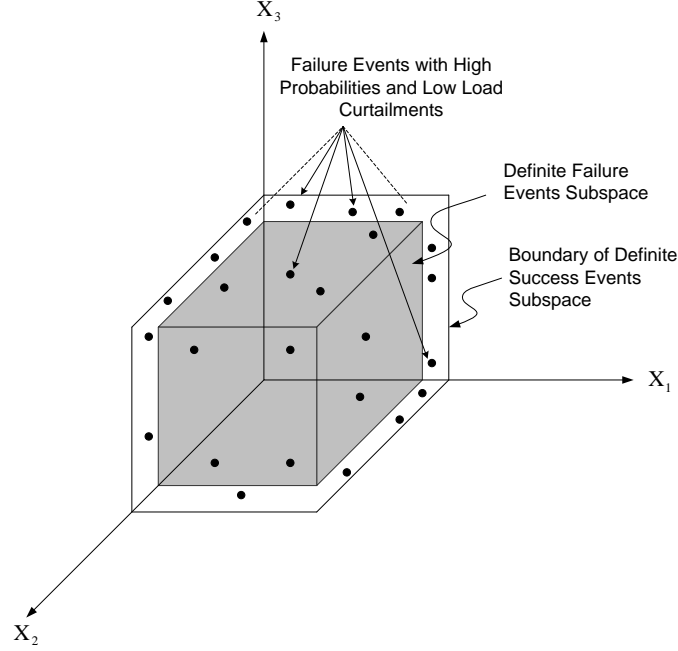
Figure 4.4: State space representation of three dimension system (three components with multiple outcomes)

4.7.2 Directed BPSO

By examining the state space, all possible outcomes of the combination of generation and transmission, the probabilities of the upper part states are larger than the probabilities of the lower part states. Further, load curtailments of the lower part states are larger than load curtailments of the upper part states. If the swarm was to fly on the upper part, it is unlikely to encounter failure states and the opposite is true for the lower part. As mentioned above, using multi-objective function does not guarantee that the particles will fly on the desired search space unless the weighting factors are chosen carefully. Figure 4.5 and Figure 4.6 show two situations for which the weighting factors of the objective function were badly chosen. Figure 4.5-(a) and Figure 4.6-(a), show the behavior of the particles and Figure 4.5-(b), and Figure 4.6-(b) show the expected profile of the reliability indices. In Figure 4.5 the swarm is trapped to the upper corner of the state space. In this case, the normalized

LOLP, (LOLP$_{norm}$) as well as the projected LOLP, (LOLP$_{proj}$), will be under estimated. As the particles continue to fly on the upper corner, most of the visited states will be success states and more likely no failure states will be captured. Therefore, no much change in the LOLP and the 1-DLOLP is sharply increasing. On the other hand, if the swarm is trapped into the lower corner of the state space as shown in Figure 4.6 most of the visited states will be failure states and unlikely to encounter success states. In this case, LOLP, (LOLP$_{norm}$) as well as the projected LOLP, (LOLP$_{proj}$), will be overestimated. The LOLP index will continue to increase whereas the 1-DLOLP index remains almost constant.
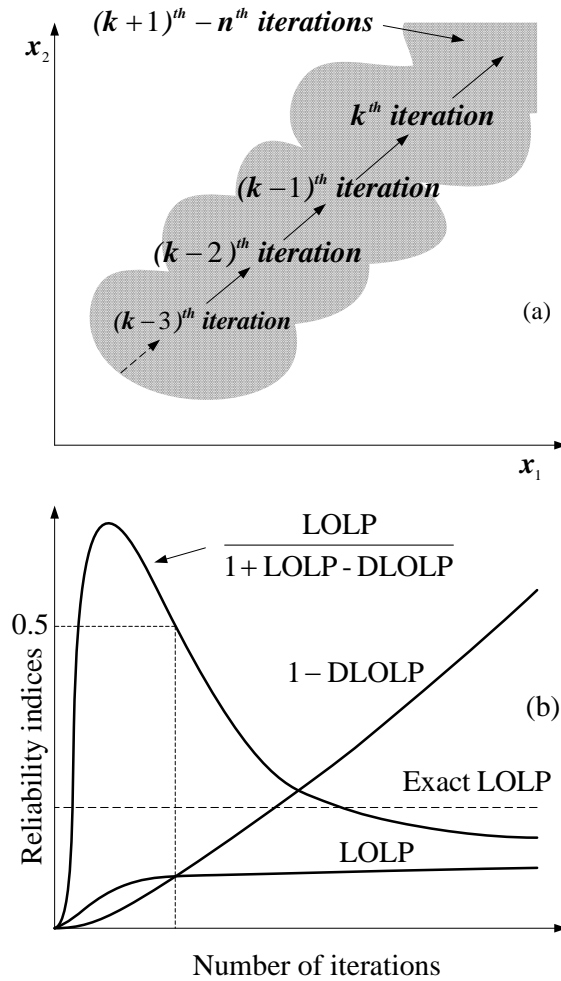
Figure 4.5: Reliability indices profile in case the particles are trapped to the upper corner of the state space

59
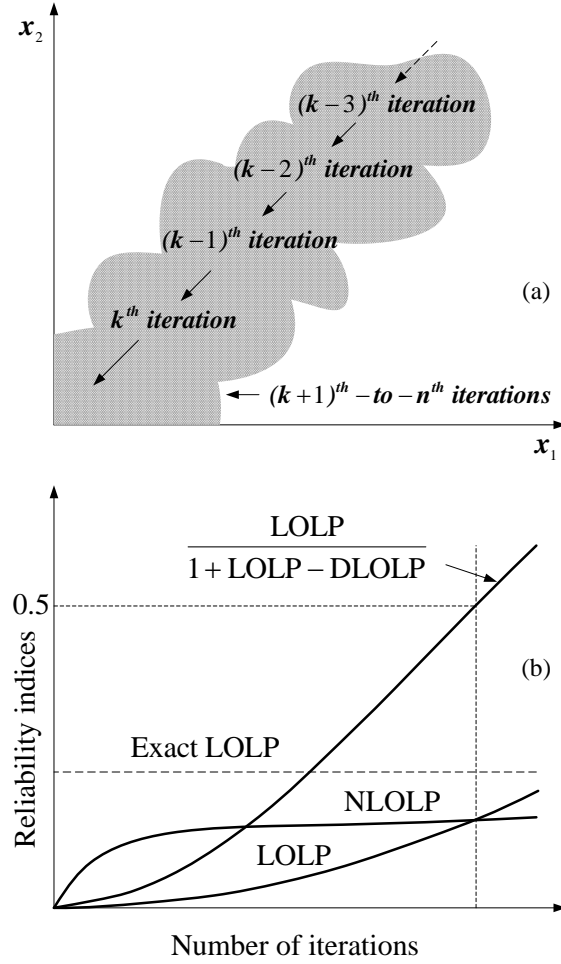
Figure 4.6: Reliability indices profile in case the particles are trapped to the lower corner of the state space

To direct the BPSO to fly on the unclassified subspace and overcome the difficulty of choosing the weighting factors as well as the change in probability limit, we propose a technique that tracks both the normalized LOLP and the number of the new visited states or the mutation rate. This technique was developed based on the normalized loss of load probability index ($LOLP_{norm}$). The $LOLP_{norm}$ has been introduced in [12, 13] to estimate the LOLP index without the need of searching the entire state space. After performing few iterations, if $LOLP_{norm}$ continues to increase that means the particles are trapped in the lower corner of the search space. On the other hand, if $LOLP_{norm}$ continues to decrease,

that means the particles are trapped in the upper corner of the search space. Also, if no new states are visited and the designated reliability index does not converge to the specified accuracy, then V_{max} is limiting the probability of bit change. Also, if the algorithm discovers that the swarm entered the classified success or failure subspaces, the weighting factor are adjusted accordingly as shown in Figure 4.7. The procedures of preventing the particles from being trapped into one area are described in detail in the solution algorithm.
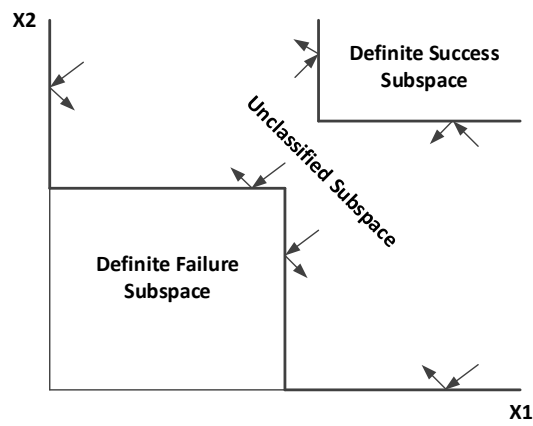
Figure 4.7: Redirecting the swarm in case it enters the success or failure subspaces

Chapter 5

Sensitivity Analysis in Composite System Reliability Using Weighted Shadow Prices

5.1   Introduction

In this chapter, a shadow-price based method is proposed for performing sensitivity analysis in composite system reliability. Shadow prices (or Lagrange multipliers) are used as a decision making tool in identifying the system's component or area that has the highest impact on system reliability; and which area or component need to be reinforced to enhance the overall system reliability. In determining components' shadow prices, power system grids are represented by the DC power flow model (chapter 2) and solving for the dual solution with an objective function of minimizing load curtailments. The proposed method relies on component availability data, generation capacity, transmission line capability and load scenarios. In most of the practical applications, the sensitivity evaluation techniques include approximations in generating capacity model, load model and the evaluation techniques. The proposed method uses a Monte Carlo simulation method that does not necessitate such approximations.

Monte Carlo simulation has been amply used in the literature in evaluating power system reliability. The use of Monte Carlo simulations also serves as a benchmark for testing the validity of the proposed state space reduction technique and the dynamically directed particle swarm optimization search method in evaluating power system reliability. In this chapter, we use Monte Carlo simulation without using any device to reduce the computation time. Therefore, the results of using the proposed techniques will be compared with results reported in this chapter.

5.2 Shadow Price Theory and Description

Shadow price principle was first proposed in 1930s by *Conte Petrovic* as an application of linear programming optimization technique [62]. Shadow price is defined as the sensitivity of the value of the objective function to the change in the right hand side of the linear programming problem constraints [27]. The objective is to minimize load curtailments and the constraints are power system network components' limitations such as generation capacities and transmission lines' carrying capabilities. From generation condition or status, total available power generation can be determined. Also, from transmission line availability and carrying capacity, the constraints can be set. From this solution, shadow prices of the generating units and transmission lines can be calculated.

In general, suppose we have m constraints with n variables, the standard *maximum* linear programming problem can be formulated as follows:

$$max(Z) = \sum_{j=1}^{n} c_j x_j \tag{5.1}$$

Subject to the following constraints,

$$\sum_{j=1}^{n} a_{ij}x_j \leq b_i \tag{5.2}$$

$$x_j \geq 0 \tag{5.3}$$

The matrix of the coefficients of the constraints is,

$$A = \begin{pmatrix} a_{11} & a_{12} & \cdots & a_{1n} \\ a_{21} & a_{22} & \cdots & a_{2n} \\ \vdots & \vdots & \ddots & \vdots \\ a_{m1} & a_{m2} & \cdots & a_{mn} \end{pmatrix} \tag{5.4}$$

The right hand side vector b of the constraints consists of m constants,

$$b = \begin{pmatrix} b_1, & b_2, & \cdots, & b_m \end{pmatrix}^T \tag{5.5}$$

The row vector of the objective function c consists of n coefficients

$$c = \begin{pmatrix} c_1, & c_2, & \cdots, & c_n \end{pmatrix}^T \tag{5.6}$$

The dual of this standard *maximum* problem is the standard *minimum* problem, that is,

$$min(W) = \sum_{i=1}^{m} b_i y_i \tag{5.7}$$

Subject to the following constraints,

$$\sum_{j=1}^{n} a_{ij} y_j \geq c_j \tag{5.8}$$

$$y_i \geq 0 \tag{5.9}$$

If the slack variables of equations (5.2) and (5.3) are imported, the standard linear programming will have the following form,

$$max(Z) = CX \tag{5.10}$$

With the equality constraints,

$$AX = b \tag{5.11}$$

$$X \geq 0 \tag{5.12}$$

The optimal and feasible solution of (5.7) can be expressed as,

$$X_b = B^{-1}b \tag{5.13}$$

where B is the optimal basis at the optimal and feasible solution and X_b is the basic variable sub-vector. In the standard problem of (5.2), the significance of the dual variables y_i is described as the ith shadow price. In other words, the y_i of the dual problem are interpreted here as the shadow prices of the linear constraints b_i.

5.3   Solution Algorithm

This section describes the approach used for calculating shadow prices of various system components. Shadow prices can be calculated for one load scenario as well as for multiple loading scenarios. However, to consider the shadow price as a reliability index, system states are to be sampled till the shadow prices of all system components converge to the pre-specified tolerance.

Since the calculation of shadow prices requires only system state and not the state duration, system state sampling approach is used in determining system states. Components outages are assumed independent events and their behavior is categorized by a uniform distribution $[0, 1]$.

For two state components, if the state of the ith component is denoted by S_i and component unavailability is denoted by q_i, system state vector S will be,

$$S = [S_1, S_2, \cdots, S_i, \cdots, S_{n-1}, S_n]$$

where, n is the number of components in the system.

A uniformly distributed random variable U_i under $[0, 1]$, using improved prime number multiplicative congruential generator method, is drawn for every component such that,

$$S_i = \begin{cases} 1 & (upstate) & if\ U_i \geq q_i \\ 0 & (downstate) & if\ 0 \leq U_i < q_i \end{cases}$$

For three state components such as generating units with derated states, let Pd_i denote

66

the probability of the derated state of the ith generating unit such that,

$$
S_i = \begin{cases}
1 & (up \ state) & if \ U_i \geq (q_i + Pd_i) \\
2 & (derated \ state) & if \ q_i \leq U_i < (q_i + Pd_i) \\
0 & (down \ state) & if \ 0 \leq U_i < q_i
\end{cases}
$$

System load is modeled by multistep model (cluster technique). Probabilities of load steps PL_i are put successively between [0, 1]. By drawing a uniformly distributed random number, the load step can be determined according to the position of the random number of the cluster discrete probability distribution function.

After sampling system states, system bus and line data are modified according to the new state. Using the DC power flow model and linear programming, components shadow prices can be calculated for each state. The procedures are illustrated in Figure 5.1.

5.4   Case Studies

The proposed method is applied on the IEEE RTS [63], the Modified IEEE RTS, and the Saskatchewan Power Corporation in Canada (SPC) and a hypothetical six bus system [64]. System descriptions are given in the appendix. Since IEEE RTS has two 400 MW and one 350 MW units which have high capacity compared to the rest of the system, it is desirable to consider the unit derated states which is given in the modified test system [63]. Accordingly, the proposed method is applied on the base case and the modified IEEE RTS test systems. Also, compared to the generating units, IEEE RTS transmission system is too reliable or over designed [63]. Due to these reasons, two additional case studies were conducted to enforce the transmission lines to become binding constraints instead of being always redundant
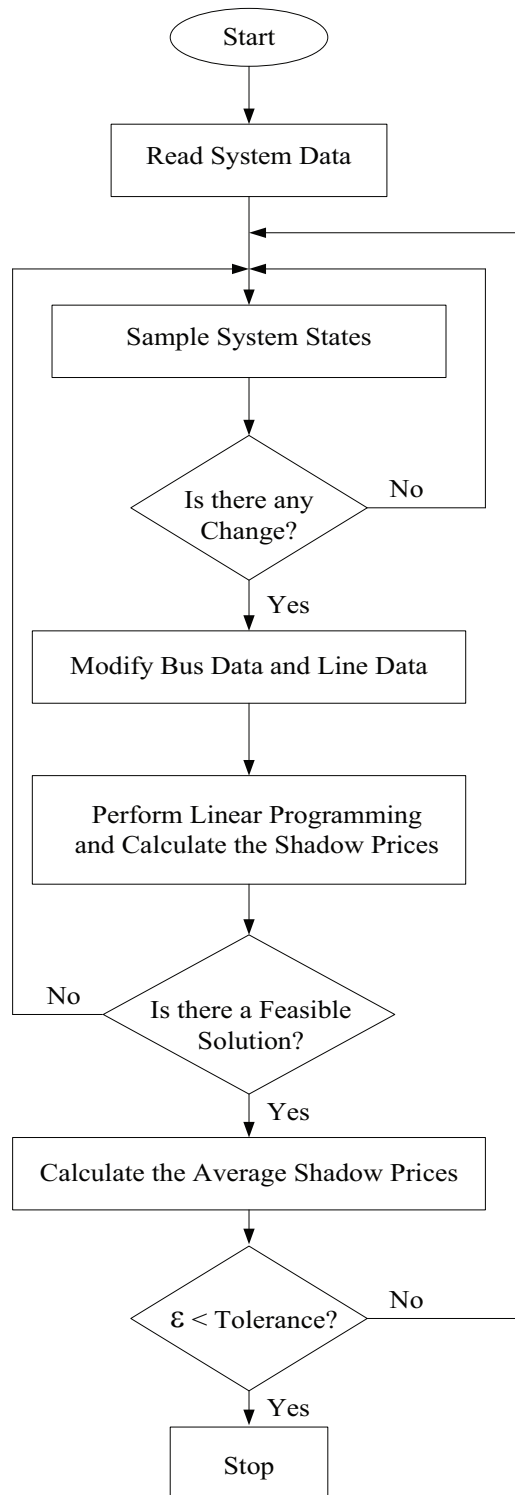
Figure 5.1: Flow chart of the proposed method

constraints. Furthermore, for the purpose of comparison, sensitivity analysis of the IEEE RTS is compared with those given in [32]. Another case study was conducted to determine the reliability indices using Monte Carlo simulation. The results of using Monte Carlo simulation will be compared with the results of using the state space reduction technique and the dynamically directed particle swarm optimization search method.

5.4.1   Case Study I: IEEE RTS Base Case

For the base case, generating units were represented by two states (up state and down state). The load levels were modeled using 20 clusters load levels. To model bus loads, the RTS peak load of 2850 MW was taken as 1 p.u. and bus loads sampled to 20 clusters as a percentage of 1 p.u. value.

Shadow prices values are given in column 2 of Table 5.1 for the generating units, column 3 of Table 5.2 for forward direction of transmission lines and column 3 of Table 5.3 for reverse direction of the transmission lines. Also, it should be noted that, transformers were modeled as transmission lines with length zero and they are placed between buses 3-24, 9-11, 9-12, 10-11 and 10-12.

5.4.2   Case Study I: Modifed IEEE RTS

As mentioned previously, the two 400 MW and one 350 MW generating units have considerably large capacity compared to the other components of the system. These three units were assumed to have derated states as it is given in [63]. In other words, every unit has three states (full capacity state, derated state and down state). In simulating these states, a cumulative distribution function was formed for every generating unit. For example, 400

MW has a cumulative probability with three steps; down, derated and full capacity levels. Shadow prices values are given in column 3 of Table 5.1, column 4 of Table 5.2 and column 4 of Table 5.3.

Table 5.1: Generators Shadow Prices

Bus No.	Case Study I	Case Study II	Case Study III	Case Study IV
1	0.40310	0.43786	0.18527	0.48389
2	0.40378	0.43881	0.18739	0.48390
7	0.15612	0.17088	0.00018	0.03040
13	0.36767	0.40017	0.16363	0.45123
15	0.36832	0.39590	0.13240	0.44642
16	1.54987	2.07930	1.16986	1.50237
18	3.69131	3.18961	3.76693	3.33811
21	4.12508	3.60711	3.62967	16.9437
22	0.36371	0.42293	0.11530	0.44142
23	0.36551	0.38899	0.15000	0.44435

5.4.3   Case Study III: Increasing Generation Capacity and Loading Level

Since the transmission lines are too reliable and have high capacity compared to the generating units, they are forced to become binding constraints by increasing generating units' capacities by two folds and increasing buses' loads by a factor of 1.8. These modifications have forced the lines to carry power near to their rated capacities. Shadow prices values of the system components are given in column 4 of Table 5.1, column 5 of Table 5.2 and column 5 of Table 5.3.

Table 5.2: Transmission Lines Shadow Prices (Forward)

From Bus	To Bus	Case Study I	Case Study II	Case Study III	Case Study IV
1	2	0.01910	0.02797	0.02478	0.02521
1	3	0.00513	0.03031	0.05207	0.03879
1	5	0.03250	0.01738	0.01347	0.01494
2	4	0.01127	0.02497	0.04716	0.02783
2	6	0.10014	0.06714	0.03747	0.07840
3	9	0.02112	0.00654	0.00682	0.01670
3	24	0.13659	0.33778	0.33118	0.29264
4	9	0.06473	0.11148	0.03406	0.03459
5	10	0.31012	0.18250	0.01780	0.00904
6	10	0.29032	0.14138	0.20795	0.08561
7	8	0.00945	0.00413	0.00594	0.02115
8	9	0.08640	0.04409	0.04403	0.06676
8	10	0.26387	0.08410	0.05354	0.02620
9	11	0.28179	0.34020	0.06319	0.27834
9	12	0.13933	0.13406	0.21986	0.22375
10	11	0.19194	0.21197	0.04182	0.26880
10	12	0.20482	0.16501	0.20676	0.33482
11	13	0.05855	0.01416	0.09561	0.02822
11	14	0.00888	0.00847	0.03080	0.02819
12	13	0.04368	0.06997	0.04625	0.02875
12	23	0.06323	0.08933	0.10376	0.05803
13	23	0.07747	0.03390	0.03663	0.01391
14	16	0.03233	0.04106	0.24144	0.07660
15	16	0.05662	0.03764	0.04132	0.01650
15	21	0.00897	0.04632	0.02449	0.00793
15	21	0.03370	0.05385	0.13175	0.01835
15	24	0.02765	0.01104	0.14698	0.06034
16	17	0.01830	0.02639	0.14053	0.02727
16	19	0.00999	0.02918	0.02474	0.01844
17	18	0.08521	0.02969	0.03175	0.02398
17	22	0.03194	0.24006	0.16942	0.08765
18	21	0.00389	0.09870	0.02135	0.02919
18	21	0.01249	0.03610	0.01660	0.01697
19	20	0.01843	0.02143	0.03792	0.05032
19	20	0.02044	0.05901	0.03024	0.16131
20	23	0.02704	0.07893	0.00847	0.02087
20	23	0.01535	0.02283	0.02537	0.01261
21	22	0.06845	0.01126	0.02745	0.07253

Table 5.3: Transmission Lines Shadow Prices (Reverse)

From Bus	To Bus	Case Study I	Case Study II	Case Study III	Case Study IV
2	1	0.02465	0.03037	0.02492	0.02345
3	1	0.00641	0.03088	0.05251	0.03763
5	1	0.03412	0.01854	0.03744	0.02722
4	2	0.01545	0.02762	0.06835	0.03738
6	2	0.10526	0.06962	0.03698	0.09066
9	3	0.01914	0.00831	0.00774	0.01517
24	3	0.10015	0.28250	0.24665	0.24444
9	4	0.05499	0.10741	0.02991	0.02632
10	5	0.07976	0.11993	0.01688	0.00853
10	6	0.05761	0.06277	0.05999	0.06797
8	7	0.55643	0.55998	0.66622	0.93444
9	8	0.08052	0.03544	0.02852	0.05715
10	8	0.02616	0.01965	0.03037	0.02211
11	9	0.21403	0.23538	0.04538	0.22259
12	9	0.07665	0.07778	0.13748	0.16371
11	10	0.23862	0.18203	0.03000	0.20555
12	10	0.52747	0.22230	0.13929	0.28966
13	11	0.04484	0.00789	0.03609	0.02184
14	11	0.00890	0.00833	0.03069	0.02696
13	12	0.02962	0.04041	0.02747	0.01715
23	12	0.03859	0.05952	0.05860	0.03715
23	13	0.07103	0.02514	0.03419	0.01051
16	14	0.02340	0.03051	0.02585	0.05528
16	15	0.06181	0.03872	0.04110	0.01688
21	15	0.00620	0.02904	0.01828	0.00520
21	15	0.02223	0.03742	0.10214	0.01022
24	15	0.04418	0.01751	0.16761	0.07624
17	16	0.01508	0.02060	0.04628	0.01816
16	19	0.01000	0.02766	0.04628	0.01816
17	18	0.08367	0.02786	0.02223	0.01563
17	22	0.01489	0.06379	0.03157	0.02138
18	21	0.00389	0.09616	0.12308	0.02764
18	21	0.00854	0.02988	0.02135	0.02533
19	20	0.01594	0.01601	0.01660	0.01185
19	20	0.02044	0.05406	0.02937	0.04566
20	23	0.01843	0.06626	0.02618	0.15679
20	23	0.01104	0.01526	0.00462	0.01408
21	22	0.03180	0.01126	0.01694	0.00780

5.4.4 Case Study IV: Reducing Lines Capacity

In this case, the carrying capacities of the transmission lines are decreased to 75% of their rated capacity. This modification was assumed to examine the effect of the lines capacities on the system reliability. The shadow prices values of the system components are given in column 5 of Table 5.1, column 6 of Table 5.2 and column 6 of Table 5.3.

5.4.5 Case Study V: Calculation of the Reliability Indices of Four Test Systems

In this case study, Monte Carlo simulation method was used to estimate the well-known annualized reliability indices of the IEEE RTS [63], the Modified IEEE RTS, and the Saskatchewan Power Corporation in Canada (SPC) and a hypothetical six bus system [64]. The annualized reliability indices are evaluated at the system peak load. The annualized indices are shown in Table 5.4.

Table 5.4: Annualized Indices of the Tested Systems.

$\hat{q}$	$\hat{d_n}$	$\hat{F}$	$\hat{L_q}$	$\hat{e_n}$	$\hat{T_c}$	Number of
	MW	occ./yr	h/yr	MWh/yr	hour	sampled states
The Hypothetical Six Bus System						
0.002400	0.034630	1.34832	21.02400	303.3588	15.59274	21,981
The IEEE RTS System						
0.08539	14.19236	18.16174	745.967	123,984	41.07354	73,925
The Modified IEEE RTS System						
0.069052	11.88175	17.14523	603.238	103,799	35.18403	67,884
Saskatchewan Power Corporation (SPC) System						
0.001081	0.039098	3.23125	9.44362	341.560	2.92259	122,941

The results of the annualized indices using Monte Carlo simulation will be used in the

next chapters as a benchmark to validate the proposed methods. Also, the number of samples will be used to test the efficiency of the proposed state space reduction technique.

5.5 Results and Discussion

From Table 5.1 it is clear that the generating unit (400 MW) at bus 21 has the highest shadow price followed by the shadow prices of the generating units of buses 18 and 16 for the four study cases. Consequently, these generating units have the largest impact on system reliability. In other words, these buses are at the highest risk and the most beneficial way to make the system more reliable is to increase the availability of these units by adding new units, decreasing repair time and/or using sophisticated methods to decrease units' failure rate. When the derated states were introduced, these shadow prices decreased due the increase in the availability of the two 400 MW and one 350 MW generating units.

In comparison to the case study I, the shadow prices of the generating units of buses 21, 18 and 16 of the case study III have slightly changed due to the unequal increase in the total installed capacity and the peak load. Such change in the installed capacity and the peak load has forced the transmission lines to have larger shadow prices than it was in case study I instead of forcing the generating units.

For the case study IV, the shadow price of the generating unit at bus 21 has increased for more than four times than it was in case study I whereas the generating units at buses 18 and 16 stayed almost the same. In addition, while buses 18 and 21 have identical generating units, they have different shadow prices; which indicates that not only the availability of components has an impact on systems' reliability, but also, components' location in the grid. By looking back to the network configuration, bus 21 is connected to bus 15 through

74

two lines with normal capacities of 500 MW and to bus 18 also with two lines with normal capacities of 500 MW and they have the highest loadings in the network.

From Table 5.2 and Table 5.3, the overhead transmission line between buses 7 and 8 has the highest shadow price followed by the transformer between buses 10 and 12 and the line that connects buses 5 and 10. From the network configuration, line 7 - 8 is the only line that connects bus 7 to the rest of the system. Also, the nominal real power injection at bus 7 is 175 MW (300 MW - 125 MW) and the normal capacity of the line 7 - 8 is 175 MW. Therefore, line 7 - 8 is almost always carrying its rated power. In addition, the transformer between buses 10 and 12 connects bus 23 which have the highest generation to bus 10 which in turn connected to load buses (buses 5, 6, 8 and 14 through bus 11).

5.6 Summary

This chapter has introduced the use of shadow price concept in estimating sensitivity of the reliability indices with respect to component parameters. The shadow price can be obtained from the dual solution of the standard linear programming problem. Four study cases have been conducted on the IEEE RTS test system. It has been found that shadow price analysis is an efficient tool for composite generation and transmission planning, expansion and operation studies when compared to the sensitivity analysis technique. Moreover, it gives essential information about which component is in unsafe state from reliability point of view and the most effective way to enhance system reliability.

Chapter 6

Power System Reliability Evaluation and Sensitivity Analysis Using the State Space Reduction Technique and Population-based Intelligent Search Methods

The task of power system reliability evaluation is becoming complicated due to the increase in the complexity of the power industry infrastructure. The time and computation efforts to evaluate power system reliability indices and their sensitivities with respect to component parameters and system operating limits are of concern in both planning and operation prospectives. In this chapter, we use the heuristic, which is introduced in 4 to prune the state space and to reduce the computational efforts in evaluating the well-known reliability indices and their sensitivities with respect to component parameters and system operating limits. In this chapter we use the DC power flow model which is given in chapter 2.

This chapter serves as a validation for the proposed state space reduction technique and the use of population-based intelligent search methods in power system reliability evaluation.

The results of these methods will be compared with results of using Monte Carlo simulation which is presented in chapter 5. The method presented in this chapter is based on particle swarm optimization search method and it is applicable to the other population-based intelligent search methods. In addition to the validation of the results, this chapter also shows the reduction in the computational time and effort. The proposed method is applied on the IEEE RTS, the Modified IEEE RTS and PSC.

6.1 Discussion on the Reduction in the Computational Time

In calculating reliability indices, an optimization problem usually needs to be performed for every system state with different loading scenarios. The process of preparing and modeling power system data to be tested for reliability analysis is performed one time. However, running an optimization problem is required for every system state or for any change in system parameters. From a study of wide variety of system sizes and configurations, the optimization problem usually takes most of the calculation time. For instance, on average, the time required to solve an optimization problem for the systems we have tested took more than 95% of the calculation time for each system state. By performing the reduction technique, not all the states need to be passed to the optimization problem. In other words, if a state is guaranteed to be a success state, no useful results can be shown by solving an optimization problem. On the other hand, failure states should be passed to the solver to calculate bus indices. It should be pointed out here that if only system indices are to be evaluated and not bus indices and the algorithm was able to capture most of the failure states, the optimization problem need not to be performed since system indices can be evaluated

from the failure states directly.

Some failure states may not be captured by using the state space reduction technique which denoted as unclassified subspace. We have used binary particle swarm optimization search method to search for such states. The problem of deciding whether we need to perform binary particle swarm optimization search method for the unclassified subspace can be solved by running the binary particle swarm optimization search method for few iterations. If the reliability index under consideration does not change, the algorithm is terminated and the indices calculated by the line capacity model will be enough to evaluate the reliability of the system.

6.1.1 Reduction in Computational Time in Case of Ignoring the Unclassified Subspace

If the transmission lines of the system under consideration are very reliable and have high power limits in comparison with system loading conditions which is the case for most power systems, the proposed state space reduction technique can capture most of the failure states. In this case, performing the binary particle swarm optimization search method is not necessary and ignoring this subspace will not cause significant errors.

If we assume the total time required to evaluate system indices by passing every single state to the solver (optimization problem) is T, the total time required to evaluate system indices by passing only the failure states to the solver is T_r, the time required to evaluate every system state is t, the time required by the optimization problem to evaluate every system state is t_r, number of samples is N and the loss of load probability of the system is LOLP, then by ignoring the unclassified subspace, the percentage of reduction in the

computational time η can be calculated as,

$$\eta = \frac{T - T_r}{T} \times 100\ \%$$ (6.1)

where $T = N \times t$ and

$$T_r \approx N \times [LOLP \times t + (1 - LOLP)(t - t_r)]$$

here T_r is approximated because the time of performing the state space reduction technique to identify the failure states is very small in comparison with the time of preparing system data for every sampled state and the time required by solving the optimization problem.

After some manipulations, equation (6.1) can be rewritten as,

$$\eta \approx (1 - LOLP)\frac{t_r}{t} \times 100\ \%$$ (6.2)

As an example, if we assume 100,000 states were sampled and evaluated in order to reach the desired tolerance and every state takes about 0.01 seconds and if we assume the LOLP of the system is 0.02 and the optimization solver takes 95% of the calculation time of each state, then the time required with solving an optimization problem for "every state" is 1000 seconds (100000×0.01) and the time required by passing only the failure states to the solver is 69 seconds,

$$T_r \approx 100000 \times [0.02 \times 0.01 + (1 - 0.02)(0.01 - 0.95 \times 0.01)] = 69\ \text{(seconds)}$$

Therefore, the percentage of time reduction of using this technique is 93.10%,

$$\eta \approx (1 - 0.02) \left(\frac{0.95 \times 0.01}{0.01} \right) \times 100 \ \% = 93.1\%$$

6.1.2 Reduction in Computational Time in Case of Including the Unclassified Subspace

If ignoring the unclassified subspace causes considerable error in evaluating system indices, the proposed binary particle swarm optimization search method should be used. In this case, calculation of the percentage of time reduction is not straight forward and system dependent. Therefore, calculation of this time cannot be determined beforehand.

To calculate the time reduction, another time which is the time spent by performing the binary particle swarm optimization search method, T_{BPSO}, should be added to the time spent to perform the line capacity model, T_r. Now, equation (6.1) can be rewritten as,

$$\eta = \frac{T - (T_r + T_{BPSO})}{T} \times 100 \ \% \tag{6.3}$$

The computational efforts required by the algorithm proposed in [13] for the entire state space is found to be only 19.31% of performing Monte Carlo Simulation with State Space Pruning [8] on the modified IEEE RTS. Since we are applying a dynamically directed binary particle swarm optimization search method on a subspace of the entire state space, T_{BPSO} in our case should be less than 19.31% of T. Also, the number of states to be visited is very small, hence, the required memory will be small too.

6.2 Solution Algorithm

The solution algorithm explains the flow of the procedures of evaluating the reliability indices and their sensitivities with respect to component parameters and the operating conditions as well as the technique used to direct and prevent the particles from being trapped in a search subspace. The steps can be explained as follows:

1. Initialize the positions and velocities of the particles, x_i and v_i respectively. Particles positions are initialized by using the forced outage rates of system components; components that are in the up state are represented by 1's and components in the down state are represented in 0's. The length of a particle string equals the number of components. Velocities are initialized to have V_{max} equals 2.2 (probability limits are between 0.9 and 0.1).

2. Check if there are identical particles. If so, discard the identical ones and save the rest of the particles in a temporary array vector by converting the binary numbers to decimal numbers. Check if there are particles already exist in the database, if so set probabilities and load curtailments of the existing particles to zeros to decrease the chance of visiting these states again. Then, save the rest in the database and go to the next step.

3. Compute the exact probability of each particle which represents the probability of a system state. If the probability of a particle is less than a threshold ε discard this particle, otherwise go to the next step. In this work, ε is chosen to be 10^{-15}.

4. Set system parameters and update generation and transmission lines status for every particle. Perform the linear programming optimization problem to check if there are

load curtailments. Update the reliability indices.

5. Determine and update personal best states' probabilities and best load curtailments. Also, determine and update best global probability and best global load curtailment. Update particles velocities using (2.16) and update particles positions using (4.7) and (4.10).

6. Check the normalized LOLP ($LOLP_{norm}$) whether it is increasing or decreasing and adjust c_1, c_2, c_3 and c_4 accordingly. If it increasing, increase the values of c_1 and c_2 and decrease the values of c_3 and c_4. Perform the opposite if $LOLP_{norm}$ is decreasing. In this work, we adjust the amount of increasing or decreasing these coefficients according to the amount of change of the $LOLP_{norm}$. Any strategy can be used to adjust these factors. However, the optimum adjustment of these factors is out of the scope of this work. We relate the amount of change of these coefficients to the amount of change in $LOLP_{norm}$, ($\Delta LOLP_{norm}$), in an exponential form as follows,

$$c_{(1,2)-new} = c_{(1,2)-old} \times e^{(100 \times \Delta LOLP_{norm})}$$

$$c_{(3,4)-new} = c_{(3,4)-old} \times e^{(-100 \times \Delta LOLP_{norm})}$$

7. Check if any of the particles has entered the success and/or failure subspaces. If a particle has entered the success subspace, redirect the particle by using the objective of maximum load curtailment only (ignoring the objective of maximum probability) by setting c_1 and c_2 to zeros. If a particle has entered the failure subspace, redirect the particle by using the objective of maximum probability only (ignoring the objective of maximum load curtailment) by setting c_3 and c_4 to zeros.

8. Check for convergence. If the stopping criterion is met, stop; otherwise go to the next step.

9. Determine the number of newly visited states since the previous few iterations. If the number of the new states is less than a threshold, adjust V_{max} and then go to step 2; otherwise go directly to step 2. The threshold is chosen to be 80% of the total number of particles for the first 10 iterations, 50% for the next 10 iterations and 20% thereafter. V_{max} is adjusted according to the direction of the LOLP$_{norm}$ index. If the particles are searching around the success subspace, adjust V_{max} to a large number. On the other hand, if the particles are searching around the failure subspace, adjust V_{max} to a small number. In this work we have chosen 4.0 to be the large number and 2.0 to the small number. Again, the optimum value of V_{max} to better improve the behavior of the search method is out of the scope of this work.

6.3   Case Studies

The proposed formulation was applied on four systems, the IEEE RTS [63], the Modified IEEE RTS, and the Saskatchewan Power Corporation in Canada (SPC) and a hypothetical six bus system [64]. More details about these system are given in the appendix. The case studies are divided into two cases: (I) calculating the reliability indices, validating the results and estimating the reduction in the computational time and (II) performing sensitivity analyses for the reliability indices.

6.4 Case Study I: Calculation of the Reliability Indices

The model was applied on the IEEE RTS and the Modified IEEE RTS with 50 particles. Analysis of the annual as well as the annualized indices was conducted on the two systems. From Table 6.1, Table 6.2, Table 6.3 and Table 6.4, it has been found that in calculating the annual indices of both systems and the annualized indices of the original IEEE RTS, the heuristic technique was able to evaluate system indices and no BPSO was performed (terminated after few iterations). On the other hand, in calculating the annualized indices of the modified IEEE RTS, the heuristic technique was not able to evaluate system indices and therefore the proposed BPSO was used to search for the unclassified subspace. Also, from Table 6.4, the unclassified subspace has a significant effect on the LOLP and LOEE indices and very small effect on the EDNS and LOLE indices. These effects can be interpreted as the unclassified subspace has failure states with relatively high probability but with relatively small load curtailments. This also can be attributed to the fact that failure states that are located far from the origin (all components are in the down state) have high probability and small load curtailments. Therefore, if we were looking for just the EDNS and LOLE indices, the heuristic technique would be enough for this case.

Table 6.5 and Table 6.6, show the reduction in the computational time by using the proposed algorithm as a percentage of the time of evaluating the same indices using Monte Carlo simulation. These times account for calculating the bus indices for all cases. The average base time using Monte Carlo simulation was found to be 1175 seconds for both systems.

Figure 6.1 shows the profiles of the LOLP, DLOLP and the projected LOLP as the algorithm progresses. As the number of visited states increases, the estimated LOLP and

Table 6.1: Annual Indices of the IEEE RTS

Algorithm		LOLP	EDNS MW/yr	LOEE MWh/yr	LOLE h/yr
Proposed	Heuristic	0.00117	0.16374	1430.465	10.22112
	BPSO	–	–	–	–
	Sum	0.00117	0.16374	1430.465	10.22112
Conventional		0.00119	0.16412	1433.752	10.39584

Table 6.2: Annualized Indices of the IEEE RTS

Algorithm		LOLP	EDNS MW/yr	LOEE MWh/yr	LOLE h/yr
Proposed	Heuristic	0.08429	14.67784	128225.60	736.360
	BPSO	–	–	–	–
	Sum	0.08429	14.67784	128225.60	736.360
Conventional		0.08451	14.59761	127524.72	738.279

Table 6.3: Annual Indices of the Modified IEEE RTS

Algorithm		LOLP	EDNS MW/yr	LOEE MWh/yr	LOLE h/yr
Proposed	Heuristic	0.00106	0.07395	645.90125	9.26016
	BPSO	–	–	–	–
	Sum	0.00106	0.07395	645.90125	9.26016
Monte Carlo		0.00105	0.07436	649.61330	9.17280

Table 6.4: Annualized Indices of the Modified IEEE RTS

Algorithm		LOLP	EDNS MW/yr	LOEE MWh/yr	LOLE h/yr
Proposed	Heuristic	0.06039	10.31755	90134.083	517.259
	BPSO	0.00976	0.12171	1063.256	85.263
	Sum	0.07015	10.43926	91197.375	612.830
Monte Carlo		0.07017	10.44237	91224.549	613.005

Table 6.5: Reduction in the computational time of the IEEE RTS

| Category | Time Spent by | | Total | Time |
	Heuristic tech. (seconds)	BPSO (seconds)	Time (seconds)	Reduction (%)
Annual	28.66	0	28.66	97.56
Annualised	144.28	0	144.28	87.72

Table 6.6: Reduction in the computational time of the Modified IEEE RTS

| Category | Time Spent by | | Total | Time |
	Heuristic tech. (seconds)	BPSO (seconds)	Time (seconds)	Reduction (%)
Annual	55.60	0	55.60	95.27
Annualised	336.15	409.75	745.90	36.52

the estimated DLOLP becomes close to each other. If the simulation were to continue to make the particles visit the entire state space which is impractical, these two indices (LOLP and DLOLP) would converge to the same value. Also, Figure 6.1 shows some changes in the LOLP_{proj} index specially at the early stages of the searching process. These changes are due to the adjustments of the weighting factors of the objective function as well as the adjustments in the velocity limit, V_{max}.

6.5   Case Study II: Sensitivity Analyses

The proposed formulation was applied on the IEEE RTS [63]. From Table 6.8, it is clear that the generating unit (400 MW) at bus 18 has the highest effect on all the studied reliability indices followed by the generating units of buses 21 and 24 for all indices. Consequently, these generating units have the largest impact on system reliability. In other words, these buses are at the highest risk and the most beneficial way to improve the reliability of the

Table 6.7: Bus Annual Indices for the IEEE RTS

Bus No.	LOLP	EDNS MW	LOEE MWh/yr	LOLE hr/yr
1	0.00032	0.00555	48.50943	2.75184
2	0.00002	0.00034	2.929904	0.17472
3	0.00006	0.00188	16.41914	0.52416
4	0.00044	0.00530	46.26799	3.80016
5	0.00124	0.01473	128.67821	10.78896
6	0.00042	0.00423	36.93749	3.66912
7	0.00021	0.00398	34.78341	1.79088
8	0.00013	0.00308	26.94283	1.09200
9	0.00005	0.00125	10.90315	0.43680
10	0.00008	0.00238	20.78260	0.69888
13	0.00028	0.01001	87.42760	2.40240
14	0.00096	0.02881	251.65359	8.34288
15	0.00070	0.03126	273.12752	6.11520
16	0.00110	0.01813	158.37621	9.60960
18	0.00018	0.00862	75.30948	1.52880
19	0.00012	0.00329	28.73840	1.04832
20	0.00037	0.00744	64.97050	3.18864

system is to increase the availability of these units by adding new units, decreasing repair time and/or using sophisticated methods to decrease units' failure rate.

6.6 Summary

The heuristic technique, which is presented in chapter 4, was applied to reduce the search space. The heuristic technique is conservative in that not all the failure states can be captured and no success state was classified as failure state. The heuristic technique produces three subspaces, definite failure subspace, definite success subspace and unclassified subspace. An
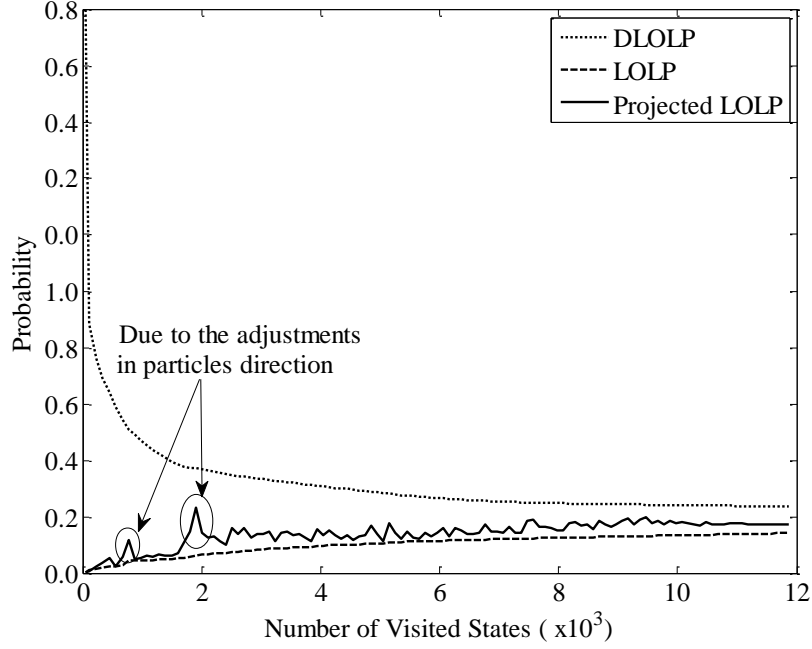
Figure 6.1: Reliability indices profile of the IEEE RTS System

Table 6.8: Sensitivity Analysis of the LOLP index

Bus No. & Gen. Cap.	$\partial LOLP/\partial u_i$ $\times 10^{-2}$	$\partial LOLP/\partial \lambda_i$ $\times 10^{-4}$	$\partial LOLP/\partial \mu_i$ $\times 10^{-4}$
#18G400	33.29905	44.15546	-6.02120
#21G400	33.18920	44.00979	-6.00134
#23G350	26.16603	25.28188	-2.19842
#13G197	20.02105	10.31336	-0.54281
#23G155	11.34010	4.77216	-0.19884
#15G155	11.01719	4.63627	-0.19318
#16G155	10.77760	4.53545	-0.18898
#22G100	4.94948	2.60356	-0.10848
#2G76	4.48367	1.96626	-0.04013
#1G76	4.36122	1.91257	-0.03903

Table 6.9: Sensitivity Analysis of the LOLF index

Bus No. & Gen. Cap.	$\partial LOLF/\partial u_i$	$\partial LOLF/\partial \lambda_i$ $\times 10^{-2}$	$\partial LOLF/\partial \mu_i$ $\times 10^{-4}$
#18G400	58.64305	77.76229	-660.80623
#21G400	57.52415	76.27860	-641.89222
#23G350	49.01718	47.36089	-202.50560
#13G197	43.04602	22.17411	-16.60056
#23G155	41.51697	17.47125	-27.43647
#15G155	39.63948	16.68116	-25.43609
#16G155	37.98464	15.98477	-23.49279
#22G100	16.69121	8.78003	-16.78555
#2G76	17.06241	7.48253	-6.30312
#1G76	16.41083	7.19679	-5.96487

Table 6.10: Sensitivity Analysis of the EDNS index

Bus No. & Gen. Cap.	$\partial EDNS/\partial u_i$	$\partial EDNS/\partial \lambda_i$ $\times 10^{-2}$	$\partial EDNS/\partial \mu_i$ $\times 10^{-4}$
#18G400	73.95452	98.06572	-1337.25977
#21G400	73.78475	97.84059	-1334.18991
#23G350	68.91659	66.58790	-579.02520
#13G197	29.80471	15.35317	-80.80615
#23G155	20.02147	8.42547	-35.10614
#15G155	18.68813	7.86438	-32.76824
#16G155	18.83241	7.92509	-33.02120
#22G100	11.23545	5.91016	-24.62565
#2G76	9.13458	4.00587	-8.17524
#1G76	8.76626	3.84434	-7.84560

intelligent search method based on binary particle swarm optimization was used to search for failure states in the unclassified subspace. From the failure states which were captured by the heuristic technique and the binary particle swarm optimization, the reliability indices and their sensitivities with respect component parameters were calculated.

An element key in using binary particle swarm optimization in composite system reliability evaluation is the selection of weighting factors of the objective function. These weighting factors are system dependent and, therefore, their appropriate values should be carefully selected, in order to prevent the swarm from being trapped to one corner of the state space. An effective particle swarm optimization technique has been proposed and used for reliability assessment of composite systems. The proposed method adjusts the weighting factors associated with the objective function in a dynamic fashion so that the swarm would always fly on the entire search space rather of being trapped to one corner of the search space. The effectiveness of the proposed method was demonstrated on four well-known test system. The results show that the reliability indices obtained by the proposed method correspond closely with those obtained using Monte-Carlo simulation, while requiring lower computational burden.

Chapter 7

Reliability and Sensitivity Analysis of Composite Power Systems Under Emission Constraints

7.1 Introduction

In view of the increasing role of environmental considerations in power generation, there is an evolving body of minimum cost and minimum emission methods that are cognizant of these emerging factors. This chapter presents a method of power system expansion planning, considering emission constraints. The method presented here uses a linearized power flow representation in the form of a linear programming (LP) model similar to those frequently used in power system studies to minimize the total operation cost and is applied to both generation and transmission expansion planning. The cost of the fuel, the cost of purchasing additional emission allowances in case a power plant reaches its maximum emission allowance and the gain from selling the excess emission credits where the emissions are less than the limit are combined to develop a piecewise linear objective function. Emissions are represented as a cost in case of buying extra emission allowances or as benefits in case of selling the excess emission allowances. It also utilizes the concept of the shadow price to perform sensitivity

analysis with respect to the operation constraints to identify the best cost effective generation and transmission expansion planning. The dual solution of the LP provides the shadow prices that are used for determining the sensitivity of the minimum cost with respect to power generation.

Following the introduction of the Clean Air Act Amendments of 1990, utilities have been required to reduce and monitor emissions from their power generating units starting from 1995. This act enforced allowances on SO_2 emissions that could be used or traded within the specified banking period [65]. The most significant reductions have occurred very recently. On November 14, 2012, California had its first auction and trading on greenhouse emission allowances [66]. Starting January 2013, California's emission cap-and-trade program came into effect, and greenhouse gas emissions from large electric power plants are required to be reduced by 16% between 2013 and 2020 [66]. The Regional Greenhouse Gas Initiative (RGGI), which consists of nine North-Eastern and Mid-Atlantic states, agreed on reduction of CO_2 budget by 45% by 2014 and the reduction will decrease by 2.5% yearly from 2015 to 2020 [67]. The American Clean Energy and Security Act of 2009 provides for the reduction of carbon emissions by 17% by 2020. The European Union Emissions Trading System reduced greenhouse gas emissions more than 8% between 2008 and 2012 and is expected to reduce greenhouse gas emissions below 20% of the 1990 levels by 2020, starting from 2013 [68].

Several methods have been proposed to reduce emissions from power generating units; these include installing post-combustion cleaning equipment, switching to fuel with less pollutants, increasing the penetration of the renewable energy, and modifying existing dispatch strategies to include emissions [69]. With these reduction methods, utilities are to operate and expand their generation within the emission allowances.

Some of the earliest work on minimum emission generation dispatch was performed by

Gent and Lamont [70]. Nada, Hari and Kothari [71] solved economic emission load dispatch with line capacity constraints. Subsequently, considerable research was reported on variations and extensions of these methods [72–78]. These variations use different means of accommodating emissions within the optimization problem. Some of the proposed formulations also take into account the different emission reduction equipment and methods described above, and thereby provide for strategies that may allow utilities to forgo, defer, or minimize additional capital costs. For example, [79] shows how a utility may avoid installation of new emission equipment by changing its commitment and dispatch schedules, or by switching to fuels with low emission (and high cost), or both.

Reducing emissions not only affects power dispatch and cost-effective planning, but also influences system reliability requirements. Imposing emission limits on some specific areas may change reliability-based expansion planning procedures. Planning decisions may comprise a trade-off between the cost of buying extra emission allowances and the cost of improving system reliability. Evaluating system reliability under the condition of reducing the emission became necessary and reliability indices need to be adapted to this new constraint. Therefore, there is an emerging need to include emission considerations in reliability, security and economy studies.

Sensitivity analyses of conventional reliability indices incorporate remedial action through load curtailment minimization under the constraints of power balance, generation capacity limits and transmission capabilities to rank system components according to their risk. However, in accommodating regulatory measures, emission allowances have been considered as additional constraints. While planning studies are concerned with reliability and cost, it is often useful to quantify the sensitivity of the reliability indices of interest to component parameters and operating constraints. In the emerging context, it is reasonable to include

emission constraints in the sensitivity analysis of the reliability indices. In other words, sensitivity of reliability indices with respect to the emission limits needs to be added to expansion planning studies. Therefore, generation expansion planning is no longer based only on reliability enhancement or cost minimization.

A considerable amount of research has been conducted on economic/emission dispatching strategies. However, incorporating emission allowances in power system reliability studies is rarely found in the literature. In [80], SO_2, NO_x and CO_2 emissions were considered as constraints in their generation expansion model which is based on multi-area reliability exponential analytic model. Minimization of emissions while maintaining reliability requirements in microgrids is presented in [81]. Most of the prior research has focused on evolutionary techniques and multiobjective minimization function to minimize emissions and generation costs in generation expansion planning [72–76, 82].

The work reported in this chapter calculates the reliability indices of composite power systems and utilizes the concept of the shadow price in ranking the generating units from the reliability point of view while considering the emission allowances as additional constraints. Therefore, this work adds another dimension to system planning processes through the inclusion of emission constraints. Sensitivity analyses of the well-known reliability indices, LOLP, LOLF and EDNS, are presented. Also, a new expression for calculating the sensitivity of the EDNS with respect to the emission limits is developed. The generating units are ranked based on their sensitivities to the emission allowances. Based on this ranking, the emission allowances of generating stations are evaluated to determine a need for expansion. For instance, if a generating plant is ranked high in terms of risk and is viewed as a candidate for reconditioning in order to increase the overall system reliability, the emission allowance should be applied. If the emission limit is reached, the planner should choose between buy-

ing emission allowances and investing in another power station that has available emission allowances. The method is applicable to any source that produces undesirable byproducts that are capped by regulatory and other policies, as long as these byproducts are a function of the output power. The method is demonstrated on the IEEE Reliability Test System (IEEE-RTS).

7.2 Emissions from Electric Generation

A significant amount of energy supply is used in producing electricity worldwide, and in most industrialized countries the bulk of electric generation comes from fossil fueled plants. According to the Environmental Protection Agency (EPA), about 16 million tons of SO_2 and 7 million tons of NO_x were emitted by electric utilities in the United States in 1985 [83]. Further, EPA reports that in 1995 about 23 million tons of SO_2 and 19 million tons of NO_x were emitted from all resources. In the UE-27, 40% of energy resources is used in generating electricity [84]. Also, in the UE-27 [84], 55% of the generated electricity in 2005 was supplied by fossil fuel resources. In 2008, 601.32 GW was generated from coal in China which is about 75.87% of the total electric energy generated [85]. Most of these emissions were produced by fossil fuel plants. In 2006, 12 million tons of Sulphur-dioxide emissions were produced in China [80].

Some regulations were introduced and categorized according to some definitions such as, "new source performance", "modified source", "reconstruction", "degree of emission limitation", etc. For instance, "new source" is defined as any source that is commissioned after the regulation is proposed and is subjected to the NSPS (New Source Performance Standards) requirements even if the regulation is not final [83]. Also, a "modified source"

is any source subjected to a physical or operation change that may increase air pollutant or produce a new air pollutant and is subject to the NSPS (CAA).

The goal of reducing the amount of emissions of SO_2 and NO_x is implemented in two stages: Phase I and Phase II. Phase I began in January 1, 1995 and Phase II began in January 1, 2000. For example, in phase I, all units with 100 MW or greater and had SO_2 emission greater than 2.5 lb/mmBtu in 1985 are subjected to emission reduction according to table A of section 404, title IV of the CAA.

7.3 CO_2, SO_2 and NO_x Emission Constraints

This section describes the formulation and incorporation of the emission in the load curtailment minimization problem (chapter 2). In this section, the emission allowances are considered as additional constraints.

Several methods have been proposed to model the emission function of the thermal generating units. Some of these models are based on the heat rate functions of the generating units with modifying the heat rate coefficients. Some other model emissions based on the heat rates with multiplying the heat rates with appropriate emission factors. In addition, some models use more detailed models such as including the valve loading effect. The heat rates themselves can be modeled in a quadratic, cubic or exponential function. Emission rates were modeled using a straight linear form as in [77,80,86], combination of a straight line and two exponentials as in [70], a quadratic form as in [71–75, 78, 79, 82, 87, 88], a quadratic and an exponential form as in [76, 89, 90], and multiplying the heat rate function with an emission factor as in [91]. In this work, for simplicity, the emissions are modeled based on the heat rates, while ignoring the valve loading effects, and linearizing the quadratic form.

The quadratic heat rate for a generating unit i can be expressed as:

$$HR = a_i + b_i P_i(t) + c_i P_i^2(t) \quad \text{(MMBtu/MWh)} \tag{7.1}$$

where HR is the heat rate, a_i, b_i and c_i are the heat rate coefficients and $P_i(t)$ is the real power generation of unit i at time t. Another widely used unit for heat rates is Btu/kWh. MMBtu/MWh has been used so as to be consistent with units of the emission rates. To convert from MMBtu/MWh to Btu/kWh, the given heat rate can be multiplied by 1,000.

Since the heat rates are functions of the output power and the emissions are functions of the heat rates, the emissions of a generating unit i can be expressed as a function of the output power as follows,

$$E_{ji} = \alpha_{ji} + \beta_{ji} P_i(t) + \gamma_{ji} P_i^2(t) \quad \text{(lbs/MMBtu)} \tag{7.2}$$

where α, β and γ are the coefficients of the emission rates, j denotes emission type (1 for ECO_2, 2 for ESO_2 and 3 for ENO_x), ECO_{2i} is the CO_{2i} emission of unit i, ESO_{2i} is the SO_{2i} emission of unit i and ENO_{xi} is the NO_{xi} emission of unit i.

Assuming a power generating plant with n thermal units at time t, the total CO_2 emission is expressed as

$$ECO_2 = \sum_{i=1}^{n} ECO_{2i}\left(P_i(t)\right) \quad \text{(ton/h)} \tag{7.3}$$

Similarly, the total SO_2 emission is expressed as

$$ESO_2 = \sum_{i=1}^{n} ESO_{2i}\left(P_i(t)\right) \quad \text{(ton/h)} \tag{7.4}$$

Also, the total NO_x emission is expressed as

$$ENO_x = \sum_{i=1}^{n} ENO_{xi}\left(P_i(t)\right) \quad (\text{ton/h}) \tag{7.5}$$

These emissions are nonlinear functions in the unit output power. In order to include these emissions as constraints in the linear programming problem, these equations are linearized around the operating points.

7.4 Sensitivity Analysis of EDNS Index with respect to the Emission Limits

The optimization is constrained by generator and transmission line capacities. However, after the introduction of the Clean Air Act, it is necessary for such analyses to accommodate emission limits. This work includes the effect of emission limits on the sensitivity analysis of the reliability indices. The most commonly used indices in composite power system are: LOLP, LOLF and EDNS. The sensitivity of the LOLP, LOLF and EDNS with respect to component parameters has been introduced in chapter 3. In this section, an analytical expression is developed to calculate the sensitivity of the EDNS with respect to emission limits. The development of this expression is based on the linearized relationship between the amount of emission and the output power. The derivation starts with utilizing the partial derivative of the EDNS to the component capacity.

The sensitivity analysis of the EDNS with respect component capacities was derived as follows [32, 33].

$$\partial EDNS/\partial C_i = \sum_{x \in X} I_f\left(x\right) P\left(x\right) \partial L_c\left(x\right)/\partial C_i \tag{7.6}$$

where C_i is the capacity of component i and $L_c(x)$ is the total load curtailment when the system is at state x.

The derivative of the total load curtailment with respect to component capacity is given in section 3.4.2. Sensitivity of EDNS with respect to circuit capacity or susceptance is inherently not affected by the emission limits; however, with generation redispatch under the condition of emission limits reduction they may become active constraints.

In section 7.3 it was stated that the emission functions are linearized about the operating points. Therefore, the effect of the emission limits on EDNS sensitivity can be evaluated by developing a relationship between shadow prices of generating units with its emission. From (2.16), the Lagrange multiplier of a generating unit can be expressed as

$$\pi_{g,i} = \partial L_c(x)/\partial g_i \tag{7.7}$$

where g_i is the capacity of generator i.

Now a new term is introduced which is the partial derivative of total load curtailment with respect to emission limit. This term can be thought of it as a new constraint to (2.16). This new constraint will produce a new Lagrange multiplier which relates the emission limit to total load curtailment. The partial derivative of total load curtailment with respect to emission limits can be expressed as

$$\pi_{E,ij} = \partial L_c(x)/\partial E_{ij} \tag{7.8}$$

where $\pi_{E,ij}$ and E_{ij} are the Lagrange multiplier or shadow price of the emission limit and

the emission limit of unit i for emission type j. $\partial L_c(x)/\partial E_{ij}$ can be expressed as

$$\partial L_c(x)/\partial E_{ij} = \partial L_c(x)/\partial g_i \cdot \partial g_i/\partial E_{ij} \tag{7.9}$$

The first term of the right hand side of (7.9) is the shadow price of the generating capacity. The second term can be calculated using the relationship of generation output power and emission. This relationship can be given as,

$$E_{ij} = E_{c,ij} \cdot g_i \tag{7.10}$$

where $E_{c,ij}$ is the linearized emission coefficient of unit i for emission type j.

Therefore, from (7.10), the partial derivative of the output power with respect to the amount of emission can be calculated as follows.

$$\partial g_i/\partial E_{ij} = 1/E_{c,ij} \tag{7.11}$$

Now, the partial derivative of the total load curtailment with respect to the emission allowances can be given by

$$\partial L_c(x)/\partial E_{ij} = \partial L_c(x)/\partial g_i \cdot 1/E_{c,ij} \tag{7.12}$$

This can be expressed in terms of shadow price or Lagrange multiplier as

$$\pi_{E,ij} = \pi_{g,i}/E_{c,ij}. \tag{7.13}$$

Therefore, the sensitivity of the EDNS with respect to emission allowances now can be defined as,

$$\partial EDNS/\partial E_{ij} = \sum_{x \in X} I_f(x)P(x)\partial L_c(x)/\partial E_{ij} \tag{7.14}$$

Expressed in terms of shadow price or Lagrange multiplier,

$$\partial EDNS/\partial E_{ij} = \sum_{x \in X} I_f(x)P(x)\left(\pi_{g,i}/E_{c,ij}\right) \tag{7.15}$$

Equations (7.14) and (7.15) calculate the sensitivity of the EDNS with respect to emission allowances. Therefore, by solving the optimization problem of (2.16) and getting the shadow prices of the generating units, the shadow prices of the emission limits are calculated by dividing the shadow prices of the generating units by the linearized emission coefficients.

7.5   Solution Algorithm

This section describes the approach used for calculating the sensitivity analysis of LOLP, LOLF and EDNS with respect to component reliability and emission allowance limits of various system components. As mentioned above, emission allowances are considered as additional constraints. The sensitivity analysis was carried out using the heuristic technique and the directed binary particle swarm optimization search method as described in chapter 4.

The stopping criterion used in this method consists of comparing the coefficient of variation of a selected index (e.g., the EDNS) to a pre-specified tolerance. The simulation steps are summarized in Figure 7.1.
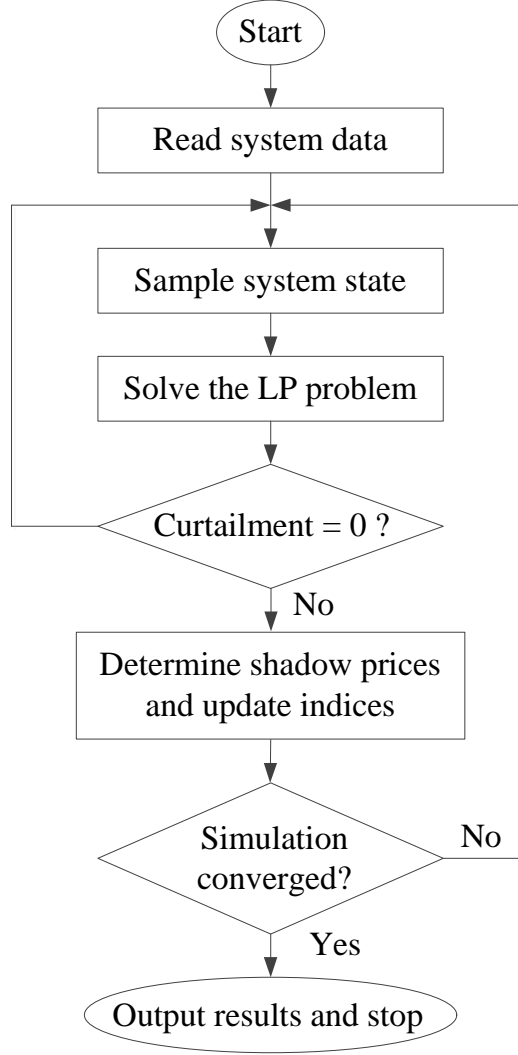
Figure 7.1: Flowchart of Estimating the Sensitivity Analysis

7.6 Case Studies

This section illustrates the method on the IEEE RTS test system [63]. The data of this system is given in the appendix. The IEEE RTS has two nuclear steam generating units each of which 400 MW and six hydro driven generating units each of which 50 MW. These units do not have SO_2, NO_x or CO_2 emissions. The emission rates were calculated from the heat rates. The emission coefficients were calculated from the emission rates based on 2nd order polynomials.

For every state, the partial derivative of the total load curtailment with respect to generation capacity is calculated from the optimization problem of (2.16). The emission curves were linearized about the operating points for two linear segments. After the simulation converges to the specified accuracy, the sensitivity of the EDNS to the emission limits is summed up as shown in (7.15).

Two case studies have been performed: a base case, and one in which the emission allowances are reduced by 5%. The annualized reliability indices of the IEEE RTS are shown in Table 7.1. The results for two more reliability indices, Loss of Load Expectation (LOLE) and Loss of Energy Expectation (LOEE, also called expected un-served energy or EUE), are also presented. LOLE and LOEE can be calculated directly from LOLP and EDNS respectively by multiplying by the study period in hours.

The sensitivity results of the LOLP with respect to reliability parameters for the base case and reduced emission case are shown in Table 7.2 and Table 7.3, respectively. The sensitivity results of the LOLF with respect to reliability parameters for the base case and reduced emission case are shown in Table 7.4 and Table 7.5, respectively. The sensitivity results of the EDNS with respect to reliability parameters for the base case and reduced emission case are shown in Table 7.6 and Table 7.7, respectively. Table 7.8 shows the sensitivity of the EDNS with respect to ESO_2, ENO_x and ECO_2 for the base case. Table 7.9, shows the sensitivity of the EDNS with respect to ESO_2, ENO_x and ECO_2 for the reduced emission case.

7.7   Results and Discussion

Is is clear that the generating unit (350 MW) at bus 23 has the highest effect on the LOLP followed by the generating units (400 MW) of buses 18 and 21 for the two study cases. Consequently, these generating units have the largest impact on system reliability. In other words, these buses are at the highest risk and the most beneficial way to make the system more reliable is to increase the availability of these stations by adding new units, or by modernizing existing units to improve reliability. When the emission allowances were reduced (case study 2), these sensitivities increased accordingly.

In comparison to the case study 1, the sensitivities of LOLP of the generating units of the case study 2 have increased due to the decrease in the emission limits. Such decrease in the emission limits has forced the generating units to have larger shadow prices values than it was in case study 1. By decreasing the emission limits, the emission limits constraints became binding constraints and generating capacities became redundant constraints.

Also, it is clear that the generating unit (350 MW) at bus 23 has the highest effect on the EDNS for both study cases. Also, after reducing the emissions, the sensitivities of the EDNS with respect to the emission limits have increased dramatically. For instance, for the SO_2 air pollutant, sensitivity of the 350 MW unit with respect to the emission has increased by about 2.6 times and for the 197 MW unit has increased by about 4.9 times. The factor of increase in the sensitivity of the EDNS with respect to emission limit due reducing the emissions are shown in Table 7.10.

From the above discussion it is obvious that reducing the emission allowance limits leads to a huge change in system reliability indices. From these studies, planners can decide where to invest by trading off between reliability requirements and the cost of reducing the

emissions or buying emission allowances for the affected areas.

Table 7.1: Annualized Indices of the IEEE Reliability Test System

	LOLP	EDNS MW	LOEE MWh/yr	LOLE hr/yr
Base Case	0.08496	14.76607	128996	742.21056
Reduced Emission	0.14093	26.49218	231435	1231.16448

Table 7.2: Sensitivity Analysis of LOLP with Respect to Reliability Parameters for the Base Case

Bus No. & Gen. Cap.	$\partial LOLP/\partial u_i$ $\times 10^{-4}$	$\partial LOLP/\partial \lambda_i$ $\times 10^{-2}$	$\partial LOLP/\partial \mu_i$ $\times 10^{-4}$
#15G12	0.23468	0.13523	-0.27598
#22G50	1.57580	0.30889	-0.31201
#16G155	14.87768	5.48451	-22.85212
#23G155	13.65057	5.03215	-20.96728
#15G155	14.49772	5.34444	-22.26849
#13G197	15.36175	6.93199	-36.48416
#23G350	42.33958	35.83622	-311.61931
#18G400	30.31500	35.21391	-480.18962
#21G400	30.42285	35.33918	-481.89795

7.8   Summary

Most of the emission studies in the literature focused on minimizing emission with economic dispatch and introducing new concepts to solve multi-objective functions. The goal was to minimize emissions and fuel costs to accommodate for the requirements of the CAA of 1990. Minimizing the emission is one solution among many methods such as utilizing fuels with less air pollutant, exploring new techniques to reduce the amount of emissions, etc.

Table 7.3: Sensitivity Analysis of LOLP with Respect to Reliability Parameters for the Reduced Emission Case

Bus No. & Gen. Cap.	$\partial LOLP/\partial u_i$ $\times 10^{-4}$	$\partial LOLP/\partial \lambda_i$ $\times 10^{-2}$	$\partial LOLP/\partial \mu_i$ $\times 10^{-4}$
#15G12	1.39303	0.80272	-1.63820
#22G50	4.97198	0.97461	-0.98445
#16G155	17.80651	6.56419	-27.35080
#23G155	16.73514	6.16924	-25.70517
#15G155	18.46648	6.80748	-28.36451
#13G197	19.05290	8.59762	-45.25063
#23G350	46.66679	39.49877	-343.46757
#18G400	33.29836	38.67937	-527.44598
#21G400	32.84112	38.14824	-520.20328

Table 7.4: Sensitivity Analysis of LOLF with Respect to Reliability Parameters for the Base Case

Bus No. & Gen. Cap.	$\partial LOLF/\partial u_i$ $\times 10^{-4}$	$\partial LOLF/\partial \lambda_i$ $\times 10^{-2}$	$\partial LOLF/\partial \mu_i$ $\times 10^{-4}$
#15G12	0.23468	0.13523	-0.27598
#22G50	1.57580	0.30889	-0.31201
#16G155	14.87768	5.48451	-22.85212
#23G155	13.65057	5.03215	-20.96728
#15G155	14.49772	5.34444	-22.26849
#13G197	15.36175	6.93199	-36.48416
#23G350	42.33958	35.83622	-311.61931
#18G400	30.31500	35.21391	-480.18962
#21G400	30.42285	35.33918	-481.89795

Table 7.5: Sensitivity Analysis of LOLF with Respect to Reliability Parameters for the Reduced Emission Case

Bus No. & Gen. Cap.	$\partial LOLF/\partial u_i$ $\times 10^{-4}$	$\partial LOLF/\partial \lambda_i$ $\times 10^{-2}$	$\partial LOLF/\partial \mu_i$ $\times 10^{-4}$
#15G12	1.39303	0.80272	-1.63820
#22G50	4.97198	0.97461	-0.98445
#16G155	17.80651	6.56419	-27.35080
#23G155	16.73514	6.16924	-25.70517
#15G155	18.46648	6.80748	-28.36451
#13G197	19.05290	8.59762	-45.25063
#23G350	46.66679	39.49877	-343.46757
#18G400	33.29836	38.67937	-527.44598
#21G400	32.84112	38.14824	-520.20328

Table 7.6: Sensitivity Analysis of EDNS with Respect to Reliability Parameters for the Base Case

Bus No. & Gen. Cap.	$\partial EDNS/\partial u_i$ $\times 10^{-4}$	$\partial EDNS/\partial \lambda_i$ $\times 10^{-2}$	$\partial EDNS/\partial \mu_i$ $\times 10^{-4}$
#15G12	0.23468	0.13523	-0.27598
#22G50	1.57580	0.30889	-0.31201
#16G155	14.87768	5.48451	-22.85212
#23G155	13.65057	5.03215	-20.96728
#15G155	14.49772	5.34444	-22.26849
#13G197	15.36175	6.93199	-36.48416
#23G350	42.33958	35.83622	-311.61931
#18G400	30.31500	35.21391	-480.18962
#21G400	30.42285	35.33918	-481.89795

Table 7.7: Sensitivity Analysis of EDNS with Respect to Reliability Parameters for the Reduced Emission Case

Bus No. & Gen. Cap.	$\partial EDNS/\partial u_i$ $\times 10^{-4}$	$\partial EDNS/\partial \lambda_i$ $\times 10^{-2}$	$\partial EDNS/\partial \mu_i$ $\times 10^{-4}$
#15G12	1.39303	0.80272	-1.63820
#22G50	4.97198	0.97461	-0.98445
#16G155	17.80651	6.56419	-27.35080
#23G155	16.73514	6.16924	-25.70517
#15G155	18.46648	6.80748	-28.36451
#13G197	19.05290	8.59762	-45.25063
#23G350	46.66679	39.49877	-343.46757
#18G400	33.29836	38.67937	-527.44598
#21G400	32.84112	38.14824	-520.20328

Table 7.8: Sensitivity Analysis of EDNS with Respect to Emission Allowance Limits for the Base Case

Bus No. & Gen. Cap.	$\partial EDNS/$ ∂ESO_2 $\times 10^{-4}$	$\partial EDNS/$ ∂ENO_x $\times 10^{-4}$	$\partial EDNS/$ ∂ECO_2 $\times 10^{-4}$
#15G12	-34.95128	-13.98051	-0.04112
#16G155	-94.96082	-37.98433	-0.09044
#23G155	-47.96955	-19.18782	-0.04569
#15G155	-94.63840	-37.85536	-0.09013
#13G197	-47.58625	-19.03450	-0.05598
#23G350	-267.88743	-107.15497	-0.25513

Table 7.9: Sensitivity Analysis of EDNS with Respect to Emission Allowance Limits for the Reduced Emission Case

Bus No. & Gen. Cap.	$\partial EDNS/ \partial ESO_2$ $\times 10^{-4}$	$\partial EDNS/ \partial ENO_x$ $\times 10^{-4}$	$\partial EDNS/ \partial ECO_2$ $\times 10^{-4}$
#15G12	-39.70206	-15.88082	-0.04671
#16G155	-274.08317	-109.63327	-0.26103
#23G155	-57.60845	-23.04338	-0.05487
#15G155	-229.14951	-91.65980	-0.21824
#13G197	-233.52268	-93.40907	-0.27473
#23G350	-702.68535	-281.07414	-0.66922

Table 7.10: Percentages of Increase in the Sensitivities of EDNS with Respect to Emission Allowance Limits Due to Reduced the Emissions

Bus No. & Gen. Cap.	Ratio of Increase
#15G12	1.14
#16G155	2.89
#23G155	1.20
#15G155	2.42
#13G197	4.90
#23G350	2.62

Minimizing the emissions can help in redispatching the existing generators. The need to establish strategies to include the CAA 1990 in future planning is necessary. Inclusion of emission constraints in planning studies as described in this chapter helps guide investment strategies with respect to reconstruction or upgrades.

The work presented here responds to the emerging need for reliability methods that are cognizant of environmental factors. This work introduced a framework for evaluating the effect of the emission rates and allowances on system reliability and determining the sensitivity of commonly used reliability indices to equipment and emission constraints.

The Expected Demand Not Supplied (EDNS) is used as a key reliability index. The sensitivity of the EDNS with respect to emission allowances is evaluated and used to study the effect of emission allowances on system reliability. From the sensitivity results, components can be ranked from reliability point of view. Therefore, the component that has the highest effect on system reliability can be identified. Also, if the reliability of the system needs to be improved, the sensitivity analyses can identify which component to increase its emission limit.

Chapter 8

Reliability and Sensitivity Analysis of Composite Power Systems Considering Voltage and Reactive Power Constraints

8.1 Introduction

There is a growing need to include the effects of voltage and reactive power constraints in power system reliability evaluation. Most of the present methods that evaluate the reliability of composite systems represent the network using the DC power flow model, which ignores the effects of the voltage and reactive power constraints on the reliability indices. Due to the integration of the renewable energy resources, the voltage and reactive power limits are expected to have more effect on the system reliability. The time and computational efforts to evaluate the reliability indices and their sensitivities with respect to the operating conditions using models that incorporate voltage and reactive power limits such as AC power flow model are of concern in both planning and operation prospectives.

Traditionally, composite system reliability methods have used transportation model and

dc power flow models to represent system flows, largely due to the complexity of AC flow-based redispatch algorithms. Evaluation of the effects of the voltage and reactive power limits has been introduced in [92]. The method presented in [92] is based on using the DC power flow model in two steps and linearizing the relationship between the reactive power injections and the voltages at the nodes. Several methods have been recently introduced in the literature of power system reliability to investigate the effects of the lack of reactive power support on the reliability indices. For example, using the AC power flow model in *two steps* to study the aspects of the reactive power on the composite system reliability has been introduced in [93–96].

Several methods have been introduced in the literature to decrease the time and computational efforts in evaluating power system reliability indices as it was mentioned in chapter 4. This chapter investigates the effects of the voltage and reactive power constraints on composite system reliability indices through performing sensitivity analyses of the Severity Index with respect to the voltage and reactive power constraints. In this chapter, expressions are developed to evaluate the sensitivity of the Severity Index with respect to these constraints. Further, four indices are used to evaluate the contributions of the minimum and maximum voltage limits at the nodes and minimum and maximum reactive power capabilities in the loss of load probability index. The full, non-linear AC power flow model, which is given in (2.14) and (2.15), is used to incorporate these constraints in the reliability evaluation. The state space pruning technique, which is introduced in chapter 3 is utilized to reduce the computational time. Also, in this chapter, composite system reliability indices using AC power flow model are provided to serve as a benchmark for future work involving power flow models. A comparison between the use of AC and DC power flow models is also provided. We have used the state space reduction technique of chapter 4.

8.1.1 Calculation of Voltage and Reactive Power Limit Indices

Calculations of the LOLP, LOLF, EDNS, LOEE and LOLE are similar to those presented in chapter 3. This section develops expressions to calculate the voltage and reactive power limit indices. In this chapter, we use four indices to represent the contributions of violations of the voltage and reactive power constraints on the loss of load probability index. These indices are defined as follows: (a) vi_{min} represents the contributions of the minimum voltage level constraints, (b) vi_{max} represents the contributions of the maximum voltage level constraints, (c) ϱi_{min} represents the contributions of the minimum reactive power level constraints and (d) ϱi_{max} represents the contributions of the maximum reactive power level constraints. For every tested state, if any of these indices is involved in the load curtailment, this index is updated. These indices are related to the failure subspace not to the system state space; these indices reflect the contributions of the violations of the voltage and reactive power constraints on the loss of load probability index. Therefore, the state space of these indices is X_f.

The estimated values of these indices can be calculated as follows,

$$f_k = E\left[q_k\right] \tag{8.1}$$

where f_k is the index under consideration, (f_1 is for the vi_{min}, f_2 is for the vi_{max}, f_3 is for the ϱi_{min} and f_4 is for the ϱi_{max}), and q_k can be evaluated as follows,

$$q_k = \frac{1}{T_f} \sum_{i=1}^{N} \xi_{ki} \tag{8.2}$$

where T_f is the sum of the durations of tested *failure* states and ξ_{ki} is an indicator function

113

for state violation that can be expressed as,

$$\xi_{ki} = \begin{cases} \tau_i, & \text{If } x_i \in X_k \\ \\ 0, & \text{otherwise} \end{cases} \tag{8.3}$$

where X_k is the set in which the index k has a contribution in the load curtailment and $X_k \subset X_f$.

8.2 Sensitivity Analysis of the EDNS Index with respect to the Voltage and Reactive Power Limit Indices

Sensitivity analyses of composite system reliability indices with respect to system parameters have been extensively addressed in the literature. To calculate the sensitivity of the EDNS index with respect to the voltage and reactive power limits; these limits need to be added to the optimization problem as shown in (2.15).

The sensitivity analyses of the reliability indices with respect to the voltage and reactive power constraints are important in identifying the impacts of these constraints on power system reliability and help in hardening power systems against catastrophic failures such as voltage collapse. Expressions for calculating the sensitivity of the EDNS index with respect to voltage and reactive power limits are developed. These expressions were developed from the Lagrange multipliers of the voltage and reactive power constraints.

8.2.1 Sensitivity of the EDNS Index with Respect to Voltage Limit Constraints

The derivation of the sensitivity of the EDNS index with respect to voltage and reactive power limits starts with utilizing the expression of (3.5). The sensitivity of the EDNS index with respect to voltage limits allowed at bus k can be expressed as follows,

$$\partial \text{EDNS}/\partial v_k = \sum_{x \in X_f} p(x) \times (\partial C(x)/\partial v_k) \tag{8.4}$$

where $\partial C(x)/\partial v_k$ is the Lagrange multiplier (π_{vk}) of the voltage constraint at bus k while the system is residing at state x.

Also, the sensitivity of the EDNS index with respect to voltage limit constraints can be evaluated using Monte Carlo state next event method as follows [97, 98],

$$\partial \text{EDNS}/\partial v_k = \frac{1}{T} \sum_{i=1}^{N} \varphi_i \times \pi_{vk}. \tag{8.5}$$

This expression can be used for both maximum and minimum voltages allowed at the buses.

8.2.2 Sensitivity of the EDNS Index with Respect to Reactive Power Limit Constraints

In the same manner, the sensitivity of the EDNS index with respect to the reactive power available at bus k can be expressed as follows,

$$\partial\rho/\partial\varrho_k = \sum_{x \in X_f} p(x) \times (\partial C(x)/\partial\varrho_k) \qquad (8.6)$$

where $\partial C(x)/\partial\varrho_k$ is the Lagrange multiplier, $\pi_{\varrho k}$, of the reactive power available at bus k while the system is residing at state x.

Similarly, the sensitivity of the EDNS index with respect to reactive power constraints at bus k can be evaluated using Monte Carlo state next event method as follows,

$$\partial\hat{\rho}/\partial\varrho_k = \frac{1}{T}\sum_{i=1}^{N}\varphi_i \times \pi_{\varrho k}. \qquad (8.7)$$

Also, this expression can be used for both maximum and minimum reactive power limits at the buses.

8.3   Case Studies

The proposed formulation was applied on the IEEE RTS [63]. The IEEE RTS system has been extensively tested for power system reliability analysis.

8.3.1   Reliability Assessment

Reliability assessments using both the AC and DC power flow models have been performed on the IEEE RTS system at the peak load (Annualized Indices). As a comparison, the results of both models for the IEEE RTS are shown in Table 8.1. As it is obvious from Table 8.1, estimates from the DC power flow model produce optimistic results in comparison with the AC power flow model counterpart.

It is well-known that the transmission lines of the IEEE RTS are very reliable with respect

Table 8.1: System Annualized Indices of the IEEE RTS

Power Flow Model	$\hat{q}$	$\hat{\rho}$ MW	$\hat{\phi}$ occ./yr	$\hat{\tau}$ hour
AC	0.10427	17.37479	22.76247	0.00458
DC	0.08455	14.72996	19.76867	0.00428

to the generation. Also, the power carrying capability limits of the transmission lines are much higher than the normal loading level even in the case of the peak load. Therefore, the contributions of the transmission lines on the system reliability of this test system are very small and can be ignored. For this reason, several studies have suggested to use the modified version of it which is the same as the original system except that the generation is multiplied by 2 and the load at the buses is multiplied by 1.8. The results of both power flow models for the Modified IEEE RTS are shown in Table 8.2. Again, from Table 8.2, the DC power flow model gives *very* optimistic results in comparison with the AC power flow model counterpart.

Table 8.2: System Annualized Indices of the Modified IEEE RTS

Power Flow Model	$\hat{q}$	$\hat{\rho}$ MW	$\hat{\phi}$ occ./yr	$\hat{\tau}$ hour
AC	0.44337	20.13860	63.82885	0.00695
DC	0.07141	10.52347	17.76162	0.00402

Since there are significant differences in the values of the indices for different power flow models, two case studies have been performed by gradually stressing the transmission lines to investigate the effects of the voltage and reactive power limits on the reliability indices and to compare the results of the AC and DC power flow models.

8.3.1.1 Case Study I: Gradually Increasing the Generation and Load Levels

In this case study, the generation and load levels are increased gradually to track the behavior of system indices. The annualized reliability indices are shown in Table 8.3. The first two columns of Table 8.3, show the factors by which the load and generation are increased respectively. From Table 8.3, not much change in the system EDNS index between the IEEE

Table 8.3: System Annualized Indices for Case I: Effect of Gradually Increasing the Generation and Load Levels

Loading Factor	Generation Factor	$\hat{q}$	$\hat{\rho}$ MW	$\hat{\phi}$ occ./yr	$\hat{\tau}$ hour
1.000	1.000	0.10427	17.37479	22.76247	0.00458
1.080	1.100	0.09245	15.73231	20.50596	0.00451
1.160	1.200	0.07459	13.91987	17.03678	0.00438
1.240	1.300	0.06243	13.07068	16.30765	0.00383
1.320	1.400	0.05668	12.99306	14.51361	0.00391
1.400	1.500	0.05551	12.74350	14.54252	0.00382
1.408	1.600	0.06897	12.51458	18.99008	0.00363
1.560	1.700	0.11062	13.18529	25.88540	0.00427
1.640	1.800	0.13719	14.96639	30.11179	0.00456
1.680	1.850	0.15788	15.37179	36.89292	0.00428
1.720	1.900	0.17134	16.72898	43.63865	0.00438
1.740	1.925	0.19511	16.66352	45.35073	0.00430
1.760	1.950	0.23595	17.61181	51.25988	0.00460
1.780	1.975	0.35426	18.56049	59.52425	0.00595
1.800	2.000	0.44337	20.13860	63.82885	0.00695

RST and Modified IEEE RTS. System loss of load probability and loss of load frequency indices are smoothly increasing with the increase in the loading and generation levels until the load level reaches around 170% of the peak load. After this point, these indices show a sharp increase. This sudden increase can be attributed to the voltage and reactive power

Table 8.4: System Annualized Indices for Case II: Effect of Gradually Increasing the Load Levels and Fixing the Generation

Loading Factor	Generation Factor	$\hat{q}$	$\hat{\rho}$ MW	$\hat{\phi}$ occ./yr	$\hat{\tau}$ hour
1.000	2.000	0.00139	0.00800	0.37248	0.00373
1.080	2.000	0.00171	0.02570	0.68971	0.00248
1.160	2.000	0.00185	0.04468	0.85359	0.00217
1.240	2.000	0.00202	0.07438	0.85251	0.00237
1.320	2.000	0.00201	0.09948	0.82788	0.00243
1.400	2.000	0.00272	0.20431	1.23875	0.00220
1.480	2.000	0.00557	0.40744	2.55331	0.00218
1.560	2.000	0.01041	1.05772	4.68652	0.00222
1.640	2.000	0.04629	2.97801	16.07442	0.00288
1.680	2.000	0.08679	4.68413	23.47966	0.00412
1.720	2.000	0.12261	7.91592	27.23764	0.00450
1.740	2.000	0.14321	10.02282	33.99955	0.00421
1.760	2.000	0.18729	12.58832	42.44476	0.00441
1.780	2.000	0.22284	15.67655	49.43979	0.00451
1.800	2.000	0.44337	20.13860	63.82885	0.00695

limits as it is explained in section 8.3.3.

8.3.1.2 Case Study II: Gradually Increasing the Load Level and Keeping the Generation Level Constant

This case study is similar to the case study I except that the generation level is kept constant by a factor of 2. The reason of performing this case study is that in Case Study I, both generation and load levels are increasing and the point at which the indices start sharply increasing due to load effect is difficult to detect. The annualized reliability indices are shown in Table 8.4.

119
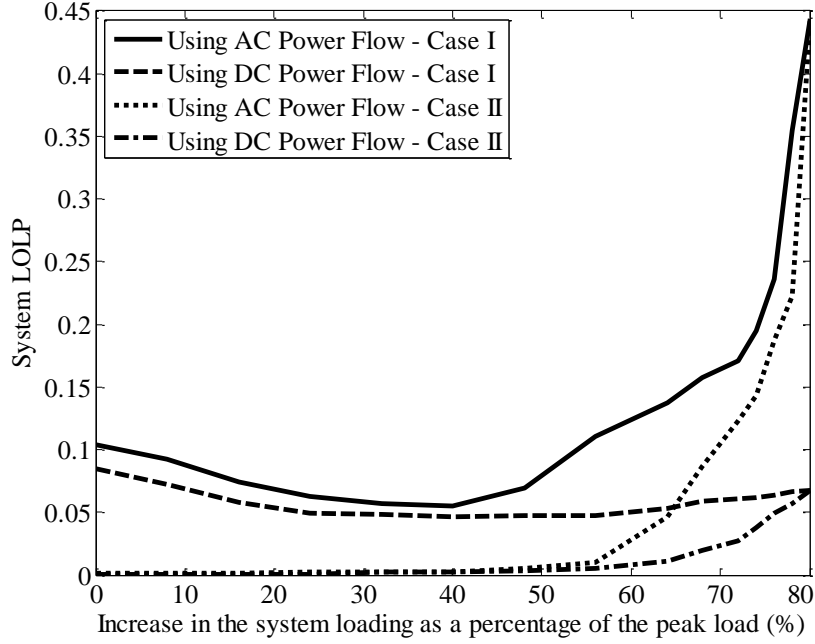
Figure 8.1: System loss of load probability (LOLP) index profile against the change in the system loading level

From Table 8.4, the system EDNS index smoothly increases and system loss of load probability and loss of load frequency indices are smoothly increasing as the load level increases until the load level reaches around 145% of the peak load. After this point, these indices increase sharply. Also, a very sharp increase for these indices happens after around 175% of the peak load. Again, this sudden increase can be attributed to the voltage and reactive power limits as it is explained in subsection 8.3.3.

8.3.2 Comparison with the DC Power Flow Model

To compare the results of the reliability indices with those found using the DC power flow model, the analyses of the above case studies were repeated using the DC power flow model. To better visualize the differences in these values, the results of the system loss of load probability index are depicted in Figure 8.1.
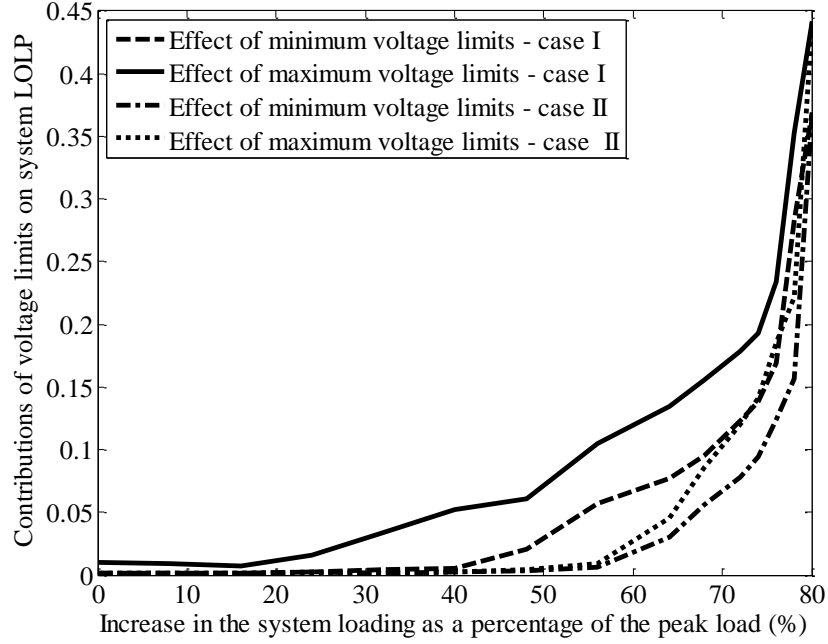
Figure 8.2: Contributions of the voltage limit violations on the system loss of load probability (LOLP) index against the change in the system loading level

From Figure 8.1, it is obvious that the DC power flow model closely depicts the AC power flow model, although optimistic, until the load reaches around 145% of the base peak load level. After this point, the differences between the results of using the AC and DC power flow models are significant where the results of the DC power flow are *very* optimistic.

8.3.3 Effects of Voltage and Reactive Power Limits on the Reliability Indices

From the above results, after a certain loading level, the two power flow models produce significantly different results. Several factors may cause this difference. The effects of the voltage and reactive power constraints on the loss of load probability index are investigated through tracking the contributions of these constraints and the estimation of the proposed indices of the voltage and reactive power limits.
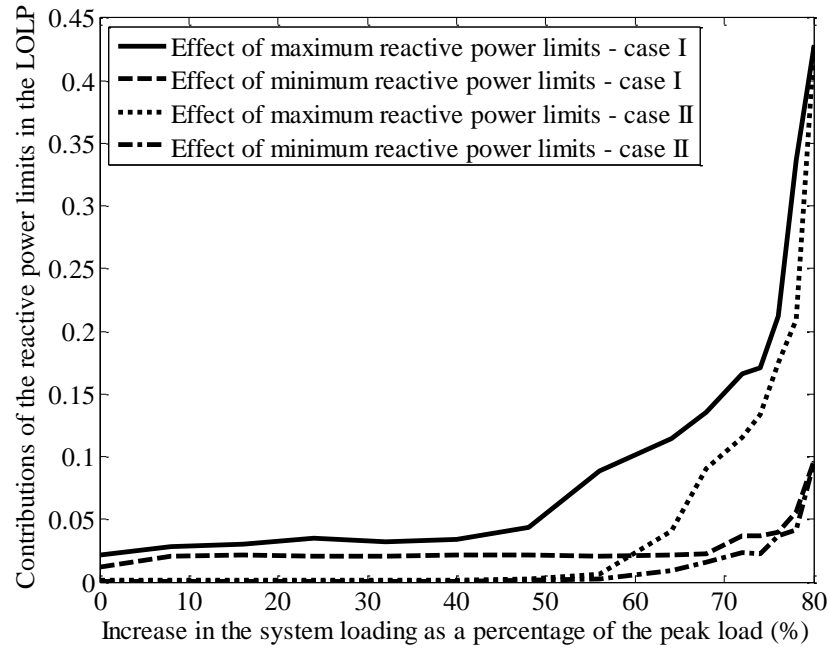
Figure 8.3: Contributions of the reactive power limit violations on the system loss of load probability (LOLP) index against the change in the system loading level

8.3.3.1 Contributions of the Voltage and Reactive Power Constraints

The contributions of the voltage limit violations on the system loss of load probability index against the change in the system loading level are shown in Figure 8.2. The contributions of the reactive power limit violations on the system loss of load probability index against the change in the system loading level are shown in Figure 8.3.

The results totally agree with the observations of the sharp increase in the loss of load probability and loss of load frequency indices using AC power flow model as it is shown in sections 8.3.1.1 and 8.3.1.2. The contributions of the voltage and reactive power violations are very small until the load level reaches about 145% of the original load level for the Case Study I and 170% for the Case Study II. Also, if the contributions of the voltage and reactive power violations are subtracted from the loss of load probability index, both models would produce similar results.

8.3.3.2 Indices of the Voltage and Reactive Power Limits

During the simulation, if the voltage or reactive power limits contributes in the load curtailment, the related index is updated according to (8.2). The results of these indices of the Modified IEEE RTS are shown in Table 8.5. From Table 8.5, it is clear that the maximum voltage limit at bus 2 has contributed in almost all the failure states. Maximum voltage limits at buses 7, 13, 21 and 22 have contributed in around 80% of the failure states. One of the possible solutions is to install condensers at these buses. Minimum voltage limit at bus 6 has contributed in around 83% of the failure states. One possible solution is to add a reactor at this bus. Maximum reactive power limit at buses 2, 3 and 15 have contributed in around 90% of the failure states. The minimum reactive power limit at bus 6 has contributed in around 15% of the failure states.

8.3.3.3 Relaxing Voltage Constraints

In this part, the voltage limit constraints are relaxed to investigate the effects of these constraints on the reliability indices of the Modified IEEE RTS. Figure 8.4 shows the profile of the loss of load probability index with relaxing the voltage constraints. The results of the system indices with relaxing voltage constraints are given in Table 8.6. From Figure 8.4 and Table 8.6, it is clear that relaxing voltage limit constraints significantly reduces system indices. However, even with relaxing these constraints, the values of these indices still high in comparison with DC power flow counterpart. This can be related to the fact that the DC power flow model ignores the losses in the lines and in the case of the AC power flow, voltage constraints have been relaxed without increasing the reactive power support.

Table 8.5: Contributions of Voltage and Reactive Power Constraints

Bus No	vi_{max}	vi_{min}	ϱi_{max}	ϱi_{min}
1	0.15438	0.00000	0.00684	0.00004
2	0.99643	0.00000	0.84201	0.00000
3	0.00059	0.00941	0.96751	0.00000
4	0.00002	0.00016	–	–
5	0.00002	0.00007	–	–
6	0.00011	0.83354	0.00309	0.15427
7	0.85299	0.00000	0.03379	0.00000
8	0.00000	0.04804	–	–
9	0.00011	0.00787	–	–
10	0.04770	0.00000	–	–
11	0.00000	0.00034	–	–
12	0.00000	0.00598	–	–
13	0.78751	0.00000	0.12792	0.00000
14	0.00259	0.00435	0.03030	0.00002
15	0.18674	0.00000	0.91008	0.00015
16	0.07582	0.00050	0.19863	0.08940
17	0.00011	0.00000	–	–
18	0.20134	0.00000	0.08019	0.00000
19	0.00018	0.00000	–	–
20	0.00050	0.00000	–	–
21	0.82095	0.00000	0.32305	0.00000
22	0.29347	0.00007	0.00003	0.00002
23	0.82510	0.00402	0.02226	0.00007
24	0.00029	0.04100	–	–

8.3.4 Sensitivity Analysis

The results of the sensitivity analyses of the EDNS index with respect to the voltage and reactive power constraints are shown in Table 8.7. The following points can be observed
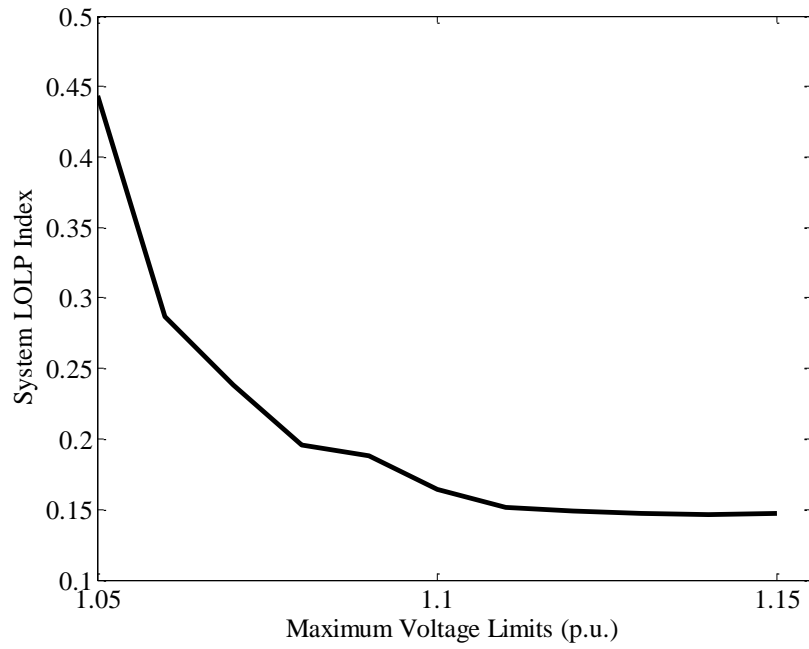
Figure 8.4: The profile of system loss of load probability (LOLP) index with relaxing voltage limit constraints

Table 8.6: Reliability Indices with Relaxing Voltage Limit Constraints

Voltage Max.	Voltage Min.	$\hat{q}$	$\hat{\rho}$ MW	$\hat{\phi}$ occ./yr	$\hat{\tau}$ hour
1.05	0.95	0.44341	19.63547	62.98836	0.00704
1.06	0.94	0.28647	18.52728	58.25106	0.00492
1.07	0.93	0.23826	18.10026	45.03072	0.00440
1.08	0.92	0.19594	17.13641	44.27397	0.00443
1.09	0.91	0.18810	16.55377	42.44361	0.00443
1.10	0.90	0.16416	16.71187	36.94868	0.00444
1.11	0.89	0.15108	16.40434	33.24840	0.00454
1.12	0.88	0.14926	16.21602	33.35913	0.00447
1.13	0.87	0.14719	15.83632	32.79869	0.00449
1.14	0.86	0.14642	15.60547	32.05549	0.00457
1.15	0.85	0.14687	15.68066	32.06075	0.00458

Table 8.7: Sensitivity Analyses of the Severity Index with respect to the Voltage and Reactive Power Constraints

Bus	Sensitivity of the Severity Index with respect to:			
No	V_{max}	V_{min}	Q_{max}	Q_{min}
1	0.32604	0.00000	0.00003	0.00001
2	1.35209	0.00000	0.01412	0.00000
3	0.00002	0.17834	0.14772	0.00000
4	0.00000	0.00431	–	–
5	0.00000	0.00102	–	–
6	0.00005	10.3881	0.02302	0.16863
7	0.11922	0.00000	0.00088	0.00000
8	0.00000	0.10789	–	–
9	0.00000	0.02155	–	–
10	0.02656	0.00000	–	–
11	0.00000	0.00126	–	–
12	0.00000	0.03430	–	–
13	0.31398	0.00000	0.00579	0.00004
14	0.00745	0.00453	0.00120	0.00001
15	0.09631	0.00000	0.02306	0.00000
16	0.06129	0.00095	0.00106	0.00164
17	0.00000	0.00000	–	–
18	0.06080	0.00000	0.00071	0.00047
19	0.00000	0.00000	–	–
20	0.00000	0.00000	–	–
21	0.81786	0.00000	0.00460	0.00000
22	0.14240	0.00000	0.00000	0.00000
23	0.51735	0.00125	0.00000	0.00005
24	0.00056	0.25576	–	–

from the sensitivity analyses: (a) bus 2 has the highest effect in terms of maximum voltage limit, therefore, the planner may consider installing a condenser at bus 2, (b) the minimum voltage limit at bus 6 has the highest effect on the EDNS index, therefore, the planner may consider installing a reactor, (c) bus 3 has the highest effect in terms of maximum reactive power limit, and (d) bus 6 has the highest effect in terms of minimum reactive power limit. It should be noted that the voltage sensitivity analyses are based on the p.u. values.

8.4 Summary

This chapter has investigated the effects of the voltage and reactive power constraints on power system reliability through developing expressions and performing sensitivity analyses of the EDNS index with respect to these constraints. Also, four indices were proposed to address the contributions of the voltage and reactive power constraints on system load curtailments. Extensive studies on the IEEE RTS and the Modified IEEE RTS were conducted to investigate the effects of the voltage and reactive power constraints on the power system reliability indices. Several case studies were performed through gradually stressing the transmission lines to track the profile of the reliability indices with increasing system loading level. A comparison between the use of the AC and DC power flow models in the composite system reliability studies are provided to test the effects of ignoring the voltage and reactive power constraints. The results show that, for the cases where the system is stressed, the accuracy of the DC power flow in evaluating the reliability indices is deteriorated. Also, the state space reduction technique has been used to reduce the computation time and burden.

Chapter 9

Hardening Power Systems Against Cascading Failures Based on Risk Sensitivity Analysis

9.1 Introduction

In response to the rapid growth of the global economics, large power grids are interconnected in order to provide the required energy. As a result of these interconnections, the number of failures also increases and may spread through these interconnections and cause cascading failures. Large blackouts in power system networks are rare in nature, however they usually start with a small triggering event that by successive sequence can cascade and develop a complete blackout. Cascading failures in power systems have been recently encountered more frequently. Examination of catastrophic events such as the August 14, 2003 blackout shows that many factors were involved in the development of the cascading failure. These factors can be classified into three categories: physical behavior of the networks, software failures and operators' mistakes. Among the physical behavior problems of the networks are overloading, inadvertent tripping, transient instability, voltage collapse, etc. Such factors are interrelated and their effect cannot be separated from each other. For instance, overloading may cause

inadvertent tripping and tripping of loaded lines may cause voltage collapse and/or transient instability. An effort to address all of these factors faces many burdens such as modeling and computational time. Most of current cascading failure mitigation methods can capture only a subset of the cascading failure phenomena mechanisms. This chapter focuses on using the sensitivity of the reliability risk index with respect to voltage limits and reactive power reserve.

9.2 Sensitivity Analysis-based Cascading Failure Mitigation

This chapter introduces a method based on risk sensitivity analysis to determine strategies to harden power systems against catastrophic failures. This method utilizes risk sensitivity analysis in mitigating the cascading failures in power systems. In other words, the proposed method utilizes sensitivity analysis of the risk index with respect to the control variables to identify vulnerabilities that can be corrected by strategic or tactical measures. For any initiating event, the sensitivity of the risk of load curtailments with respect to the power quality constraints such as voltage and reactive power is derived, and thereby preventive/correction actions are determined. In addition to the insertion of compensation devices, rescheduling of generation is considered to increase the reactive power reserve. In order to evaluate the sensitivity of the risk index with respect to the power quality constraints, voltage and reactive power constraints are incorporated with the optimization problem with an objective of minimum load curtailments.

Cascading failures usually occurs as a sequence of events within a time horizon of seconds to minutes and in the best scenarios the time horizon is hours. In order to evaluate

the sensitivity of the risk index with respect to the power quality within a short time, the linearized power flow model that accounts for voltage and reactive power was used (chapter 2). The linearized power flow model was incorporated with a linear programming optimization problem with objective of minimum load curtailments. For any initiating event, the sensitivity of the risk of load curtailment with respect to the control variables is used to mitigate the risk of cascading failures. The risk sensitivity was combined with the WORMS and the Dynamic Decision-Event Tress (DDET) techniques for searching for the chain of the events and preventing the risk of the cascading failures.

From the sensitivity of the risk index with respect to voltage limits and reactive power reserve, generation rescheduling can be performed to move the system from being close to a voltage collapse to a state where the system resides within the safe operating limits. For example, if one of the expected next events may cause the voltage at a certain bus will be less than or larger than the operating limits, the remedial action can be reactive power compensation at that bus. However, if there is no reactive power compensator nearby that bus, the real power output of generators that are close to that bus have to be reduced to increase the reactive power reserve. This chapter provides suggestions for the control action but specifically identifying which corrective action should be performed. This model was applied on the IEEE RTS and the results are presented.

9.3   Remedial Actions

A remedial action scheme based on the sensitivity analysis with economic dispatch helps the operator in the control room to choose an action that appropriate for the conditions on hand. The proposed sensitivity analysis-based remedial action scheme can be combined with

the other tools using multi-decision-making techniques to choose the "best" option that has minimum risk and minimum cost. The remedial action scheme can be run periodically as well as after every triggering event. From the results of the analyzer (sensitivity analysis of the risk index with respect to voltage limits and reactive power reserve), a remedial action scheme produces a list of actions that can alleviate the violation if there is any.

The remedial action scheme is intended to act as a preventive/corrective action control. The ability of distinguishing between these two actions depends upon the initial conditions of the system and the triggering events. For example, in case there is no disturbance, the remedial action scheme examines the designated contingencies for possible voltage limit violations. In case of possible violations, the scheme lists possible generation rescheduling alternatives based on the sensitivity of the risk index with respect to control parameters and the best action can be chosen based on multi-decision-making techniques. Possible actions from the preventive action scheme are insertion of reactive power compensation and generation rescheduling. The preventive action scheme can help operators to discard the unsafe alternatives. Also, the suggested actions can be combined with the other tools and control parameters such as equipment actuation time, cost, available means, etc. using multi-decision-making techniques.

In case of corrective action mode, the scheme can be used to prevent the possibility of cascading failures. The corrective action scheme is less costly than the preventive action; however, it is the last defense line and if the correction actions suggested by this scheme cannot be applied, the system more likely to go under cascading failures. Therefore, a careful selection of the proposed actions needs to be implemented in this scheme. Possible actions from the corrective action scheme are generation rescheduling and load shedding.

In many situations where loss of one of the critical lines may cause the system to go under

131

cascading failures and a fast action needs to be initiated. Based on the preventive action scheme, the power flowing in the critical lines can be alleviated by generation rescheduling but this might be costly prohibitive. In such cases, the critical lines will be allowed to work at their power transfer limits and perform corrective action control in case of tripping of these lines. The most commonly control actions is one or combination of generation tripping, load shedding and braking resistor insertion.

9.4   Case Studies

The proposed formulation was applied on the modified IEEE RTS. System's data are given in the appendix.

It is well known that the transmission lines of the IEEE RTS are very reliable and they have high power carrying capabilities in comparison with the loading level of the system. The contributions of the failures of these transmission lines and their capacity limits on the annual and annualized indices are very small and can be ignored $[17, 99, 100]$. For instance, the annualized LOLP index of the IEEE RTS using DC load flow model is 0.08344. On the other hand, if we relax the power carrying capability limits and assume the transmission lines are perfectly reliable, the LOLP becomes 0.0829. The modified IEEE RTS is the same as the IEEE RTS except that the generation is multiplied by 2.0 and the loads are multiplied by 1.8 to stress the transmission lines. However, these modifications cause the voltage limit at bus 3 to contribute in every sampled state. We have added a 30 MVar synchronous condenser at bus 3.

In evaluating the sensitivity of the risk index with respect to the control variables, the state space reduction technique was not able to entirely classify the state space into success

and failure subspaces. This can be interpreted as the unclassified subspace has failure states with relatively high probability but with relatively small load curtailments. This also can be attributed to the fact that failure states that are located far from the origin (all components are in the down state) have high probability and small load curtailments. Therefore, the proposed dynamically directed binary particle swarm optimization search method was used to search for the unclassified subspace. To investigate the benefits of the state space reduction technique and the dynamically directed binary particle swarm optimization search method, we have performed the same a case study on the modified IEEE RTS using Monte Carlo simulation. The computation time using the state space reduction technique with the dynamically directed binary particle swarm optimization search method was around 45% less than the computation time using Monte Carlo simulation.

The sensitivities of the risk index of the modified IEEE RTS with respect voltage and reactive power limits are shown in Table 9.1, Table 9.2, Table 9.3 and Table 9.4.

Table 9.1: Sensitivity of the risk index with respect to minimum reactive power limits for the modified IEEE RTS

Power limit	Minimum Reactive Power Limit				
Bus No.	22	21	16	18	15
Value	-0.00078	-0.00045	-0.00007	-0.00006	-0.00004

Table 9.2: Sensitivity of the risk index with respect to maximum reactive power limits for the modified IEEE RTS

Power limit	Maximum Reactive Power Limit				
Bus No.	6	14	16	13 & 15	1
Value	-0.00362	-0.00036	-0.00014	-0.00005	-0.00003

Table 9.3: Sensitivity of the risk index with respect to under voltage limits for the modified IEEE RTS system

Voltage limit	Minimum Voltage Limit				
Bus No.	3	8	6	24	7
Value	-0.06538	-0.03226	-0.01649	-0.01345	-0.01313
Bus No.	4	18	20	19	13
Value	-0.00795	-0.00218	-0.00032	-0.00027	-0.00032

Table 9.4: Sensitivity of the risk index with respect to over voltage limits for the modified IEEE RTS system

Voltage limit	Maximum Voltage Limit				
Bus No.	1	2	13	14	10
Value	-0.03888	-0.02926	-0.02710	-0.01370	-0.01228
Bus No.	6	23	7	22	15
Value	-0.01205	-0.01157	-0.00586	-0.00335	-0.00075

Form Table 9.1, we can see that among the minimum reactive power limits, bus 22 has the highest effect on the risk index. Also, buses 15, 16, 18, 21 and 22 are generation buses. Therefore, one of the options to harden this system against catastrophic failures is to reschedule the generation at these buses to increase the minimum reactive power limits.

Table 9.2 shows the effect of maximum reactive power limits on the risk index. Buses 1, 13, 15 and 16 are generator buses. Again, one of the options to harden this system against catastrophic failures is to reschedule the generation at these buses to increase the maximum reactive power limits. Bus 14 has a synchronous condenser. Another condenser may be added at this bus. At bus 6 there is a fixed reactor with 100 MVar. A condenser may be

added at this bus.

Table 9.3 and Table 9.4 show the effect of under and over voltage limits on the risk index. The buses that hit the limits consist of load and generation buses. At load buses that have only under voltage problems, condensers may be added. At load buses that have only over voltage problems, reactors may be added. As in the case of the effect of reactive power limits, at generation buses that have under or over voltage problems or both, generation rescheduling to increase the reactive power margin may solve the problem. Buses 6, 7 and 13 appear in both under and over voltage violations. These buses have special property. Bus 6 is connected to bus 10 through a cable with high line susceptance. The high line susceptance makes bus 6 sensitive to loading levels and line status. Buses 7 and 13 are connected with a line with capacity of 175 MVA and it is the only line connects bus 7 to the rest of the system. Any failure in this line, the system will be separated.

9.5 Summary

Several power system networks operate at their capacity and voltage limits and a tool to harden power systems against cascading failures is of necessity. A risk sensitivity analysis with respect to voltage and reactive power limits is introduced in this chapter. To account for voltage and reactive power constraints, the linearized power flow model was used and incorporated with a linear programming optimization problem with the objective of minimum load curtailments to calculate the sensitivity of the reliability risk index with respect to voltage limits and reactive power reserve. The most vulnerable components as well as the most buses that have voltage collapse and reactive support problems were identified. The results obtained from the risk sensitivity analysis are used to harden power systems against

cascading failures. In addition, these results can be used in preventive or corrective remedial actions. It is noteworthy pointing out here that the method presented in this chapter differs from the existing cascading failure mitigation methods in the sense that it evaluates the sensitivity of the risk index with respect to voltage and reactive power limits for N-k events, instead of considering sequence of events.

In performing the sensitivity analyses, large number of states has to be tested. The state space reduction approach in conjunction with the dynamically directed particle swarm optimization search method was used to reduce the search space, and thereby speed up the computations. The proposed method was applied on the modified IEEE RTS. The results of the sensitivity analysis of the risk index with respect to voltage and reactive power limits have identified the buses that have most effect on system availability and possibility of cascading failures.

Chapter 10

Conclusions and Future Work

Summaries of the findings have been provided at the end of each chapter. These summaries discuss specific findings related to each chapter. This chapter provides a general conclusion about the methods that have been used, the general outcomes of this work and suggestions. Also, this chapter provides possible future developments that can be built on or added to the presented work.

10.1   Concluding Remarks

The objective of this work was to develop a comprehensive formulation of the sensitivity analysis and an efficient solution algorithms and methods to decrease the computation burden. The work presented in this thesis uses sensitivity analysis-based method to develop strategies to improve power system reliability. Lagrange multipliers were used in estimating the sensitivity of the reliability indices with respect to component parameters. The Lagrange multipliers can be obtained from the dual solution of a standard linear/non-linear programming problem. Three power flow models were utilized in modeling power system networks, namely, DC power flow model, AC power flow model and a linearized power flow model. A state space reduction technique in conjunction with a dynamically directed particle swarm optimization search method was used to reduce the computational time and burden.

The state space reduction technique, which is presented in chapter 4, was proposed and

applied to reduce the search space. This technique is conservative in that not all the failure states can be captured and no success state was classified as failure state. The state space reduction technique classifies the state space into three subspaces, definite failure subspace, definite success subspace and unclassified subspace. An intelligent search method based on a dynamically directed binary particle swarm optimization was developed and used to search for failure states in the unclassified subspace. From the failure states, which were captured by the state space reduction technique and the dynamically directed binary particle swarm optimization search method, the reliability indices and their sensitivities with respect to component parameters were calculated.

An element key in using binary particle swarm optimization in composite system reliability evaluation is the selection of weighting factors of the objective function. These weighting factors are system dependent and, therefore, their appropriate values should be carefully selected in order to prevent the swarm from being trapped to one corner of the state space. An effective particle swarm optimization search method was proposed and used for reliability assessment of composite systems. The proposed method adjusts the weighting factors associated with the objective function in a dynamic fashion so that the swarm would always fly on the desired search space rather of being trapped to one corner of the search space.

The effectiveness of the proposed methods was tested on several standard test systems and the results correspond closely with those obtained using Monte-Carlo simulation, while requiring lower computational burden. The proposed methods were applied on several practical problems such as the effects of the voltage and reactive power limits on power system reliability, the effects of imposing the regulations of reducing the emissions from power generation, and hardening power systems against cascading failures.

The effects of the voltage and reactive power constraints on power system reliability

were investigated through developing expressions and performing sensitivity analyses of the expected demand not supplied (EDNS) index with respect to these constraints. Four indices were proposed to address the contributions of the voltage and reactive power constraints on system load curtailments. Extensive studies on the IEEE RTS and the Modified IEEE RTS were conducted to investigate the effects of the voltage and reactive power constraints on the power system reliability indices. Several case studies were performed through gradually stressing the transmission lines to track the profile of the reliability indices with increasing system loading level. A comparison between the use of the AC and DC power flow models in the composite system reliability studies are provided to test the effects of ignoring the voltage and reactive power constraints. The results show that, for the cases where the system is stressed, the accuracy of the DC power flow in evaluating the reliability indices is deteriorated.

The effects of the inclusion of the emission constraints were investigated through performing sensitivity analysis of the EDNS index with respect to the emission constraints. Most of the emission studies in the literature have focused on minimizing emissions through economic dispatch and introducing new concepts to solve multi-objective functions. This work introduced a framework for evaluating the effect of the emission rates and allowances on system reliability and determining the sensitivity of commonly used reliability indices to equipment and emission constraints. From the sensitivity results, components can be ranked from reliability point of view. Therefore, components that have the highest effect on system reliability can be identified. Also, if the reliability of the system needs to be improved, the sensitivity analyses can identify which component to increase its emission limit. Inclusion of emission constraints in planning studies helps guide investment strategies with respect to reconstruction or upgrades.

Hardening power systems against cascading failures by improving voltage stability was also introduced. The sensitivity of the reliability EDNS index with respect to voltage limits and reactive power reserve was used to identify the most vulnerable components as well as the most buses that have voltage collapse and reactive support problems. In addition, the results of the sensitivity analysis can be used in establishing preventive or corrective remedial action schemes.

10.2   Future Work

Although the results presented in this thesis show the powerfulness of the use of the sensitivity analysis in power system planning and operation and the effectiveness of the use of state space reduction technique with the population-based intelligent search methods, the work could be extended and further developed by considering some of the following points:

1. Adding another constraints: Another constraints can be added to the system operating constraint such as transient stability limits, voltage stability limits, operating cost, etc. Inclusion of such constraints would increase the complexity of the optimization problem but it would make the solution for optima more realistic.

2. Using different population-based intelligent search methods: In this thesis, we have used particle swarm optimization due to its simplicity; the other population-based intelligent search methods could be used and a comparison between these methods in terms of efficiency and reduction in the computational time could be established.

3. Combining the proposed state space reduction method with the existing methods: In this work, we have used minimum generation vector for determining the boundary of

the success subspace. The state space pruning could be combined with the proposed method to decrease the size of the unclassified subspace.

4. Determining the effective region of the Lagrange multipliers: In this work, we have used the value of the Lagrange multipliers in performing sensitivity analysis, but without accounting for the effective region. The effective region can be defined as the region in which the Lagrange multipliers of the corresponding constraints are binding. In other words, there will be a limit for a Lagrange multiplier after which the corresponding constraint becomes redundant.

APPENDIX

Derivation of the Sensitivity Relationships

Here, only the derivations of the sensitivity of the LOLP index with respect to reliability parameters are provided. The remaining sensitivities for LOLF and EDNS can be easily derived in the same manner. Some of the derivations presented below have been adapted from [32]. However, this reference does not provide the complete derivations.

Sensitivity of LOLP to Component Failure Probability

$$\partial LOLP/\partial u_i$$

$$= \sum_{x \in X} \{[\partial I_f(x)/\partial u_i]P(x) + I_f(x)[\partial P(x)/\partial u_i]\}$$

$$= \sum_{x \in X} I_f(x)\{[\partial [P(S_1)P(S_1) \cdots P(S_i) \cdots P(S_m)]/\partial u_i]\}$$

$$= \sum_{x \in X} I_f(x)P(x)[1/P(S_i)][\partial P(S_i)/\partial u_i]$$

If $S_i = 1$,

$$[1/P(S_i)][\partial P(S_i)/\partial u_i]$$

$$= (1/P(S_i = 1))(\partial P(S_i = 1)/\partial u_i)$$

$$= (1/a_i)(\partial a_i/\partial u_i) = -1/a_i = -S_i/a_i$$

If $S_i = 0$,

$$[1/P(S_i)][\partial P(S_i)/\partial u_i]$$

$$= (1/P(S_i = 0))(\partial P(S_i = 0)/\partial u_i)$$

$$= (1/u_i)(\partial u_i/\partial u_i) = 1/u_i = (1 - S_i)/u_i$$

Therefore, in general,

$$[1/P(S_i)][\partial P(S_i)/\partial u_i] = (1 - S_i)/u_i - S_i/a_i$$

$$= (1/u_i) - S_i/(a_i u_i)$$

Then,

$$\partial LOLP/\partial u_i = \sum_{x \in X} I_f(x)P(x)[(1/u_i) - S_i/(a_i u_i)]$$

Sensitivity of LOLP to Component Failure Rate

$$\partial LOLP/\partial \lambda_i$$

$$= \sum_{x \in X} \{[\partial I_f(x)/\partial \lambda_i]P(x) + I_f(x)[\partial P(x)/\partial \lambda_i]\}$$

$$= \sum_{x \in X} I_f(x)\{[\partial[P(S_1)P(S_1)...P(S_i)...P(S_m)]/\partial \lambda_i]\}$$

$$= \sum_{x \in X} I_f(x)P(x)[1/P(S_i)][\partial P(S_i)/\partial \lambda_i]$$

144

If $S_i = 1$,

$$[1/P(S_i)][\partial P(S_i)/\partial \lambda_i]$$

$$= (1/P(S_i = 1))(\partial P(S_i = 1)/\partial \lambda_i)$$

$$= (1/a_i)(\partial a_i/\partial \lambda_i) = -S_i/(\lambda_i + \mu_i)$$

If $S_i = 0$,

$$[1/P(S_i)][\partial P(S_i)/\partial \lambda_i]$$

$$= (1/P(S_i = 0))(\partial P(S_i = 0)/\partial \lambda_i)$$

$$= (1/u_i)(\partial u_i/\partial \lambda_i)$$

$$= (a_i/u_i)(1/(\lambda_i + \mu_i))$$

$$= (a_i/u_i)((1 - S_i)/(\lambda_i + \mu_i))$$

Therefore, in general,

$$[1/P(S_i)][\partial P(S_i)/\partial \lambda_i]$$

$$= -S_i/(\lambda_i + \mu_i) + (a_i/u_i)((1 - S_i)/(\lambda_i + \mu_i))$$

$$= a_i/\lambda_i - S_i/\lambda_i$$

Then,

$$\partial LOLP/\partial \lambda_i = \sum_{x \in X} I_f(x) P(x)[a_i/\lambda_i - S_i/\lambda_i]$$

145

Sensitivity of LOLP to Component Repair Rate

$\partial LOLP / \partial \mu_i$

$$= \sum_{x \in X} \{[\partial I_f(x)/\partial \mu_i]P(x) + I_f(x)[\partial P(x)/\partial \mu_i]\}$$

$$= \sum_{x \in X} I_f(x)\{[\partial[P(S_1)P(S_1)...P(S_i)...P(S_m)]/\partial \mu_i]\}$$

$$= \sum_{x \in X} I_f(x)P(x)[1/P(S_i)][\partial P(S_i)/\partial \mu_i]$$

If $S_i = 1$,

$$[1/P(S_i)][\partial P(S_i)/\partial \mu_i] = (1/P(S_i = 1))(\partial P(S_i = 1)/\partial \mu_i)$$

$$= (1/a_i)(\partial a_i/\partial \mu_i)$$

$$= (u_i/a_i)(1/(\lambda_i + \mu_i))$$

$$= (u_i/a_i)(S_i/(\lambda_i + \mu_i))$$

If $S_i = 0$,

$$[1/P(S_i)][\partial P(S_i)/\partial \mu_i]$$

$$= (1/P(S_i = 0))(\partial P(S_i = 0)/\partial \mu_i)$$

$$= (1/u_i)(\partial u_i/\partial \mu_i)$$

$$= -1/(\lambda_i + \mu_i) = -(1 - S_i)/(\lambda_i + \mu_i)$$

Therefore, in general,

$$[1/P(S_i)][\partial P(S_i)/\partial\mu_i]$$

$$= (u_i/a_i)(S_i/(\lambda_i + \mu_i)) - (1 - S_i)/(\lambda_i + \mu_i)$$

$$= -a_i/\mu_i + S_i/\mu_i$$

Then,

$$\partial LOLP/\partial\mu_i = \sum_{x \in X} I_f(x)P(x)[-a_i/\mu_i + S_i/\mu_i]$$

Test Systems

IEEE RTS

The IEEE RTS System has been extensively tested for power system reliability analysis [63]. IEEE RTS consists of 24 buses, 38 transmission lines/transformers (33 transmission lines and 5 transformers) and 32 generating units on 10 buses. The total generation of this system is 3405 MW and total peak load is 2850 MW.

Modified IEEE

The modified IEEE RTS System is the same as the original IEEE RTS System except that the generation is doubled and the loads are multiplied by a factor of 1.8. The reason of this modification is because the transmission lines of the original system have high power carry capabilities in comparison with the generation and loading conditions. Therefore, this modification will make the transmission lines more stressed. Also, this modification will allow us to test the robustness of the proposed method.

A Six Bus Hypothetical System

The six bus system is a hypothetical system consists of 16 generating units on two generating buses, five load buses and 9 transmission lines. Line and generation data are given in [64]. The total generation of this system is 240 MW and the total real power load is 185 MW.

The Saskatchewan Power Corporation in Canada

The SPC system is the network of the Saskatchewan Power Corporation in Canada [64]. The system consists of 45 buses, 29 generating units on 8 buses and 71 transmission lines/transformers. Four of the 45 buses are used to represent equivalent assistance from the Manitoba Hydro System. One of these four buses is a fictitious bus that represents the power import from Manitoba Hydro System which is 300 MW. This bus is connected to the other three buses and the sum of the 300 MW is represented by three generating units each of which 100 MW. The total generation is 2530 MW and total load is 1802.5 MW. System data are given in [64].

BIBLIOGRAPHY

BIBLIOGRAPHY

[1] S. Elsaiah, M. Benidris and J. Mitra, "Analytical approach for placement and sizing of distributed generation on distribution systems," *IET Generation, Transmission & Distribution*, vol. 8, no. 6, pp. 1039–1049, Dec. 2013.

[2] T. N. Santos and A. L. Diniz, "A dynamic piecewise linear model for DC transmission losses in optimal scheduling problems," *IEEE Trans. Power Syst.*, vol. 26, no. 2, pp. 508–519, May 2011.

[3] H. Zhang, V. Vittal, G. T. Heydt and J. Quintero, "A mixed-integer linear programming approach for multi-stage security-constrained transmission expansion planning," *IEEE Trans. Power Syst.*, vol. 27, no. 2, pp. 1125–1133, May 2012.

[4] N. Alguacil, A. L. Motto and A. J. Conejo, "Transmission expansion planning: a mixed-integer LP approach," *IEEE Trans. Power Syst.*, vol. 18, no. 3, pp. 1070–1077, Aug. 2003.

[5] Wenyuan Li, *Risk Assessment of Power Systems*. USA, IEEE Press: Wiley-Interscience, 2005.

[6] C. Singh and J. Mitra, "Composite System Reliability Evaluation Using State Space Pruning," *IEEE Trans. on Power System*, vol. 12, no. 1, pp. 471–479, Feb. 1997.

[7] J. Mitra and C. Singh, "Incorporating the DC Load Flow Model in the Decomposition–Simulation Method of Multi-Area Reliability Evaluation," *IEEE Trans. on Power Syst.*, vol. 11, no. 3, pp. 1245–1254, Aug. 1996.

[8] J. Mitra and C. Singh, "Pruning and Simulation for Determination of Frequency and Duration Indices of Composite Systems," *IEEE Trans. on Power Syst.,* vol. 14, no. 3, pp. 899–905, Aug. 1999.

[9] J. He, Y. Sun, D. S. Kirschen, C. Singh and L. Cheng, "State-space partitioning method for composite power system reliability assessment," *IET Gener. Transm. Distrib.*, vol. 4, no. 7, pp. 780–792, 2010.

[10] M. Benidris and J. Mitra, "Composite Power System Reliability Assessment Using Maximum Capacity Flow and Directed Binary Particle Swarm Optimization," Proc. *North American Power Symposium*, pp. 1–6, 2013.

[11] M. Benidris, S. Elsaiah and J. Mitra, "Composite System Reliability Assessment Using Dynamically Directed Particle Swarm Optimization," Proc. *North American Power Symposium*, pp. 1–6, 2013.

[12] S. B. Patra, J. Mitra and R. Earla, "A New Intelligent Search Method for Composite System Reliability Analysis," Proc. of the *IEEE-PES Transmission and Distribution Conference and Exposition*, Dallas, TX, May 21–24, 2006, pp 803–807.

[13] J. Mitra and X. Xu, "Composite System Reliability Analysis Using Particle Swarm Optimization," *IEEE 11th International Conference on Probabilistic Methods Applied to Power Systems (PMAPS),* pp. 548–552, 2010.

[14] L. Wang and C. Singh, "Population-Based Intelligent Search in Reliability Evaluation of Generation Systems With Wind Power Penetration," *IEEE Trans. on Pow. Syst.*, vol. 23, no. 3, pp. 1336–1345, 2008.

[15] J. Mitra and M. R. Vallem, "Determination of storage required to meet reliability guarantees on island-capable Microgrids with intermittent sources," *IEEE Trans. Pow. Syst.*, vol. 27, no. 4, pp. 2360–2367, Nov. 2012.

[16] M. Benidris and J. Mitra, "Reliability and Sensitivity Analysis of Composite Power Systems Under Emission Constraints," *IEEE Trans. Power Syst.*, vol. 29, no.1, pp. 404–412, Jan. 2014.

[17] M. Benidris, S. Elsaiah and J. Mitra, "Sensitivity Analysis in Composite System Reliability Using Weighted Shadow Prices," *IEEE PES General Meeting 2011,* pp. 1–6, Detroit, MI, USA.

[18] A. C. G. Melo, M. V. F. Pereira and A. M. Leite da Silva, "A Conditional Probability Approach to the Calculation of Frequency and Duration Indices in Composite System Reliability Evaluation," *IEEE Trans. Power Syst.*, vol. 8, no. 3, pp. 1118–1125, Aug. 1993.

[19] A. C. G. Melo, M. V. F. Pereira and A. M. Leite da Silva, "Frequency and Duration Calculation in Composite Generation and Transmission Reliability Evaluation," *IEEE Trans. Power Syst.*, vol. 7, no. 2, pp. 469–476, May 1992.

[20] C. Singh, "Calculating the Time-Specific Frequency of System Failure," *IEEE Trans. on Reliability*, vol. R-28, no. 2, pp. 124–126, June 1979.

[21] C. Singh, "Rules for Calculating the Time-Specific Frequency of System Failure," *IEEE Trans. on Reliability*, vol. 30, no. 4, pp. 364–366, Oct. 1981.

[22] R. Billinton and W. Li, *Reliability Assessment of Electric Power Systems Using Monte Carlo Methods*, Plenum Press, New York, USA 1994.

[23] C. Singh and Q. Chen, "Generation System Reliability Evaluation Using a Cluster Based Load Model," *IEEE Trans. on Power Systems*, Vol. 4, No. 1, pp. 102–107, Feb. 1989.

[24] C. Singh and A. Lago-Gonzalez, "Improved Algorithms for Multi-Area Reliability Evaluation Using the Decomposition-Simulation Approach," *IEEE Trans. on Power Systems*, vol. 4, no. 1, pp. 321–328, Feb. 1989.

[25] A. Lago-Gonzalez and C. Singh, "The Extended Decomposition–Simulation Approach for Multi-Area Reliability Calculations," *IEEE Trans. on Power Systems*, vol. 5, no. 3, pp. 1024–1031, Aug. 1990.

[26] C. Singh and Z. Deng, "A New Algorithm for Multi-Area Reliability Evaluation-?Simultaneous Decomposition–Simulation Approach," *Electric Power Systems Research*, vol. 41, no. 2, pp. 129–136, June 1991.

[27] P. Ramanujan, Z. Li, and L. Higham, "Shadow prices versus Vickery prices in multipath routing," *IEEE conference on Information and Communication*, pp. 2956–2960, 2009.

[28] S. Cunda, M. Pereria, L. Pinto and G. Oliveira, "Composite Generation and Transmission Reliability Evaluation in Large Hydroelectric Systems," *IEEE Trans. Power Appar. and Syst.*, vol. 104, no. 10, pp. 2657–2663, Oct. 1985.

[29] G.Li, C. Liu, and H. Salazar, "Forecasting transmission congestion using day-ahead shadow prices," *IEEE Power Syatems Conference*, pp. 1705–1709, 2006.

[30] Z. Hui, Y. Pei, and L. Jie, "Study on the estimating model of shadow prices for national economy evaluation of construction projects," *IEEE, International Conference on Management and Service Science*, pp. 1–4, 2009.

[31] A. C. G. Melo and M. V. F. Pereira, "Sensitivity Analysis of Reliability Indices with Respect to Equipment Failure and Repair Rates," *IEEE Trans. Power Syst.*, vol. 10, no.2, pp. 1014–1021, May 1995.

[32] Y. Zhao, N. Zhou, J. Zhou and X. Zhao, "Research on Sensitivity Analysis for Composite Generation and Transmission System Reliability Evaluation," *IEEE International Conference on Power System Technology*, pp. 1–5, 2006.

[33] T. X. Zhu, "A New Methodology of Analytical Formula Deduction and Sensitivity Analysis of EENS in Bulk Power System Reliability Assessment," *IEEE PES, Power Systems Conference and Exposition, PSCE*, pp. 825–831, 2006.

[34] M. V. F. Pereira and L. M. V. G. Pinto, "Application of Sensitivity Analysis of Load Supplying Capability to Interactive Transmission Expansion Planning," *IEEE Trans. Power Appar. and Syst.*, vol. PAS–104, no.2, pp. 381–389, Feb. 1985.

[35] Z. Deng and C. Singh, "A new approach to reliability evaluation of interconnected power systems including planned outages and frequency calculations," *IEEE Trans. on Power Systems*, vol. 7, no. 2, pp. 734–743, May 1992.

[36] J. Mitra, M. R. Vallem and S. B. Patra, "A Probabilistic Search Method for Optimal Resource Deployment in a Microgrid," Proc. of the *9th International Conference on Probabilistic Methods Applied to Power Systems*, Stockholm, Sweden, June 11–15, 2006.

[37] G. C. Oliveira, M. V. F. Pereira, and S. H. F. Cunha, "A technique for reducing computational effort in Monte Carlo based composite reliability evaluation," *IEEE Trans. on Power Systems*, vol. 4, no. 4, pp. 1309–1315, Nov. 1989.

[38] R. C. Green, Z. Wang, L. Wang, M. Alam, and C. Singh, "Evaluation of Loss of Load Probability for Power Systems Using Intelligent Search Based State Space Pruning," *IEEE 11th International Conference on Probabilistic Methods Applied to Power Systems (PMAPS),* pp. 319–324, 2010.

[39] R. C. Green, L. Wang and C. Singh, "State Space Pruning for Power System Reliability Evaluation Using Genetic Algorithms," *IEEE Power and Energy Society General Meeting,* pp. 1–6, 2010.

[40] D. Zhao and C. Singh, "Modified Genetic Algorithm in State Space Pruning for Power System Reliability Evaluation and Its Parameter Determination," *IEEE North American Power Symposium,* pp. 1–6, 2010.

[41] R. C. Green, L. Wang, Z. Wang, M. Alam, and C. Singh, "Power System Reliability Assessment Using Intelligent State Space Pruning Techniques: A Comparative Study," Proc. *IEEE International Conference on Power System Technology (POWERCON),* pp. 1–8, 2010.

[42] R. C. Green, L. Wang, M. Alam and C. Singh, "State Space Pruning for Reliability Evaluation Using Binary Particle Swarm Optimization," *IEEE/PES Power Systems Conference and Exposition,* pp. 1–7, 2011.

[43] R. C. Green, L. Wang, M. Alam and C. Singh, "An Examination of Artificial Immune System Optimization in Intelligent State Space Pruning for LOLP Estimation," *IEEE North American Power Symposium (NAPS),* pp. 1–7, 2011.

[44] R. C. Green, L. Wang, M. Alam and C. Singh, "Intelligent State Space Pruning Using Multi-Objective PSO for Reliability Analysis of Composite Power Systems: Observations, Analyses, and Impacts," *IEEE Power and Energy Society General Meeting,* pp. 1–8, 2011.

[45] J. Mitra, "Application of Computational Intelligence in Optimal Expansion of Distribution Systems," Proc. of the *IEEE-PES Annual General Meeting*, Pittsburgh, PA, July 20–24, 2008.

[46] J. Mitra, S. B. Patra, M. R. Vallem and S. J. Ranade "Optimization of Generation and Distribution Expansion in Microgrid Architectures," Proc. of the *6th WSEAS International Conference on Power Systems*, Lisbon, Portugal, Sept. 22–24, 2006, pp. 14–21.

[47] S. A. Al-Askari, S. J. Ranade and J. Mitra, "Optimal Allocation of Shunt Capacitors Placed in a Microgrid Operating in the Islanded Mode," Proc. of the *37th annual North American Power Symposium*, Ames, IA, Oct. 23–25, 2005, pp. 406–411.

[48] X. Xu and J. Mitra, "Reliability Evaluation of Composite System Using Bacterial Foraging Algorithm," Proc. of the *17th Power System Computation Conference*, Stockholm, Sweden, August 22–26, 2011.

[49] S. J. Ranade and R. Kolluru and J. Mitra, "Identification of Chains of Events Leading to Catastrophic Failures of Power Systems," Proc. of the *IEEE International Symposium on Circuits and Systems*, 2005, Kobe, Japan, May 23–26, 2005, pp. 4187–4190.

[50] Y. del Valle, G. K. Venayagamoorthy, S. Mohagheghi, J.-C. Hernandez and R. G. Harley, "Particle swarm optimization: basic concepts, variants and applications in power systems," *IEEE Trans. Evol. Comp.*, vol. 12, no. 2, pp. 171–195, Apr. 2008.

[51] M. Benidris and J. Mitra, "Use of Intelligent Search Methods in Performing Sensitivity Analysis of Power System Reliability Indices," Proc. of the *IEEE-PES Annual General Meeting*, Washington, DC, July 27–31, 2014.

[52] R. Earla, S. B. Patra and J. Mitra, "A Particle Swarm Based Method for Composite System Reliability Analysis," Proc. of the *36th annual North American Power Symposium*, Moscow, ID, Aug. 8–10, 2004, pp 294–298.

[53] V. Miranda, L. M. Carvalho, M. A. Rosa, A. M. L. Silva and C. Singh, "Improving Power System Reliability Calculation Efficiency With EPSO Variants," *IEEE Trans. on Pow. Syst.*, vol. 24, no. 4, pp. 1772–1779, 2009.

[54] F. Yang and C. S. Chang, "Optimisation of maintenance schedules and extents for composite power systems using multi-objective evolutionary algorithm," *IET Gener. Transm. Distrib.*, vol. 3, no. 10, pp. 930–940, 2009.

[55] K. Suresh and N. Kumarappan, "Generation maintenance scheduling using improved binary particle swarm optimisation considering aging failures," *IET Gener. Transm. Distrib.*, vol. 7, no. 10, pp. 1072–1086, 2013.

[56] S. Elsaiah, M. Benidris and J. Mitra, *Reliability-Constrained Optimal Distribution System Reconfiguration,* to appear in Computational Intelligence Applications in Modeling and Control, Springer, 2015.

[57] J. Mitra, S. B. Patra, S. J. Ranade and M. R. Vallem, "Reliability-Specified Generation and Distribution Expansion in Microgrid Architectures," *WSEAS Transactions on Power Systems*, vol. 1, no. 8, pp 1446–1453, Aug. 2006.

[58] M. R. Vallem and J. Mitra, "A Particle Swarm-based Method for Reliability-driven DG Deployment and Feeder Augmentation in Microgrids," Proc. of the *15th National Power System Conference*, Mumbai, India, Dec. 16–18, 2008.

[59] J. Mitra, S. B. Patra and S. J. Ranade, "Reliability Stipulated Microgrid Architecture Using Particle Swarm Optimization," Proc. of the *9th International Conference on Probabilistic Methods Applied to Power Systems*, Stockholm, Sweden, June 11–15, 2006.

[60] J. Kennedy and R. Eberhart, "Particle Swarm Optimization," *IEEE International Conference on Neural Networks*, pp. 1942–1948, 1995.

[61] J. Kennedy and R. Eberhart, "A Discrete Binary Version of the Particle Swarm Algorithm," *IEEE International Conference on Computational Cybernetics and Simulation,* pp. 4104–4108, 1997.

[62] B. Li, J. Qu and Y. Cui, "The resources purchase quantity algorithm based on the shadow price and its application in the enterprise management," *IEEE International Conference on Test and Management*, pp. 346–349, 2009.

[63] Reliability Test System Task Force of the Application of Probability Methods Subcommittee, "IEEE Reliability Test System," *IEEE Trans. on Power Apparatus and Systems*, Vol. PAS–98, No. 6, pp. 2047–2054, Nov./Dec. 1979.

[64] R. Billinton and S. Kumar, "Effect of Higher–Level Independent Generator Outages in Composite-System Adequacy Evaluation," *IEE Proceedings on Generation, Transmission and Distribution,* vol. 134, no. 1, pp. 17–26, Jan. 1987.

[65] F. Lee, J. Liao and A. Breipohl, "Coordination of SO2 emission allowance trading, energy and spinning reserve transactions, and consumption of take–or–pay fuels," *IEEE Trans. on Power Systems*, vol. 9, no. 3, pp. 1243–1252, Aug. 1994.

[66] Center for Climate and Energy Solutions. (2013, January). *California Cap–And–Trade Program Summary (1st ed.)* [Online]. Available: http://www.c2es.org/docUploads/calif-cap-trade-01-13.pdf

[67] Regional Greenhouse Gas Initiative, Inc. (2013, February 7). *RGGI States Propose Lowering Regional CO2 Emissions Cap 45%, Implementing a More Flexible Cost–Control Mechanism (1st ed.)* [Online] Available: http://www.rggi.org/docs/PressReleases/PR130207_ModelRule.pdf

[68] L. M. Brown, A. Hanafi and A. Petsonk. (2012). *The EU Emissions Trading System–Results and Lessons Learned (1st ed.)* [Online]. Available: http://www.edf.org/climate/eu-emissions-trading-system-report

[69] J. Kabouris and F. Kanellos, "Impacts of Large–Scale Wind Penetration on Designing and Operation of Electric Power Systems," *IEEE Trans. on Sustainable Energy*, vol. 1, no. 2, pp. 107–114, July 2010.

[70] M. Gent and J. Lamont, "Minimum–Emission Dispatch," *IEEE Trans. on Power Apparatus and Systems*, vol. PAS–90, no. 6, pp. 2650–2660, June 1971.

[71] J. Nanda, L. Hari and M. Kothari, "Economic emission load dispatch with line flow constraints using a classical technique," *IEE Proceedings—Generation, Transmission and Distribution*, vol. 141, no. 1, pp. 1–10, Jan. 1994.

[72] M. AlRashidi and M. El-Hawary, "Emission–Economic Dispatch Using a Novel Constraint Handling Particle Swarm Optimization Strategy," *IEEE Canadian Conference on Electrical and Computer Engineering, CCECE '06.*, pp. 664–669, 2006.

[73] H. Rughooputh and R. Ah King, "Environmental/economic dispatch of thermal units using an elitist multiobjective evolutionary algorithm," *IEEE International Conference on Industrial Technology*, vol. 1, pp. 48–53, 2003.

[74] L. Wang and C. Singh, "Reserve–Constrained Multiarea Environmental/Economic Dispatch Using Enhanced Particle Swarm Optimization," *IEEE, Systems and Information Engineering Design Symposium*, pp. 96–100, 2006.

[75] T. Prasanna and P. Somasundaram, "Fuzzy mutated evolutionary programming based algorithm for combined economic and emission dispatch," *IEEE Region 10 Conference*, pp. 1–5, 2008.

[76] M. Abido, "Environmental/Economic Power Dispatch Using Multiobjective Evolutionary Algorithms," *IEEE Trans. on Power Systems*, vol. 18, no. 4, pp. 1529–1537, Nov. 2003.

[77] J. Choi, S. Jeong, S. Bo, J. Park, A. El-Keib and J. Watada, "CO2, SOx and NOx Emissions Constrained Multi–Criteria–Best Generation Mix Using Fuzzy Set Theory," *IEEE Conference on Large Engineering Systems*, pp. 118–124, 2007.

[78] D. Yamashita, T. Niimura, R. Yokoyama and M. Marmiroli, "Trade–off Analysis of CO2 versus Cost by Multi–objective Unit Commitment," *IEEE PES General Meeting*, pp. 1–6, 2010.

[79] W. Spens and F. Lee, "Interactive search approach to emission constrained dispatch," *IEEE Trans. on Power Systems*, vol. 12, no. 2, pp. 811–817, May 1997.

[80] R. Sun, L. Chen, Y. Song, and Y. Sun, "Generation Expansion Planning based on multi–area reliability exponential analytic model and emission control," *IEEE/PES Transmission and Distribution Conference and Exposition*, pp. 1–6, 2008.

[81] A. Prasai, A. Paquette, Yi Du, R. Harley and D. Divan, "Minimizing emissions in microgrids while meeting reliability and power quality objectives," *IEEE International Power Electronics Conference (IPEC)*, pp. 726–733, 2010.

[82] P. Venkatesh, R. Gnanadass and N. P. Padhy, "Comparison and Application of Evolutionary Programming Techniques to Combined Economic Emission Dispatch With

Line Flow Constraints," *IEEE Trans. on Power Systems*, vol. 18, no. 2, pp. 688–697, May 2003.

[83] J. R. Domike and A. C. Zacaroli, *The Clean Air Act Handbook*, American Bar Association, Chicago, USA, 2011.

[84] W. Graus and E. Worrell, "Trend in efficiency and capacity of fossil power generation in the EU," *Elsevier, Energy Policy*, vol. 37, no. 6, pp. 2147–2160, June 2009. Bar Association, Chicago

[85] X. Yang, Y. Song, G. Wang and W. Wang, "A Comprehensive Review on the Development of Sustainable Energy Strategy and Implementation in China," *IEEE Trans. on Sustainable Energy*, vol. 1, no. 2, pp. 57–65, July 2010.

[86] Y. Kim and B. Ahn, "Multicriteria generation–expansion planning with global environmental considerations," *IEEE Trans. on Engineering Management*, vol. 40, no. 2, pp. 154–161, Aug. 2002.

[87] V. Mendes, S. Mariano, J. Catalao and L. Ferreira, "Emission constraints on short–term schedule of thermal units," *Universities Power Engineering Conference, 39th International*, vol. 2, pp. 1068–1072, 2004.

[88] Z. Yong, "Control of CO2 Emissions of China Under Kyoto Protocol," *IEEE International Conference on Energy and Environment Technology, ICEET*, pp. 32–35, 2009.

[89] A. Farag, S. Al-Baiyat, and T. C. Cheng, "Economic load dispatch multiobjective optimization procedures using linear programming techniques," *IEEE Trans. Power Syst.*, vol. 10, pp. 731–738, May 1995.

[90] D. B. Das and C. Patvardhan, "New multi-objective stochastic search technique for economic load dispatch," *Proc. Inst. Elect. Eng.-Gen. Transm. Dist.*, vol. 145, no. 6, pp. 747–752, 1998.

[91] H. Chang, C. Kuo, J. Jiang and S. Lu, "Generation Dispatch Strategy under Environment Protection Consideration," *IEEE/ACM International Conference on Green Computing and Communications*, pp. 242–247, 2011.

[92] P. L. Noferi, L. Paris "Effects of Voltage and Reactive Power Constraints on Power System Reliability," *IEEE Trans. Power Appar. and Syst.*, vol. PAS-94, no. 2, pp. 482–490, March/April 1975.

[93] W. Qin, P. Wang, X. Han and X. Du, "Reactive Power Aspects in Reliability Assessment of Power Systems," *IEEE Trans. Power Syst.*, vol. 26, no. 1, pp. 85–92, Feb. 2011.

[94] P. Wang, W. Qin, X. Han and X. Du, "Reliability Assessment of Power Systems Considering Reactive Power Sources," *IEEE Power & Energy Society General Meeting*, pp. 1–7, 2009.

[95] W. Qin, P. Wang, J. Song and Z. Wang, "Reactive Power Impact on Reliability of 220kV Taiyuan Power System," *IEEE 11th International Conference on Probabilistic Methods Applied to Power Systems (PMAPS)*, pp. 648–653, 2010.

[96] D. Gaikwad and S. Mehraeen, "Reactive Power Considerations in Reliability Analysis of Photovoltaic Systems," *IEEE Green Technologies Conference*, pp. 1–6, 2012.

[97] C. Singh, T. Pravin, M. P. Bhavaraju and M. Lauby, "A Monte Carlo Tool for Estimating Contingency Statistics," *In Proceedings of the Joint International Power Conference*, vol. 2, pp. 670–674, Athens Power Tech, 1993.

[98] R. Billinton and W. Li, "A System State Transition Sampling Method for Composite System Reliability Evaluation," *IEEE Trans. Power Syst.*, vol. 8, no. 3, pp. 761–770, Aug. 1993.

[99] M. Benidris and J. Mitra, "Composite Power System Reliability Assessment Using Maximum Capacity Flow and Directed Binary Particle Swarm Optimization," *North American Power Symposium,* pp. 1–6, 2013.

[100] M. Benidris, S. Elsaiah and J. Mitra, "Composite System Reliability Assessment Using Dynamically Directed Particle Swarm Optimization," *North American Power Symposium,* pp. 1–6, 2013.